Natural Product Reports

ROYAL SOCIETY OF CHEMISTRY

REVIEW

View Article Online
View Journal



Cite this: DOI: 10.1039/d5np00092k

# Fungal polyketide biosynthesis as a platform for designer natural products

Pingxin Lin, [abc] Zhenhao Fu, [d] Ye Li, [e] Yeo Joon Yoon [f] and Sang Yup Lee *[abcgh]

Covering: 2010 to 2025

Polyketides constitute a vast family of structurally and functionally diverse natural products that underpin numerous pharmaceuticals, nutraceuticals, and materials. Among them, fungal typve I iterative polyketide synthases (iPKSs) orchestrate highly programmable catalytic cycles that transform simple acyl-CoA precursors into architecturally complex molecules. Understanding the programming logic of these multidomain enzymes has revealed how chain-extension, reduction, and cyclization patterns are encoded, offering a foundation for rational pathway engineering. Recent advances in structural biology, cryo-electron microscopy (cryo-EM) analysis, and computational modelling have clarified the conformational dynamics of iPKSs and their collaborating enzymes, while combinatorial biosynthetic strategies now enable the creation of non-natural scaffolds and expanded chemical diversity. Parallel progress in fungal and yeast cell-factory engineering—spanning metabolic rewiring, organelle compartmentalization, and dynamic control—has substantially improved the efficiency and scalability of polyketide production. This review integrates mechanistic insights with biotechnological innovation, highlighting emerging rules for programmable PKS design and discussing future directions toward AI-assisted, high-throughput platforms for sustainable industrial biosynthesis of fungal polyketides.

Received 25th December 2025

DOI: 10.1039/d5np00092k

rsc.li/npr





[a]*Metabolic and Biomolecular Engineering National Research Laboratory, Systems Metabolic Engineering and Systems Healthcare Cross-Generation Collaborative Laboratory, Korea Advanced Institute of Science and Technology (KAIST), Daejeon 34141, Republic of Korea*

[b]*Department of Chemical and Biomolecular Engineering (BK21 Four), KAIST, Daejeon 34141, Republic of Korea. E-mail: leesy@kaist.ac.kr; Web: https://twitter.com/mbelmbel99; Fax: +82-42-350-3910; Tel: +82-42-350-3930; https://mbel.kaist.ac.kr/*

[c]*KAIST Institute for the BioCentury, KAIST, Daejeon 34141, Republic of Korea*

[d]*School of Biotechnology and Key Laboratory of Industrial Biotechnology of Ministry of Education, Jiangnan University, 1800 Lihu Road, Wuxi 214122, China*

[e]*Department of Bioengineering, School of Food and Liquor Engineering, Sichuan University of Science and Engineering, Yibin, Sichuan 644005, China*

[f]*College of Pharmacy, Seoul National University, Gwanak-ro, Gwanak-gu, Seoul 151-742, Republic of Korea*

[g]*BioProcess Engineering Research Center, KAIST, Daejeon 34141, Republic of Korea*

[h]*Graduate School of Engineering Biology and Center for Synthetic Biology, KAIST, Daejeon 34141, Republic of Korea*

## 1. Introduction

Natural products constitute a major source of structurally diverse small molecules that continue to inspire drug discovery

and chemical biology.[1,2] Analyses of approved small-molecule therapeutics over the past four decades consistently show that a substantial fraction are either unmodified natural products, close analogues or inspired by natural product scaffolds, highlighting the enduring impact of nature-derived chemotypes on modern medicine and agrochemistry.[3–5] Among these, polyketides represent one of the most prolific and functionally versatile superfamilies, encompassing antibacterial, antifungal, immunosuppressive, anticholesterolemic, and anticancer agents, as well as pigments and signalling molecules.[6] Classic clinical examples include the macrolide antibiotic erythromycin, the immunosuppressant rapamycin, and the cholesterol-lowering drug lovastatin, alongside more recently exploited fungal metabolites such as griseofulvin (Fig. 1).[6–9] Polyketide frameworks from diverse microorganisms further serve as privileged starting points for semi-synthetic modification, combinatorial chemistry and biosynthetic tailoring, thereby feeding a broad pipeline of lead optimization programmes.

Fungi are particularly rich producers of polyketides with both beneficial and deleterious activities. On the beneficial side,

**Pingxin Lin**

*Pingxin Lin obtained his MS in Fermentation Engineering from Jiangnan University in 2023, where his research focused on genome mining of fungal polyketide biosynthetic gene clusters, combinatorial biosynthesis, and yeast compartmental engineering. He is currently pursuing his PhD in the Department of Chemical and Biomolecular Engineering at the Korea Advanced Institute of Science and Technology (KAIST) under the supervision of Prof. Sang Yup Lee. His research focuses on modular and systems-level engineering of natural and non-natural flavonoids and polyketides to develop programmable biosynthetic platforms for generating high-value bioactive molecules and structurally diverse natural products.*

**Zhenhao Fu**

*Zhenhao Fu obtained his MS in Light Industry Technology and Engineering from Jiangnan University in 2022, where his research focused on rapid food detection, quality control, and process analytical technologies for the food industry. He is currently pursuing his PhD in Fermentation Engineering at the School of Biotechnology, Jiangnan University, under the supervision of Prof. Zhonghu Bai. His doctoral research focuses on yeast metabolic engineering and organelle engineering to develop highly efficient microbial platforms for the biosynthesis of natural products.*

**Ye Li**

*Ye Li received his PhD in 2016 from the Department of Chemical and Biomolecular Engineering at the University of Houston under the supervision of Prof. Pat Cirino. He conducted postdoctoral research with Prof. István Molnár at the University of Arizona from 2016 to 2019, followed by six years of research at Jiangnan University. He is currently an assistant professor at Sichuan University of Science and Engineering. His work integrates protein engineering, metabolic engineering, and synthetic biology to engineer yeast and* E. coli *for value-added compounds and to study underlying mechanistic insights.*

**Yeo Joon Yoon**

*Yeo Joon Yoon is a Professor at the College of Pharmacy, Seoul National University. He received his BS (1992) and PhD (2000) from Seoul National University, conducting his doctoral research on polyketide biosynthesis under the guidance of Prof. C. Richard Hutchinson at the University of Wisconsin–Madison. He later worked with Prof. David H. Sherman at the University of Minnesota as a postdoctoral researcher. His research focuses on the characterization of biosynthetic pathways for polyketides/aminoglycosides/nonribosomal peptides and the application of combinatorial biosynthesis/synthetic biology to the production of secondary metabolites.*

**Sang Yup Lee**

*Sang Yup Lee is Distinguished Professor and Senior Vice President for Research at KAIST. He is recognized for pioneering systems metabolic engineering to develop high-performance microbial cell factories. He has received numerous prestigious awards, including the most prestigious Order of Science and Technology Merit-Changjo Medal from Korean government and the Eni Award from Italian President. He is an International Member of both the National Academy of Sciences and the National Academy of Engineering in USA, and a Foreign Member of the Royal Society (UK) and the Chinese Academy of Engineering.*

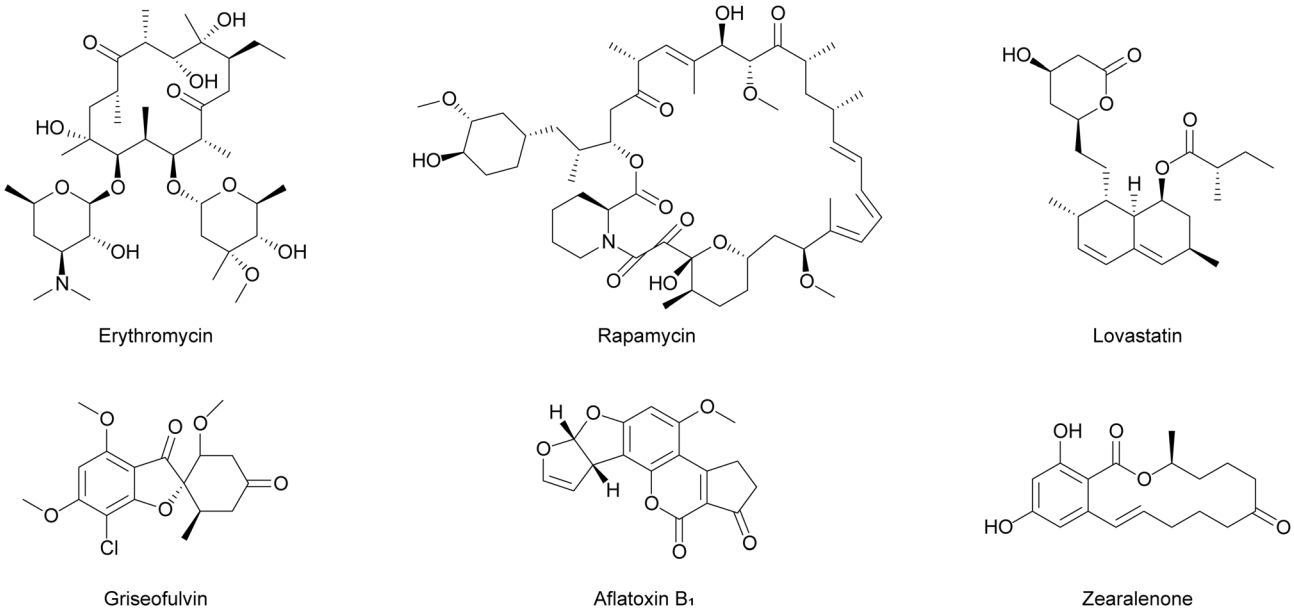


Fig. 1 Representative fungal-derived type I polyketides. Structures of widely distributed fungal polyketide natural products synthesized by type I PKSs, illustrating the chemical and functional diversity of this family. Shown are the macrolide antibiotic erythromycin, the immunosuppressant rapamycin, the cholesterol-lowering agent lovastatin, the antifungal precursor griseofulvin, and the mycotoxins aflatoxin $B_1$ and zearalenone, which highlight the broad biosynthetic and biological scope of fungal polyketides. Adapted from ref. 6–9 and 11–13.

filamentous fungi furnish industrial statins, antifungals, anticancer leads and crop-protection agents, many of which exploit unique carbon skeletons or dense stereochemistry that are difficult to access by purely synthetic routes.[6,10] Conversely, fungal polyketides also underpin major classes of mycotoxins—including aflatoxins, fumonisins, zearalenone, ochratoxins and related toxins (Fig. 1)—that contaminate food and feed, threatening human and animal health and causing substantial agricultural losses.[8,11–13] The same biosynthetic logic that yields life-saving drugs thus also generates potent virulence factors and ecological weapons, illustrating both the opportunity and the risk inherent in fungal polyketide metabolism.[6,14]

At the heart of polyketide biosynthesis are polyketide synthases (PKSs), large multidomain enzymes that assemble acyl-CoA building blocks into complex carbon scaffolds.[15] Based on domain organization and catalytic mechanism, PKSs are broadly classified into type I, type II and type III systems.[16] Type I PKSs are giant multidomain assemblies that operate either in a modular, non-iterative fashion—where each module is used once per cycle—or in an iterative mode, where the same catalytic domains are reused multiple times during chain extension and tailoring.[17] While bacteria often exploit modular type I PKSs, fungi rely almost exclusively on monomodular iterative type I PKSs (iPKSs) to construct their polyketide backbones.[16,18–20] iPKSs also occur in certain bacteria, but their organization and catalytic logic closely parallel fungal systems, reinforcing the generality of the fungal iPKS paradigm.[21]

Fungal iPKSs can be broadly grouped into highly reducing (hrPKSs), partially reducing (prPKSs) and non-reducing (nrPKSs) classes, reflecting the extent of β-keto processing and the nature of the resulting scaffolds (Fig. 2).[22,23] HrPKSs possess a full complement of reductive domains—ketoreductase (KR), dehydratase (DH) and enoylreductase (ER)—alongside ketosynthase (KS), acyltransferase (AT), acyl carrier protein (ACP) and often a *C*-methyltransferase (cMT), enabling the construction of highly functionalized, non-aromatic chains that can be further cyclized or merged into hybrid natural products.[24–26] PrPKSs typically retain only a subset of these reductive functions, generating partially reduced chains that cyclize into simple but bioactive lactones and related motifs,[27] whereas nrPKSs lack reductive domains altogether and instead combine starter-unit selection, iterative extension and programmed cyclization to yield complex aromatic polyketides (Fig. 2).[28] Together, these three iPKS subclasses, often assisted by *trans*-acting tailoring enzymes and hybridization with nonribosomal peptide synthetases (NRPSs), account for the vast majority of known fungal polyketide scaffolds.[29]

Over the past few years, rapid advances in cryo-electron microscopy (cryo-EM), X-ray crystallography and structure-prediction tools such as AlphaFold have profoundly reshaped our understanding of fungal iPKS programming, as emphasized in recent structural and mechanistic reviews on hrPKSs and related megasynthases.[15,30] Recent high-resolution work on the lovastatin synthase complex LovB–LovC has illustrated how distinct conformational states coordinate starter-unit selection, chain elongation, β-processing and product release within a single fungal megasynthase.[31] In parallel, systematic analysis of domain architectures and inter-domain communication across multiple iPKSs has begun to define how intrinsic domain selectivity and extrinsic protein–protein interactions together encode "programming rules" for chain length, reduction pattern and cyclization outcome.[30] Notably, combining cryo-EM

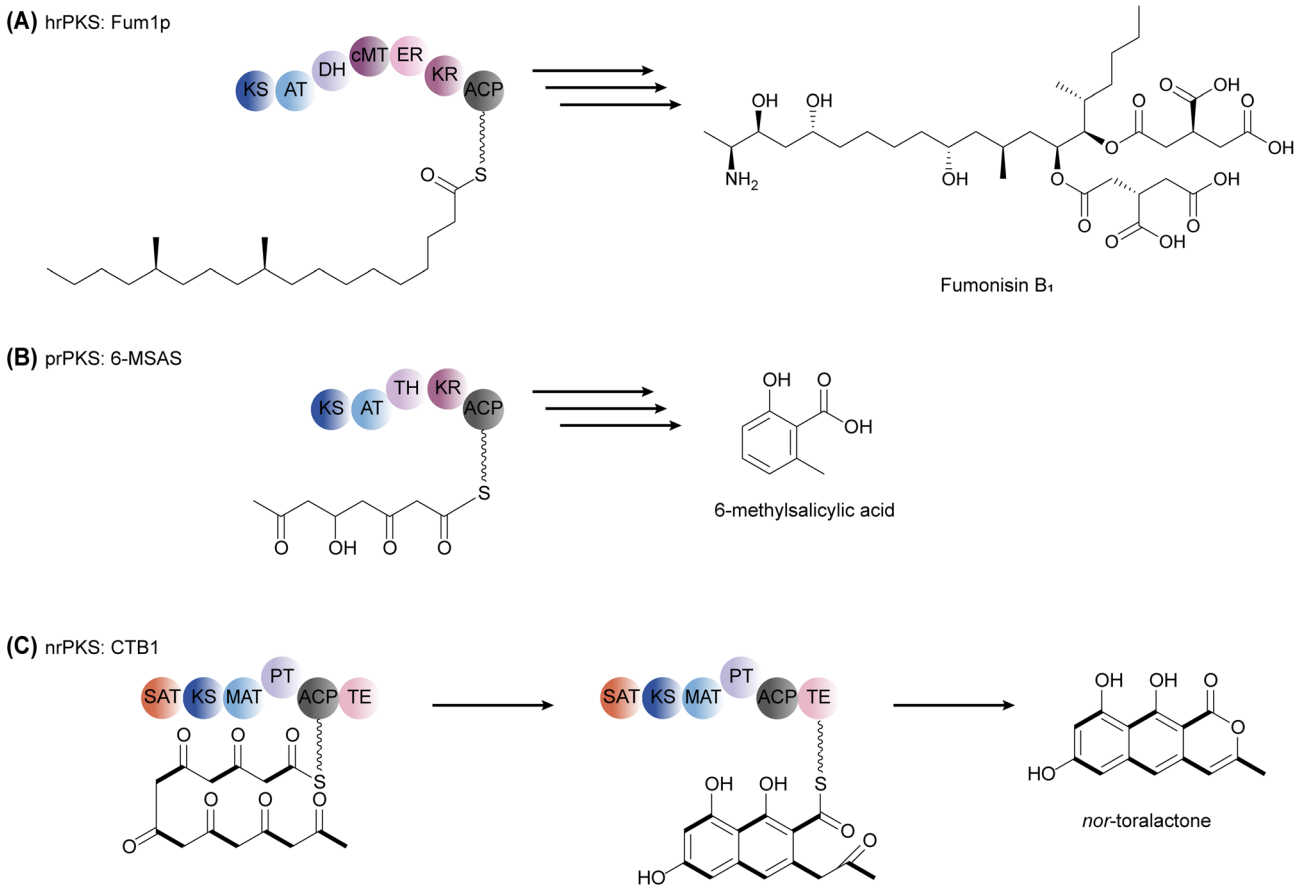


Fig. 2 Domain organization and representative biosynthetic products of fungal type I iterative PKSs. (A) The highly reducing PKS Fum1p, showing its characteristic hrPKS domain architecture (KS–AT–DH–cMT–ER–KR–ACP) and the corresponding product fumonisin B1. Adapted from ref. 27 and 28. (B) The partially reducing PKS 6-MSAS, featuring the canonical prPKS domain ensemble (KS–AT–TH–KR–ACP) and producing 6-methylsalicylic acid. Adapted from ref. 76. (C) The non-reducing PKS CTB1 with the typical nrPKS domain set (SAT–KS–MAT–PT–ACP–TE), together with its representative aromatic product *nor*-toralactone, illustrating nrPKS-controlled cyclization and release. Adapted from ref. 86. Domain abbreviations: KS, ketosynthase; AT, acyltransferase; DH, dehydratase; cMT, *C*-methyltransferase; ER, enoylreductase; KR, ketoreductase; ACP, acyl carrier protein; TH, thiohydrolase; SAT, starting-unit acyltransferase; MAT, malonyl-CoA:ACP transacylase; PT, product template; TE, thioesterase.

data with AlphaFold-based modelling has enabled direct visualization of ACP trajectories and gating motions during successive iterations in representative hrPKSs such as the tenellin synthase TENS, providing a concrete structural basis for chain-length control in these systems.[32]

Concomitant with these mechanistic insights, computational and synthetic-biology approaches have increasingly been used to reprogram iterative PKSs toward non-natural scaffolds. Detailed biochemical and structural dissection of programming in hrPKSs has highlighted specific catalytic motifs and dynamic elements as promising engineering handles.[33] iPKSs are now often treated as modular engineering platforms in which domain swaps, loop mutations and interface redesign can be guided by structure-based modelling and sequence analysis, as demonstrated for chain-length reprogramming of TENS *via* targeted mutations in the KR substrate-binding helix.[32] However, many reprogramming attempts still fail due to subtle mismatches in domain dynamics and substrate channeling, underscoring the need for structure-guided and data-driven design principles, a challenge highlighted in broader engineering perspectives on fungal natural product biosynthesis.[34] Complementary to direct enzyme engineering, combinatorial biosynthesis that mixes and matches iPKSs with tailoring enzymes has produced libraries of hybrid scaffolds—including polyketide–peptide and polyketide–terpenoid natural products—through rational pathway recombination and mutasynthesis.[35]

At the same time, the emergence of advanced genome-mining and heterologous expression technologies has greatly expanded access to fungal biosynthetic gene clusters (BGCs). Early work on expressing filamentous fungal pathways in tractable hosts such as *Aspergillus nidulans* and *A. oryzae* established robust platforms for reconstructing complex fungal secondary-metabolite pathways and exploring cryptic gene clusters.[36] More recently, CRISPR-Cas-based genome editing and activation systems have become central tools for turning on silent BGCs and fine-tuning their expression in native and heterologous fungal hosts.[37] These enabling methods are increasingly

 

combined with plug-and-play expression cassettes and high-throughput liquid chromatography-mass spectrometry (LC-MS) screening to systematically map the biosynthetic output of orphan BGCs in *Aspergillus*, *Penicillium* and other fungi, revealing large reservoirs of unexplored polyketide chemical space.[38] In parallel, metabolic engineering of chassis organisms such as *Saccharomyces cerevisiae* and the oleaginous yeast *Yarrowia lipolytica* has demonstrated that complex fungal-like polyketides can be produced at increasingly industrially relevant titers—for example, *via* acetyl-CoA and malonyl-CoA rewiring to boost triacetic acid lactone and 4-coumaroyl-CoA-derived polyketides in *Y. lipolytica*.[39,40] Together, these developments point toward an era in which fungal polyketide pathways can be designed and controlled across multiple levels—from enzyme structure and domain programming, through pathway and BGC architecture, to host metabolism and bioprocess optimization.

In this review, we synthesize these emerging mechanistic and engineering insights to present fungal polyketide biosynthesis as a programmable platform for designer natural products. Building on the foundational understanding of iPKS programming rules and structural determinants,[15,24] we first outline how different classes of fungal iPKSs (hrPKSs, prPKSs and nrPKSs) encode chain-length, reduction state and cyclization logic. We then survey combinatorial biosynthesis and enzyme-engineering strategies that expand chemical diversity beyond natural scaffolds, before highlighting the integration of these advances within fungal and yeast cell-factory frameworks for sustainable production. By emphasizing rational design, computational prediction and multi-scale engineering, we aim to bridge fundamental enzymology with industrial application and to provide a conceptual roadmap for the next generation of fungal polyketide research.

## 2. Programming rules and mechanistic logic of fungal iPKSs

### 2.1. Overall architecture and catalytic cycle

Fungal type I iPKSs are giant multidomain enzymes that resemble eukaryotic fatty acid synthases (FASs) in both overall architecture and reaction logic, yet exhibit far greater catalytic versatility.[30] In both systems, a single polypeptide (or homodimer) harbors all the activities required to iteratively extend acyl chains from simple acyl-CoA precursors, but iPKSs combine this FAS-like scaffold with expanded tailoring domains and additional control elements that enable diverse, highly functionalized products (Fig. 3A).[41] A comprehensive comparative analysis of yeast-type FAS (yFAS), mammalian FAS (mFAS) and fungal iPKSs has shown that these megasynthases assemble into large supramolecular structures in which catalytic domains are spatially arranged to support efficient intramolecular acyl carrier protein (ACP) shuttling and vectorial catalysis.[30]

Despite differences in domain composition among hrPKSs, prPKSs and nrPKSs, the core catalytic cycle of fungal iPKSs follows a conserved three-stage logic of initiation, iterative extension and termination.[25,42] In a typical cycle, a starter unit—often acetyl-, propionyl- or a more elaborate acyl group—is loaded onto the active-site cysteine of the KS domain *via* an acyltransferase-mediated transacylation step.[26] For hrPKSs and prPKSs, the acyltransferase is usually embedded as an AT domain;[43] for nrPKSs, a dedicated starter-unit acyltransferase (SAT) domain transfers the starter acyl group to the KS, while a malonyl:ACP acyltransferase (MAT) loads malonyl units onto ACP for chain extension.[44] Subsequent decarboxylative Claisen condensation catalysed by KS yields a β-ketoacyl intermediate tethered to ACP, which then undergoes variable processing by reductive domains (KR-DH-ER) in hrPKSs and prPKSs, or is left unreduced in nrPKSs for downstream aromatic cyclization (Fig. 2).[27,45,46]

Recent structural and mechanistic studies have begun to reveal how this apparently simple cycle is diversified into a wide range of programmed reaction sequences. High-resolution analyses of isolated domains and larger assemblies from multiple iPKSs—including hrPKSs involved in lovastatin and related pathways—have shown that KS, AT/MAT and ACP form a dynamic core module that repeatedly executes loading and condensation steps, while flexible linkers and docking interfaces guide ACP to different reductive or cyclization domains in a defined order.[15,33] Time-resolved biochemical experiments and structural models support a "tethered substrate shuttle" model in which ACP oscillates between multiple catalytic sites within a confined reaction space, and where the probability of visiting specific domains in each iteration—KR, DH, ER, or, in nrPKSs, product-template (PT) domains—encodes the final reduction pattern and ring-formation logic.[30,47]

Termination of the iterative cycle is mediated by product-releasing enzyme (PRE) domains located at the C-terminus of iPKSs or by discrete *trans*-acting factors.[46] In fungal nrPKSs, terminal release domains fall into three principal classes: (i) canonical α/β-hydrolase fold thioesterase (TE) domains that catalyse hydrolytic, macrolactonization or cross-coupling release; (ii) TE/CLC (Claisen cyclase) domains that promote C–C bond formation during programmed cyclization; and (iii) reductase (R) domains that mediate NAD(P)H-dependent reductive off-loading.[46] In addition, some nrPKSs lack a terminal release domain and instead recruit *trans*-acting metallo-β-lactamase-type thioesterases (MβL-TEs).[48] Systematic sequence–structure–function analysis of PRE domains in fungal nrPKSs has shown that these off-loading modules not only catalyse hydrolysis, macrolactonization or Dieckmann-type cyclization, but can also perform proofreading or editing functions that shape product fidelity and scaffold topology.[48] In hrPKSs and prPKSs, termination is typically mediated by embedded α/β-hydrolase-type release domains, historically annotated either as thioesterases (TE) or thiohydrolases (TH) depending on pathway context; these domains generally catalyse hydrolytic off-loading rather than Claisen-type cyclization, and may operate either as integral PKS domains or as discrete *trans*-acting factors.[49,50]

Collectively, these architectural and mechanistic insights support a unified view of fungal iPKSs as monomodular but multifunctional megasynthases that execute a conserved

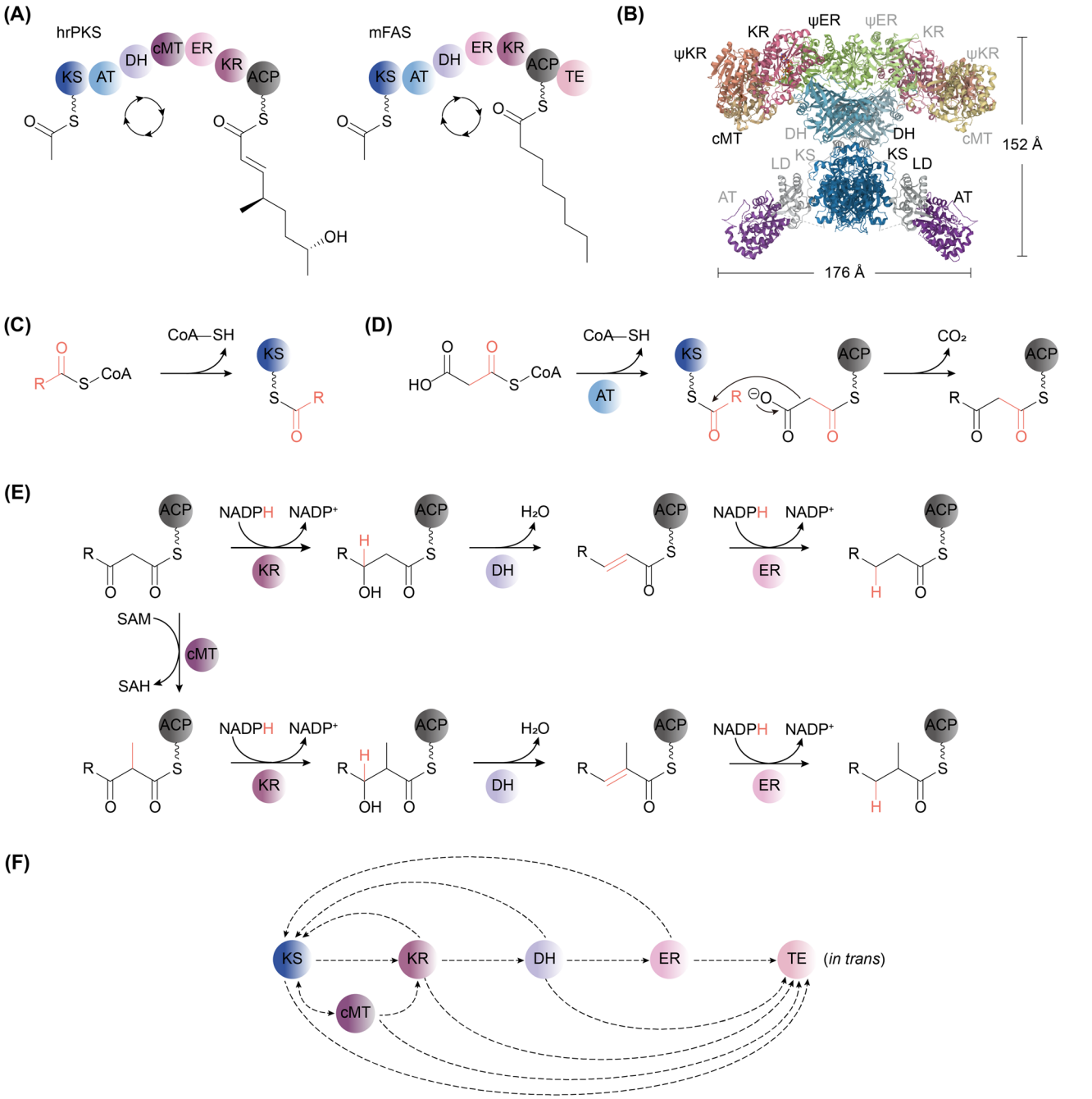


Fig. 3 Structural features and iterative programming of hrPKSs. (A) Comparison of the canonical domain organization and reductive programming logic between fungal hrPKSs and mammalian fatty acid synthase (mFAS), highlighting both conserved catalytic modules and differences in iterative reduction rules. (B) Cryo-EM structure of the hrPKS LovB (LNKS), the megasynthase responsible for assembling the nonaketide intermediate monacolin J acid in the lovastatin biosynthetic pathway, resolved at 2.91 Å (PDB: 7CPX). Individual domains are color-coded, and inactive modules are indicated with leading $\psi$ (pseudo) symbols. LD, linker domain. Adapted from ref. 31. (C) The KS domain initiates polyketide assembly by selecting and loading the appropriate starter acyl unit. (D) Chain elongation proceeds through malonyl-CoA incorporation mediated by the AT and KS domains. (E) Iterative β-keto processing occurs through the coordinated action of the KR, DH, ER, and cMT domains, generating variably reduced and α-methylated intermediates. (F) Representative programming trajectories of hrPKSs, illustrating selective domain engagement and kinetic competition between cMT and KR during chain extension. Chemical modifications introduced by each domain are highlighted in red.

initiation–extension–termination cycle while embedding tunable "decision points" at each iteration. In hrPKSs and prPKSs, the number and order of visits to KR, DH and ER domains determine the extent of β-reduction and hence the degree of saturation and hydroxylation of the final product;[30] in nrPKSs, SAT specificity, KS chain-length control and PT-mediated cyclization are key determinants of aromatic scaffold topology.[16,51] To consolidate these distributed mechanisms

Table 1 Core programming decision nodes in fungal iPKSs

| Decision node | PKS class | Programming role | Representative examples | References |
|---|---|---|---|---|
| Starter-unit loading (SAT or embedded AT) | nrPKS (SAT); hr/prPKS (AT) | Defines starter identity and initial oxidation bias | CazM/CazF; CTB1; LovB | 31, 88, and 90 |
| Condensation cassette (KS–AT/MAT–ACP) | All classes | Controls chain elongation and iteration number | CTB1; SQTKS; LovB | 31, 64, and 90 |
| Reductive loop (KR–DH–ER) | hrPKS; prPKS (KR ± DH) | Determines β-reduction pattern and oxidation state distribution | LovB/LovC; SQTKS; SN477 | 31, 57, 76, and 85 |
| cMT (embedded or *trans*-acting) | hrPKS; nrPKS; *trans* systems | Introduces α-methylation and modulates elongation or reduction timing | PksCT; PsoF; SQTKS | 58–60, and 94 |
| Product template (PT) domain | nrPKS | Directs first- and second-ring cyclization regioselectivity | PksA; CTB1; PhnA | 96, 97, 100, 103, and 104 |
| Embedded product-releasing enzymes (TE/CLC/R) | prPKS; nrPKS; some hrPKS | Defines mode of off-loading (hydrolysis, macrolactonization, Dieckmann, reduction) | PksA; Pks1; AquA | 108, 111, 114, and 120 |
| *Trans*-acting release/editing enzymes (TE, TE/CLC, MβL-TE) | hrPKS; nrPKS | Enforces chain-length window; proofreading; selective termination | LovG; Bref-TH; CitA; ACTE | 22, 66, 132, 133, and 135 |
| Multi-megasynthase handover (hrPKS–nrPKS; PKS–NRPS) | Dual/hybrid systems | Branch specificity and scaffold hybridization | CazF/CazM; EquiS; TwmB | 88, 150, 151, and 154 |

into a central framework, the core programming decision nodes across hrPKSs, prPKSs and nrPKSs are summarized in Table 1. These emerging "programming rules" provide the conceptual foundation for the subsequent sections, where we discuss in detail how different classes of fungal iPKSs and their collaborating enzymes encode specific chain-extension, reduction and cyclization patterns, and how these features can be exploited for rational engineering.

### 2.2. Highly reducing PKSs (hrPKSs)

Fungal iterative hrPKSs comprise a KS–AT–ACP minimal "loading/condensing" set that executes repeated decarboxylative Claisen condensations, while additional modifying domains (KR, DH, ER, and frequently cMT) are arranged to be accessed iteratively by the ACP during chain growth; this FAS-like scaffold has been visualized and compared across fungal megasynthases using structural and biochemical analyses.[23,30] In the lovastatin pathway, cryo-EM structures of the LovB core (2.91 Å) (Fig. 3B) and the LovB–LovC complex (3.60 Å) (Fig. 4A) revealed an X-shaped face-to-face dimer and an L-shaped catalytic chamber, respectively, illustrating how a *trans*-acting ER (LovC) docks laterally near the AT region and helps organize iterative processing within a confined reaction space.[31] During initiation, a simple acyl starter (commonly acetyl- or propionyl-derived) is loaded to KS—by the embedded AT in hrPKSs—followed by iterative malonyl-ACP extensions; this division of labor (starter loading *vs.* extender supply) parallels but is mechanistically distinct from nrPKSs where SAT and MAT split the roles (Fig. 3C and D).[52] Collectively, these data support a model in which ACP shuttling and flexible inter-domain linkers orchestrate a cyclical sequence of loading → condensation → optional β-processing before the next round of extension, setting the stage for programmable selectivity in downstream steps.

After each condensation, β-ketoacyl intermediates are variably processed by KR, DH and ER to yield β-alcohol, enoyl or fully reduced segments (Fig. 3E);[53] biochemical and structural work on hrPKSs shows that the order and frequency of ACP visits to these reductive domains encode the final reduction pattern, in contrast to the more uniformly reducing cycles of metazoan FAS.[54] Methylation by the embedded cMT often acts as a checkpoint that branches the itinerary of the growing chain: cMT can compete kinetically with KS-catalysed extension and with KR access, thereby altering both chain-length programming and downstream reduction outcomes (Fig. 3E and F).[55,56] At the case-study level, recent cryo-EM-guided analyses of LovB/LovC, together with reconstituted domain biochemistry, highlight how *trans*-ER engagement and cMT timing together affect stereochemical outcomes and the fidelity of iterative processing in a paradigmatic hrPKS system.[31]

In squalestatin tetraketide synthase (SQTKS), the isolated *cis*-acting ER forms a discrete dimer in solution and displays broad substrate tolerance toward natural and non-natural enoyl thioesters—an observation that explains how subtle features such as local methylation patterns can "gate" enoyl reduction and, consequently, iteration-dependent termination.[57] Beyond changing reduction, cMT can also influence chain-length decisions: studies on fungal hrPKSs revealed the molecular basis by which cMT intercepts ACP-bound intermediates and biases whether KS proceeds to the next round of condensation, rationalizing how methylation state and β-processing co-define scaffold topology.[58] Finally, in hybrid iPKS systems such as

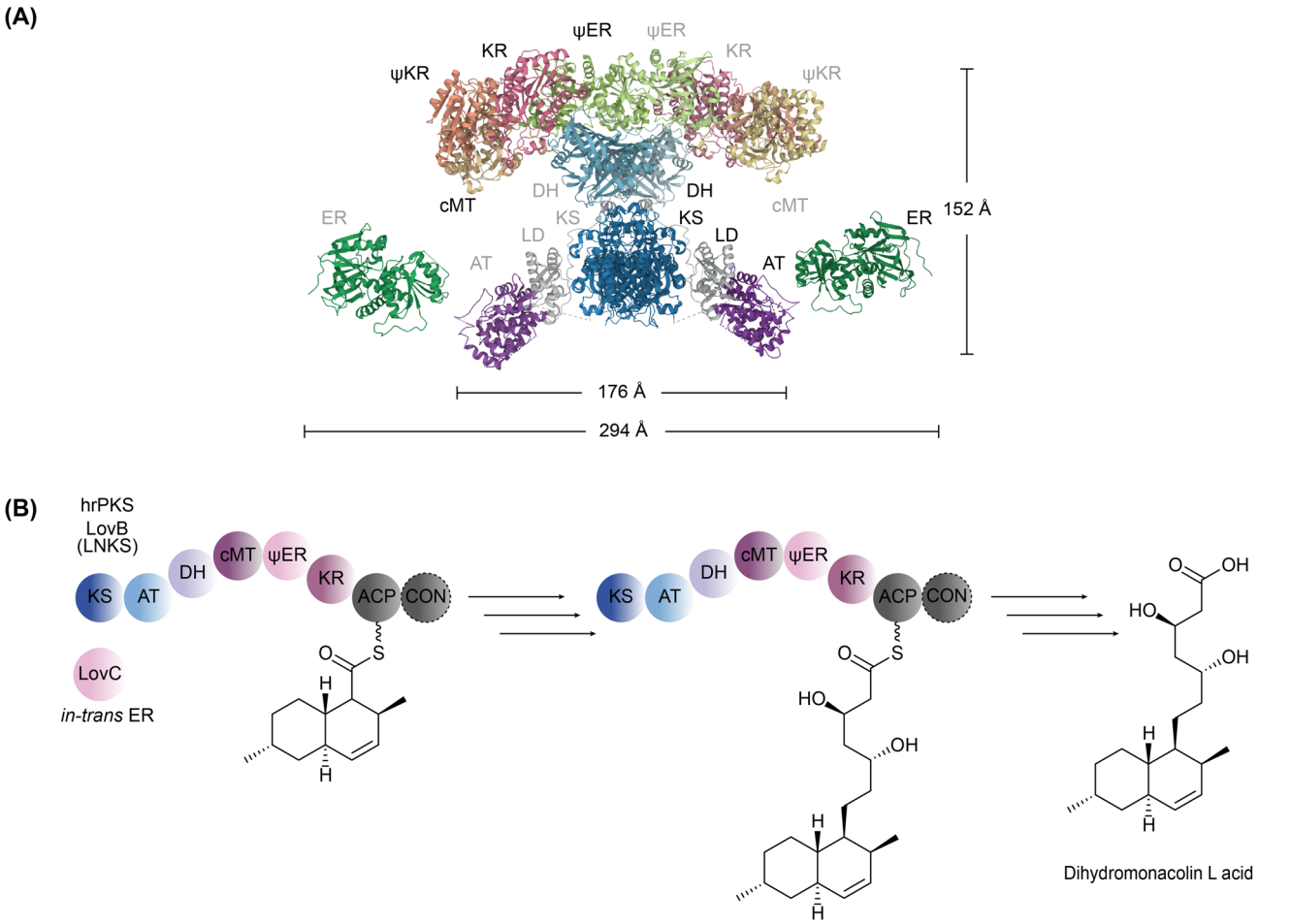


Fig. 4 Structural organization and biosynthetic role of the LovBC complex. (A) Cryo-EM structure of the LovB–LovC complex resolved at 3.60 Å (PDB: 7CPY), illustrating the docking interface between the megasynthase LovB and the *trans*-acting ER LovC. Adapted from ref. 62. (B) General process by which the LovBC complex mediates iterative chain tailoring and reduction to assemble dihydromonacolin L acid, with LovC supplying *trans*-ER activity to specific cycle-defined intermediates. Inactive modules are indicated with leading $\psi$ (pseudo) symbols. CON, unresolved C-terminal condensation domain. Adapted from ref. 31.

the pseurotin pathway, a bifunctional PsoF (epoxidase-*C*-methyltransferase) collaborates with the PKS-NRPS machinery to tailor intermediate reactivity and geometry—directly illustrating how MT chemistry shapes programming windows available to KR/DH/ER in later iterations (Fig. 3F).[59,60]

LovB (lovastatin nonaketide synthase, LNKS) represents one of the best-characterized fungal hrPKSs and has long served as a model for understanding iterative programming in polyketide biosynthesis (Fig. 3B).[31] Its accompanying *trans*-acting ER LovC acts in concert with LovB to produce dihydromonacolin L acid, the first committed intermediate of lovastatin biosynthesis (Fig. 4B).[61] Structural and biochemical analyses have revealed that LovB alone accumulates aberrantly reduced or truncated polyketides, whereas co-expression with LovC restores correct chain reduction and product fidelity.[31]

Recent cryo-EM reconstructions of the LovB–LovC complex at near-atomic resolution uncovered an X-shaped "head-to-tail" dimeric arrangement, with a flexible docking interface near the AT–KS junction that accommodates transient association of LovC (Fig. 4A).[31,62] This structural snapshot provided the first direct visualization of a fungal hrPKS-*trans*-ER assembly and explained how LovC engages the β-enoyl intermediate during selective iteration.[31] Complementary cross-linking mass-spectrometry and mutagenesis experiments further showed that LovC recognizes the ACP-tethered substrate through a hydrophobic docking groove and stabilizes its NADPH-binding loop only when positioned near the AT domain, ensuring precise timing of reduction.[63] Functionally, the LovB–LovC system exemplifies conditional domain crosstalk in fungal hrPKSs: LovB's internal reductive loop (KR–DH) executes partial β-processing, whereas LovC provides an auxiliary ER activity only in iterations requiring full reduction, thereby modulating the oxidation state of specific chain segments.[31] Single-particle cryo-EM analysis coupled with AlphaFold modeling demonstrated that LovB alternates between "open" and "closed" conformations that expose or sequester the active-site cavities in coordination with LovC binding.[31] Collectively, these results establish LovB/LovC as a prototype for *trans*-acting enzyme assistance in hrPKS systems, highlighting how transient protein–protein interactions expand the catalytic repertoire and

control the iterative sequence of reductions and methylations during fungal polyketide assembly.

SQTKS is another representative hrPKS that demonstrates how the intrinsic selectivity of reductive domains influences product patterning.[64] Biochemical reconstitution of SQTKS revealed that its internal reductive domains perform three rounds of chain extension and β-processing, producing the squalestatin core from acetate, malonate, *S*-adenosylmethionine (SAM) and NADPH.[64,65] In the first two iterations, complete reduction and α-methylation yield saturated intermediates, whereas the third round omits ER-catalyzed reduction, halting the cycle and defining the final oxidation pattern.[24]

Purified SQTKS ER functions as a discrete homodimer that displays remarkably broad substrate tolerance toward both natural diketide/triketide and synthetic enoyl substrates, and the enzyme's activity is modulated by the methylation state of its substrate: a dimethylated 2,4-dimethyl-oct-2-enoyl-ACP analog fits within the active site but resists reduction.[57] These observations reveal a kinetic gating mechanism, where methylation pattern and intermediate geometry determine whether ER can engage, thereby controlling which iterations undergo full β-processing. Mechanistically, structural models suggest that subtle conformational changes in the ER substrate-binding loop adjust access to the NADPH cofactor and stabilize the transition state only for properly oriented intermediates. This property explains how hrPKSs can generate alternately reduced and unreduced segments within a single iterative cycle, yielding molecules of mixed oxidation state and stereochemical complexity.[57] Together, SQTKS illustrates the broader principle that reductive-loop plasticity and kinetic control—rather than rigid sequential processing—govern product specificity in fungal hrPKSs, providing critical insight for future reprogramming efforts that aim to tune redox and methylation patterns in engineered systems.

Beyond *trans*-ERs, fungal iPKS pathways frequently rely on stand-alone factors—including hydrolases or thioesterases (THs or TEs, including TEIIs), ATs, and *trans*-acting cMTs—to control chain release, proofreading, chain-length decisions, and methylation checkpoints that together enforce hrPKS programming fidelity.[15] In lovastatin biosynthesis, the serine hydrolase LovG functions as a chain-release/"editing" factor for LovB, removing aberrant intermediates and releasing the correctly programmed nonaketide prior to downstream processing; *in vitro* and genetic evidence established LovG-dependent quality control as a key layer of programming.[66] Analogously, in brefeldin A biosynthesis, a partnering thiohydrolase (Bref-TH) truncates the chain one iteration earlier: the hrPKS alone favors a nonaketide, but with Bref-TH the octaketide is specifically off-loaded, demonstrating *trans*-releaser-controlled chain length.[22] Recent structural enzymology consolidates these cases and shows how such hydrolases/hot-dog fold TEs set release chemistries and chain-length windows across fungal systems.[67]

A complementary control point arises from *trans*-acting cMTs that intercept ACP-tethered intermediates and thereby compete with KR/KS steps. Two structurally characterized cMTs—PsoF (from the pseurotin pathway) and CalH′/CalH (from calbistrin)—provide direct, stand-alone methylation of PKS intermediates; crystallographic work pinpointed SAM-binding motifs and substrate channels that rationalize timing-dependent interception of β-ketoacyl intermediates.[68,69] Functionally, such *trans*-cMT "checkpoints" can bias whether the chain undergoes further β-processing or proceeds to the next elongation step, thereby re-wiring oxidation state and termination logic at the iteration where methylation occurs.[70]

*Trans*-acting TEIIs have seen important mechanistic updates. A 2024 study delineated TEII editing functions embedded in fungal PKS gene clusters[71]—showing that dedicated TEIIs can rescue stalled ACP-bound species and improve product fidelity, extending the "proofreading" paradigm beyond LovG-like hydrolases. Meanwhile, structural snapshots of α/β-hydrolase fold *trans*-TEs (*e.g.*, DcsB for decarestrictine C1; GrgF for gregatin A)[50,72] highlight dimeric assemblies and catalytic triads that accommodate poly-β-keto chains and enable off-loading *via* cyclization or C–C coupling—providing a generalizable release architecture now used to interpret newer pathways. Beyond hydrolases, *trans*-acting ATs can also "intercept and deliver" polyketide chains: in lovastatin maturation, LovD accepts the diketide from LovF-ACP and transfers it to monacolin J, and structure-guided engineering has dramatically accelerated its catalytic cycle, underscoring how stand-alone ATs remodel flux at pathway junctions.[31]

Recent primary studies further broaden the repertoire of non-ER *trans* partners. In 2025, Takekawa *et al.* dissected two *trans*-ERs (PhiaB/PhomB) from phialotide/phomenoic-acid pathways and uncovered distinct chain-length preferences by X-ray structure and *in vitro* assays, directly linking enzyme architecture to iteration-specific engagement;[73] these data, together with kinetic gating observed in hrPKS systems, reinforce the concept that *trans* partners partition iterations by chain length, not only by redox state (*i.e.*, a general rule for stand-alone reductive/checkpoint enzymes). Beyond reductive gating, auxiliary enzymes can also diversify scaffolds through other *trans*-acting modifications. In parallel, *Org. Lett.* 2024 reported a noncanonical fungal PKS pathway (PF1163A) in which a stand-alone *trans*-acting *N*-methyltransferase (PfaC) functions with the PKS–NRPS megasynthase to diversify the scaffold, while subsequent oxidative tailoring steps further modify the released intermediate.[74] Together with updated structural enzymology showing how *trans*-releasing enzymes (*e.g.*, Bref-TH, Fma-AT)[22] precisely enforce where the hrPKS stops and how the product is ejected, these examples establish a unifying view: stand-alone partners act as programmable gates that modulate when to reduce, when to methylate, and when to release in each iteration, thereby expanding chemical space without altering the embedded hrPKS domain set.

### 2.3. Partially reducing PKSs (prPKSs)

PrPKSs are iterative type I PKSs that lack an ER but retain a β-keto processing set focused on KR and often DH, operating on a KS–AT–ACP minimal scaffold;[75] the canonical 6-methylsalicylic acid synthase (6-MSAS) clade exemplifies the architecture KS–AT–KR–ACP, frequently accompanied by a TH domain

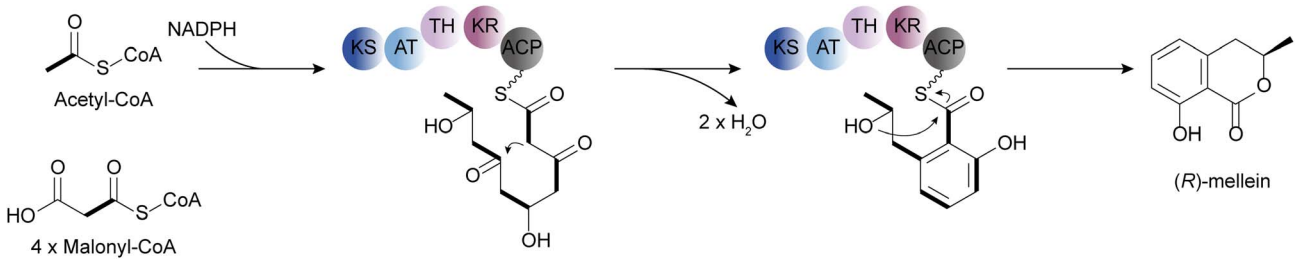


Fig. 5 Biosynthetic mechanism of (*R*)-mellein formation by the prPKS SN477 assembles (*R*)-mellein from one acetyl-CoA starter unit and four malonyl-CoA extender units, generating a pentaketide intermediate that undergoes programmed β-keto processing and cyclization. In the structural representation, each bold bond highlights a $C_2$ extender-derived building block, and five bold segments denote the five sequential chain-extension steps leading to the final (*R*)-mellein scaffold. Adapted from ref. 76 and 85.

that mediates stereoselective cyclization and release (Fig. 2B).[76] Recent transcriptome-guided discovery in plant-associated fungi again recovered prPKS candidates with KS–AT–DH–KR–ACP features, reinforcing this architecture as the prevalent prPKS pattern in nature.[77] In parallel, genome-scale mining of *Penicillium* species uncovered 6-MSAS-like clusters co-localized with downstream tailoring genes, supporting the view that prPKSs often sit at the entrance of multi-step pathways producing salicylate- or isocoumarin-derived scaffolds.[78] Functionally, prPKSs generate partially reduced polyketide intermediates that are pre-organized for regio-defined cyclization and release by the embedded or partner TH or TE domain, a division of labor that distinguishes them from hrPKSs and aligns with the single-pass reduction logic summarized below.[77]

In prPKSs, each extension round is followed by at most a single β-reduction event (KR ± DH) before the system proceeds to the next condensation, setting up hydroxylated or dehydrated handles that bias aldol-type ring formation and lactonization at termination.[79] Heterologous reconstitution of prPKS routes in *Y. lipolytica* has demonstrated this programming at production scale: by supplying malonyl-CoA and SAM flux, engineered strains produced 6-MSA and an isocoumarin-type scaffold (bostrycoidin), showing that limited β-processing coupled to efficient TH/TE-mediated off-loading is sufficient to build salicylate/isocoumarin cores and that these prPKS products function as gateway metabolites for downstream diversification.[80] Complementarily, transcriptome-guided identification of prPKSs with KS–AT–DH–KR–ACP organization verified that the absence of ER correlates with products bearing discrete hydroxylation patterns rather than fully reduced segments, consistent with single-reduction programming that precedes TH-controlled ring closure.[77] Together, these recent studies consolidate a unified rule: prPKSs encode chain growth with limited β-processing, and the timing/chemistry of TH- or TE-driven release fixes ring topology and oxidation state, positioning prPKS products as programmable entry points for fungal polyketide and isocoumarin pathways.[78,81]

The small molecule 6-MSA, produced by the 6-MSAS clade of prPKSs, remains a prototypical example of partially reducing fungal PKSs and their downstream biosynthetic potential. A recent heterologous production study in *Y. lipolytica* achieved titers of ≈ 400 mg $L^{-1}$,[80] thereby validating 6-MSA's role as a production gateway for derived natural products (*e.g.* patulin, terreic acid, yanuthones).[27,82–84] Meanwhile, the (*R*)-mellein synthase SN477 from *A. oryzae* (heterologously studied in *S. cerevisiae*) extends the prPKS logic by performing four rounds of extension and selective β-ketone reduction before TH-mediated lactonization, offering a close parallel to 6-MSA biosynthesis albeit with additional chain length and stereochemical complexity (Fig. 5).[76,85] These cases illustrate how prPKSs embed one-pass β-processing + TH- or TE-mediated termination logic and how their products become entry points for larger tailoring enzyme networks.

In summary, prPKSs enforce a single-reduction logic followed by TH- or TE-controlled release, making them inherently more tractable than multifunctional hrPKSs for engineering scaffold libraries. The architecture KS–AT ± DH–KR–ACP ± TH positions prPKSs as programmable entry points into fungal polyketide diversification. Nonetheless, engineering challenges remain: ensuring TH or TE compatibility, balancing extender unit flux, and controlling unintended full reduction events are critical. Leveraging the accumulating structural and genomic data, future work can treat prPKSs not just as natural curiosity but as designable modules within broader synthetic biology workflows.

### 2.4. Non-reducing PKSs (nrPKSs)

Fungal nrPKSs construct fully unreduced poly-β-keto backbones that undergo programmed intramolecular cyclization to yield aromatic scaffolds (Fig. 2C).[86] As summarized in Table 1, nrPKSs encode a layered logic in which condensation, methylation and cyclization checkpoints act sequentially to define aromatic scaffold topology. This behavior reflects their characteristic SAT–KS–MAT–ACP–PT–TE domain organization, which lacks the β-processing domains (KR, DH, ER) present in hrPKSs and prPKSs.[87] Recent phylogenomic analysis of nrPKSs across ascomycota and basidiomycota revealed that most nrPKSs maintain this canonical domain set, although several basidiomycete lineages lack a SAT domain entirely while retaining robust aromatic programming, indicating that nrPKSs can use KS-based direct loading when SAT is absent.[16]

The SAT domain remains the defining gateway for starter-unit selection in ascomycete nrPKSs. A 2023 structure-informed analysis demonstrated that SAT domains favor

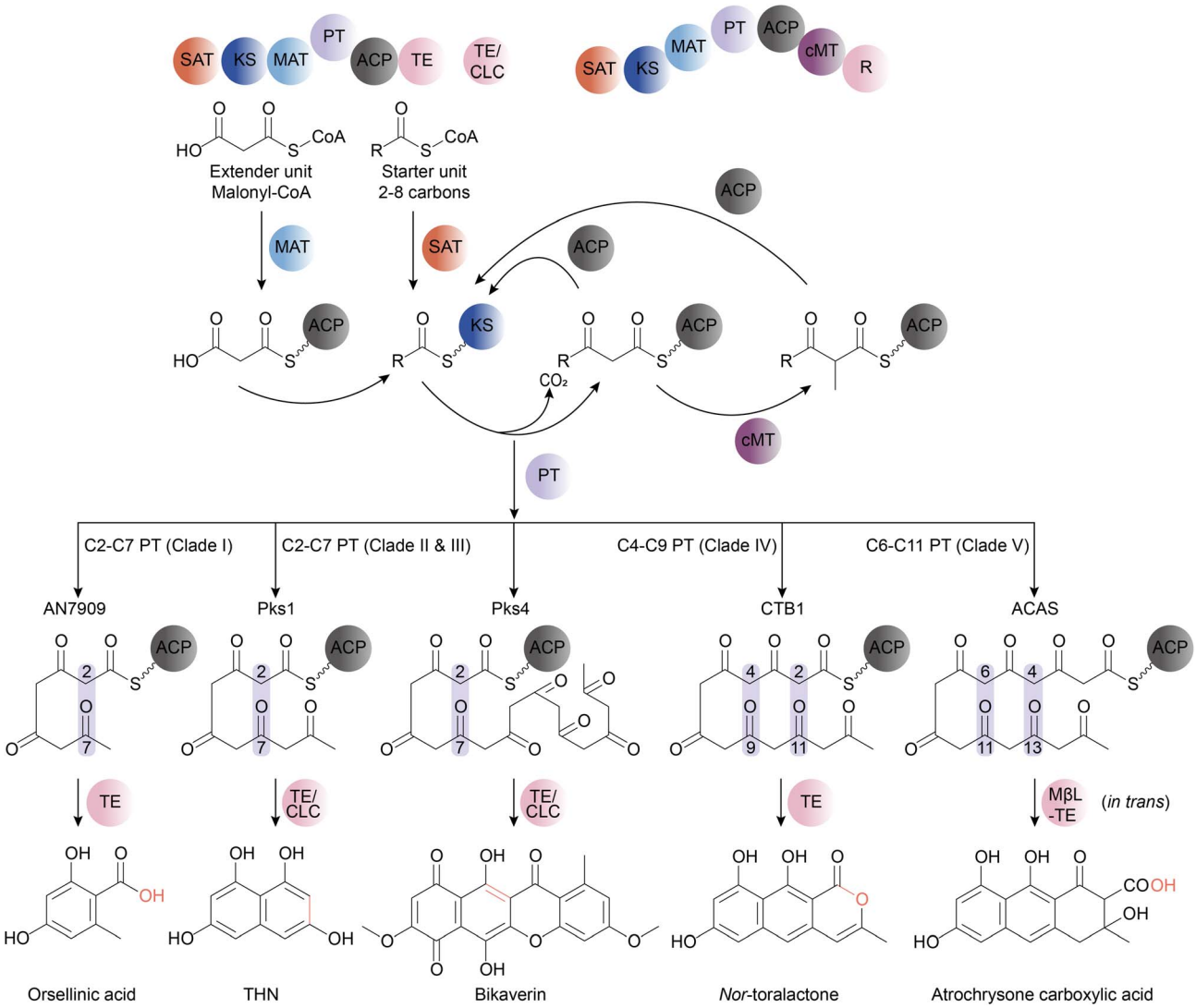


Fig. 6 Overview of nrPKS domain organization and iterative programming. nrPKSs initiate and extend polyketide chains either with or without a cMT domain, generating highly programmed β-keto-processing patterns prior to cyclization and product release. The PT domain governs the first- and second-ring cyclization trajectories and can be classified into five major clades, whose active-site geometries correlate with distinct folding modes: clades I–III catalyze C2–C7 first-ring closures on tetra-, hexa-, or longer ketide chains (*e.g.*, clade I: orsellinic acid from AN7909; clade II: 1,3,6,8-tetrahydroxynaphthalene (THN) from Pks1; clade III: bikaverin from Pks4); clade IV mediates C4–C9 followed by C2–C11 cyclization (*e.g.*, *nor*-toralactone from CTB1); and clade V promotes C6–C11/C4–C13 modes (*e.g.*, atrochrysone carboxylic acid from ACAS). Cyclization modes dictated by the PT domain are highlighted in purple, whereas chemical modifications introduced by the TE domain are highlighted in red. Domain abbreviations: TE/CLC, thioesterase/Claisen cyclase domain; MβL-TE, metallo-β-lactamase-type thioesterase; R, reductase. Adapted from ref. 90 and 98–101.

acetyl- or longer acyl-CoA units, thereby determining the oxidation-state and chain-length bias of downstream poly-β-keto chains (Fig. 6).[15] This selectivity is also evident in the CazM/CazF azaphilone pathway, where CazM-SAT selectively accepts the highly reduced (*S*,*E*)-4-methyl-hex-2-enoyl triketide from the upstream hrPKS CazF while rejecting the more oxidized triketide intermediate needed for late-stage tailoring (Fig. 7A).[88] This selective gating ensures that nrPKS-specific cyclization only proceeds from the correct reduced starter, demonstrating that starter identity, not only chain length, is a SAT-encoded programming checkpoint.[89] Together, these insights from comparative genomics and biochemical reconstitution reinforce a unifying principle: nrPKS programming begins at the SAT/KS interface, where starter-unit identity and the physical arrangement of the condensation domains drive the fate of the aromatic backbone.

After starter-unit transfer, nrPKSs extend the chain exclusively with malonyl-ACP units *via* the MAT domain, while the KS orchestrates iterative Claisen condensations to generate long poly-β-keto intermediates (Fig. 6).[87] Because these chains are unreduced, the KS must precisely determine how many elongation rounds occur before PT-mediated cyclization can begin. This concept is strongly supported by structural work on CTB1, the nrPKS forming *nor*-toralactone in *Cercospora nicotianae*.[90] Cryo-EM coupled with mechanism-based ACP–KS crosslinking revealed a rhombus-shaped KS–MAT dimer with

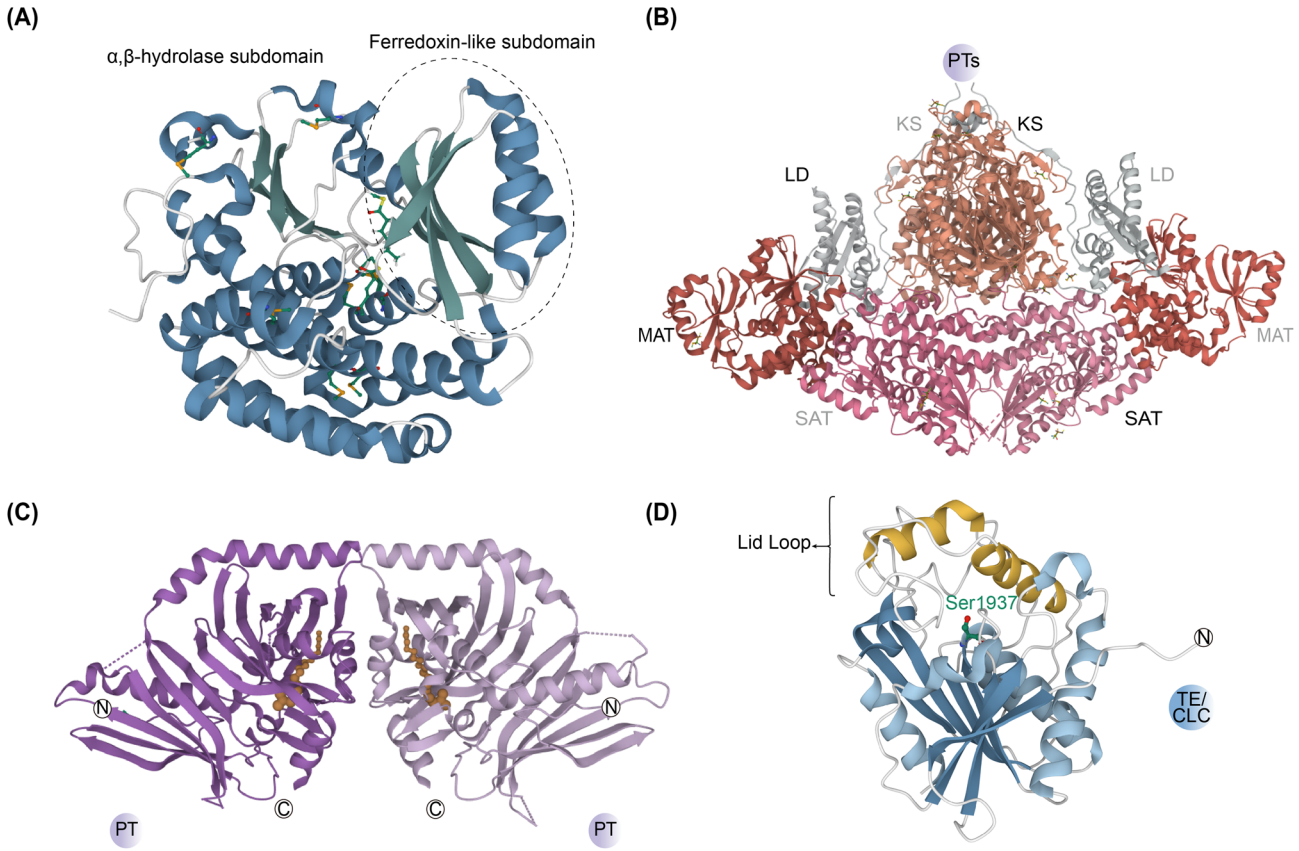


Fig. 7 Structural snapshots of key domains from non-reducing PKSs (nrPKSs). (A) Crystal structure of the CazM SAT domain bound to hexanoyl-CoA, showing a monomeric architecture composed of a large α/β-hydrolase-like subdomain and a smaller ferredoxin-like subdomain (PDB: 4RPM). Adapted from ref. 88. (B) Structure of the CTB1 loading/condensing region comprising the SAT–KS–MAT tri-domain module, which coordinates starter-unit selection and chain initiation (PDB: 6FIJ). Adapted from ref. 91. (C) PksA PT domain structure with bound palmitate or substrate analog (PDB: 3HRQ); the PT adopts a modified double-hot-dog (DHD) fold, with PT dimers shown as purple cartoons and palmitate ligands represented as orange spheres. Adapted from ref. 97. (D) Ribbon representation of the PksA TE/CLC domain, exhibiting an α/β-hydrolase fold with its core catalytic scaffold in blue and a distinctive lid loop in yellow, adjacent to the active-site Ser1937 (shown as green ball-and-stick) (PDB: 3ILS). Adapted from ref. 108.

a pseudodimeric SAT inserted asymmetrically into the condensation region.[91] The ACP interacts preferentially with one KS protomer in a 1 : 2 binding mode, implying that nrPKSs may determine chain-length by biased ACP access rather than a symmetric dimeric cycle (Fig. 7B).[91]

New comparative analyses published in 2023 further support this logic: nrPKSs from recently characterized fungal clades show that single amino-acid substitutions in the KS active-site loops are sufficient to shift product chain length by two carbons, confirming that KS micro-architecture fine-tunes iteration count.[16] These findings align with earlier functional studies on CazM/CazF, where SAT selectivity and KS timing cooperate to distinguish between early-stage triketides *vs.* late-stage oxidized intermediates, establishing the precise window in which nrPKS cyclization can proceed.

Together, these structural and mechanistic data illustrate that nrPKS condensation is not a passive cycle but rather a geometrically constrained, domain-position-dependent system in which: (i) SAT selects the correct starter, (ii) MAT supplies uniform extender units, and (iii) KS encodes the iteration number through conformational bias, ACP trajectory, and domain stoichiometry.[92] These rules place the condensation cassette (SAT–KS–MAT) at the center of nrPKS programming, providing the biochemical framework for the PT-controlled cyclization logic described in the following sections.

Beyond the SAT–KS–MAT condensation cassette, many nrPKSs also harbour an internal cMT domain that introduces α-methyl groups into ACP-bound β-keto intermediates, adding a second layer of programming on top of chain length control (Fig. 6).[93] Mechanistic dissection of the citrinin nrPKS PksCT showed that its cMT methylates the growing polyketide only at a defined chain length and oxidation state, and that this modification is strictly required for formation of the trimethylated pentaketide precursor, establishing cMT as a timing-sensitive checkpoint rather than a constitutive decorator.[94] The SAH-bound crystal structure of the isolated PksCT cMT domain further revealed a two-subdomain Class-I SAM-dependent fold in which a C-terminal SAH-binding core and an N-terminal helical subdomain together form a narrow hydrophobic tunnel that accommodates the elongated polyketide chain and positions it for catalysis, with a His/Glu pair acting as the catalytic base–acid dyad.[94] Recent domain-focused

 

genome-mining and phylogenetic analyses of fungal nrPKSs have shown that cMT-containing enzymes cluster into distinct clades whose active-site motifs and predicted substrate tunnels correlate with specific product families and methylation patterns, indicating that α-methylation is encoded as a clade-specific programming feature rather than an optional add-on.[95] Together with the SAT–KS–MAT rules discussed above, these data place cMT at a strategic position between condensation and cyclization: by selectively modifying particular intermediates, it biases which chain conformations and substitution patterns are presented to the downstream PT domain, thereby pre-shaping the set of aromatic cyclization trajectories that nrPKSs can access.

Downstream of the condensation and cMT checkpoints, the PT domain provides the key layer of programming that converts a linear, unreduced poly-β-keto chain into a defined aromatic scaffold.[96] PT domains are unique to nrPKSs and adopt a conserved double hot-dog (DHD) fold, as first revealed by the crystal structure of the dissected PT monodomain from the aflatoxin NR-PKS PksA, which showed a dimeric DHD architecture with a deep hydrophobic pocket that can bind both linear and bicyclic polyketide mimics (Fig. 7C).[96,97] This pocket is functionally partitioned into a hexanoyl/"starter" binding region, an amphiphilic cyclization chamber that pre-folds the nascent chain for intramolecular aldol condensation, and a PPT-binding groove that positions the ACP-tethered substrate—features that are fully consistent with PksA PT and have since been corroborated by subsequent structural and modeling work.[92,96,98] On this structural foundation, large-scale sequence–structure analyses of >600 fungal nrPKS PT domains demonstrated that PTs can be grouped into five major clades whose active-site geometries correlate with distinct first- and second-ring cyclization modes: groups I–III catalyze C2–C7 first-ring closures on tetraketide, hexaketide or longer chains (*e.g.*, clade I: orsellinic acid from *A. nidulans* AN7909; clade II: 1,3,6,8-tetrahydroxynaphthalene (THN) from *Colletotrichum lagenarium* Pks1; clade III: bikaverin from *Fusarium fujikuroi* Pks4);[99] group IV catalysis C4–C9 followed by C2–C11 cyclization (*e.g.*, *nor*-toralactone from *Cerospora nicotianae* CTB1);[100] and group V favors C6–C11/C4–C13 patterns (*e.g.*, atrochrysone carboxylic acid from *A. terreus* ACAS) (Fig. 6).[98,101] These studies, together with earlier mapping of common C2–C7, C4–C9 and C6–C11 cyclization modes in fungal polyketides, firmly establish PT domains as regioselective aldol cyclases whose clade membership and cavity architecture largely dictate core ring topology and substitution pattern.[102]

Beyond these canonical patterns, individual PT domains can display strikingly specialized behavior that further illustrates how subtle changes in the cavity-lining residues (CLRs) remodel cyclization programming.[96] The phenalenone nrPKS PhnA, for example, produces an angular naphtho-γ-pyrone core in cooperation with a flavin monooxygenase, and its PT domain was shown biochemically and structurally to catalyze only a single C4–C9 aldol condensation, without the usual accompanying C2–C11 closure observed for PksA and CTB1—an unprecedented selectivity that was traced to differences in the size and shape of the PT cyclization chamber.[103,104] Comparative modeling and recent 2025 analyses of nrPKS diversity further revealed that PT cavity volume varies systematically across clades (for example, intermediate ∼750 Å$^3$ pockets in WA/PksP/Bik1-type enzymes *versus* larger ∼1400 Å$^3$ pockets in PksCT/Sor2/AfoE-type enzymes), and that these volumetric and electrostatic features correlate with both elongation cycle number and preferred cyclization regiochemistry.[92,105] Importantly, mutational studies and rational domain swaps between PT domains—from, for instance, asperthecin ApdA into the bikaverin PKS—have successfully redirected ring-closure patterns and yielded new anthraquinone-type scaffolds, demonstrating that PTs are not only diagnostic of product class but can also be treated as portable, engineerable cyclization modules in combinatorial biosynthesis efforts.[35,96,101] Taken together, these structural, phylogenetic and engineering data refine and extend PT section: they support the view that PT domains act as substrate tunnels that prefold specific chain lengths and α-substitution states (set upstream by KS and cMT) into defined conformers, enforcing clade-specific first- and second-ring cyclization rules that can now be predicted from sequence and increasingly reprogrammed by targeted design.

Downstream of PT-catalyzed cyclisation, fungal nrPKSs employ a suite of PREs—canonical TEs and TE/CLC domains, R domains and MβL-TEs—to both terminate synthesis and edit off-programme intermediates (Fig. 6).[106,107] Crystal and mechanistic studies on the aflatoxin nrPKS PksA first established the TE/CLC domain as a Claisen/Dieckmann cyclase that sits at the end of a hydrophobic substrate chamber, where lid-loop motions gate access of the ACP-tethered polyketide and enforce C–C bond formation over simple hydrolysis; mutations that perturb the catalytic Ser–His–Asp triad or distort the chamber switch the balance toward hydrolysis and abortive release, underscoring how TE cavity shape and dynamics help define macrolactone size and substitution (Fig. 7D).[108–110] TEs can also perform more complex chemistry, and this has been substantiated by work on the THN, a key intermediate of melanin, nrPKS Pks1 whose C-terminal TE/CLC is a true bifunctional Claisen cyclase–deacetylase: *in vitro* reconstitution showed that a single α/β-hydrolase fold catalyzes both cyclization of a monocyclic hexaketide and subsequent deacetylation in one continuous reaction sequence, with lid-loop swaps between related TE/CLCs demonstrating how subtle structural changes redistribute activity between cyclisation and hydrolysis.[111] More recently, studies on depside-forming nrPKSs have expanded this picture: the lecanoric-acid synthase Preu6 from *Preussia isomera* uses a TE that must physically collaborate with the SAT domain to forge the didepside bond, and engineered SAT–TE fusion proteins were shown to efficiently reprogramme the same nrPKS chassis toward alternative didepsides.[112,113] Likewise, the aquastatin nrPKS AquA employs a TE that catalyzes both depside formation and hydrolysis, with phylogenetic analysis revealing distinct TE clades depending on whether the depside bond is made by TE or by SAT—again linking active-site residues and cavity architecture to specific release chemistries.[48,114,115]

Beyond classical α/β-hydrolase TEs, nrPKS systems also recruit R domains and MβL-TEs to diversify product off-loading and to

maintain programming fidelity.[116] R domains embedded at the C-terminus of some cMT-containing nrPKSs catalyze NAD(P)H-dependent reductions of enzyme-bound thioesters to aldehydes or alcohols, coupling redox tailoring directly to product release,[117] while MβL-TEs—first characterized in anthracenone and naphthacenedione pathways—use a dimetal center to promote tetracyclization or hydrolysis of highly reactive poly-β-keto intermediates.[118,119] Importantly, several TE and TE/CLC domains also act as proofreading/editing factors rather than simple terminators: detailed kinetic and crosslinking experiments on PksA demonstrated that its TE/CLC can rapidly hydrolyze mis-loaded starter units (hexanoyl/acetyl-ACP) and off-programme short intermediates while sparing correctly extended malonyl-ACP species, thereby clearing stalled ACPs and enforcing processive extension to full-length product.[108,120] Together with the SAT–KS–MAT, cMT and PT layers discussed above, these product-releasing enzyme modules complete the multi-checkpoint control logic of nrPKSs: they not only dictate how and in what form aromatic scaffolds are released (macrolactone, hydrolysate, depside, reduced product), but also continuously "edit" the assembly line to suppress side-pathway chemistry, a principle that needs to be explicitly considered when re-engineering nrPKSs for designer scaffolds or when swapping TE/R/MβL-TE domains in combinatorial biosynthesis.[121,122] Taken together, these advances turn nrPKSs from enigmatic megasynthases into increasingly predictable, though still delicate, programmable platforms for exploring fungal aromatic chemical space and for building designer polyketide libraries in heterologous hosts.

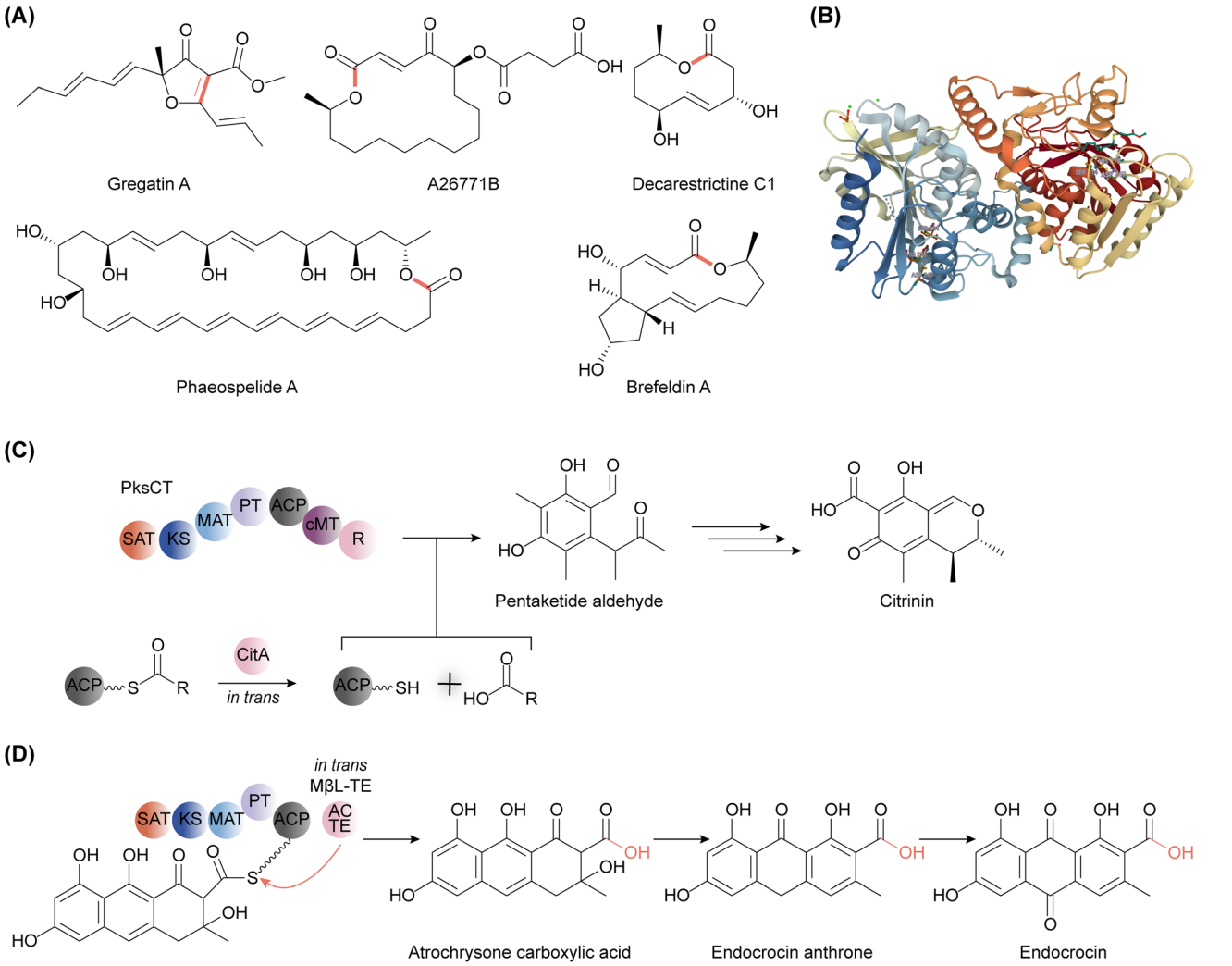


Fig. 8 *Trans*-acting hydrolases enable polyketide release or C–C bond formation. (A) Representative cases in which *trans*-acting hydrolases collaborate with hrPKSs to mediate C–C bond formation or product release, including the biosynthesis of gregatin A, A26771B, phaeospelide A, decarestrictine C1, and brefeldin A. Bonds forged or cleaved by the *trans*-acting hydrolases are shown in red. Adapted from ref. 50 and 126–129. (B) Crystal structure of DcsB, the α/β-hydrolase-folded homodimeric *trans*-TE involved in decarestrictine C1 biosynthesis (PDB: 7D79). Adapted from ref. 50. (C) Citrinin biosynthesis directed by the nrPKS PksCT, with the α/β-hydrolase CitA proofreading and hydrolyzing off-program acyl intermediates to maintain pathway fidelity. Adapted from ref. 132 and 133. (D) TE-free nrPKS ACAS collaborates with *trans*-acting MβL-TE ACTE, which hydrolyzes ACP-bound thioesters to release carboxylic acids and, in related contexts, can additionally promote Claisen-type cyclization to generate anthrone-like scaffolds. Transformations mediated by the *trans*-acting MβL-TE are indicated by red arrows and red bond highlights. Adapted from ref. 135 and 136.

### 2.5. Collaborating and *trans*-acting enzymes

In contrast to the relatively self-contained nrPKSs discussed above, many fungal iPKSs depend on discrete, *trans*-acting product-releasing and editing enzymes to complete turnover and enforce programming fidelity.[123] Large-scale analyses of chain-release mechanisms across fungal PKS and NRPS systems have shown that α/β-hydrolase thioesterases, MβL-TEs, and more unusual carnitine acyltransferase-like domains act as key "off-switches" that determine when and in what form a growing chain is released, while also excising stalled or mis-programmed intermediates.[124,125] This logic is clearly illustrated by hrPKS–TE pairs highlighted in Fig. 8A and B. In the gregatin A pathway, a single hrPKS GrgA produces two chain fragments that are fused and released by the *trans*-acting α/β-hydrolase TE GrgF, which catalyzes a Claisen condensation between two polyketide chains followed by hydrolytic off-loading to give a linear dimer that spontaneously cyclizes to the furanone core (Fig. 8A).[50,126] For the 16-membered macrolide A26771B, the hrPKS BerkA collaborates with the stand-alone TE BerkB to generate the macrolactone backbone, with recent work on the berkelylactone family and on subcellular localization in *Penicillium* confirming that BerkB acts as the dedicated chain-off-loading enzyme in a BGC that also encodes short-chain dehydrogenase (SDR), flavin-containing monooxygenase (FMO), cytochrome P450 enzyme (CYP) and acetyltransferase tailoring partners (Fig. 8A).[49,127] Alternatively, hrPKS ApmlA provides an intermediate polyketide backbone through 16-cycle carbon chain elongation and then transfers the mature levulinic acid-linked carbon chain to the serine residue of *trans*-acting independent TE ApmlB for intramolecular macrolactonization to generate 34-membered polyene macrolide compound phaeospelide A (Fig. 8A).[128] Even more strikingly, the medium-ring (10-membered) lactone core of decarestrictine C1 is forged not by the PKS itself but by the *trans*-acting TE DcsB, which was shown by Gao and co-workers to be an α/β-hydrolase dimer with broad substrate promiscuity, able to catalyze energetically disfavored medium-ring lactonizations on linear polyketides of varying length and substitution, suggesting its potential as a general lactonization biocatalyst (Fig. 8A and B).[50] Similarly, in brefeldin A biosynthesis, the hrPKS Bref-PKS generates a family of octaketide intermediates with different reduction patterns, while a dedicated *trans*-acting thiohydrolase Bref-TH selectively off-loads chains at a defined length; *in vitro* reconstitution showed that in the absence of Bref-TH, the PKS performs one extra extension–reduction cycle and produces a non-native nonaketide, demonstrating that chain length is co-programmed by the KS and by the partner TE (Fig. 8A).[22,129]

Beyond simple turnover, several *trans*-acting partners have been shown to act as proofreading hydrolases that maintain programming fidelity.[130,131] The lovastatin pathway is a textbook example: the hrPKS LovB and *trans*-ER LovC construct dihydromonacolin L, but the intermediate is only efficiently released when the cryptic serine hydrolase LovG is present. Xu and co-workers demonstrated that LovG hydrolyses incompletely processed β-ketothioesters which accumulate on LovB, thereby clearing stalled intermediates and enabling productive release of correctly programmed dihydromonacolin L acid.[31,130] An analogous *trans*-editing logic operates in the citrinin nrPKS system PksCT (Fig. 8C): the neighboring α/β-hydrolase CitA was shown to hydrolyze ACP-bound acyl intermediates in *trans*, specifically removing off-programme acetyl and short-chain species while sparing properly extended malonyl-ACP, thus preventing premature decarboxylation and stalling of chain extension.[132,133] Together, LovG and CitA exemplify a broader theme emerging from recent biochemical work: many accessory hydrolases in fungal BGCs serve as quality-control nodes rather than classical "tailoring" enzymes, and engineering efforts that ignore these nodes often suffer from low titers and shunt products.

Fungal systems have also revealed non-canonical release strategies encoded within hrPKSs themselves, again emphasizing how collaborating domains shape product diversity. A distinct clade of hrPKSs, typified by Tv6-931 from *Trichoderma virens*, carries a C-terminal carnitine *O*-acyltransferase (cAT) domain instead of a TE; Hang and co-workers showed that this cAT can reversibly transfer the polyketide chain from ACP to external polyol nucleophiles, generating polyol esters and allowing product release and recapture *in vitro*,[70] while later work and genome-mining studies have highlighted Tv6-931-like systems as versatile nodes for derivatization and glycosylated polyketide formation.[134] Complementing this, Tang and colleagues recently characterized two hrPKSs with fused C-terminal TE domains that catalyze ATP-independent amino-acylation and thiolation of polyketide chains: their TEs select cysteine or homocysteine side chains and perform reverse thioesterification or direct amidation to release aminoacylated products, revealing a new domain architecture for fungal hrPKSs and suggesting that TE fusions can be harnessed as plug-in biocatalysts to diversify polyketide termini.[123] At the other end of the spectrum, several nrPKSs lack any C-terminal TE or R domain and instead rely on physically discrete MβL-TE such as ACTE in the atrochrysone/anthracenone pathways (Fig. 8D);[135] nrPKS ACAS first synthesizes atrochrysone carboxylic acid on its ACP, and ACTE hydrolyses the ACP–thioester to release the carboxylic acid and, in related systems, can even catalyze Claisen-like cyclization.[135,136] The TAN-1612 pathway provides yet another variation: the nrPKS AdaA, which lacks a terminal off-loading domain, cooperates with a *trans*-acting MβL-TE (AdaB) and a FMO (AdaC) to achieve controlled ring closure and hydroxylation;[118] recent study in engineered yeast has shown that perturbing AdaB/AdaC leads to hydrolytic shunts and altered ring fusion patterns, underscoring how release and tailoring enzymes act together as a coupled termination module.[137] Collectively, the examples in Fig. 8A–E support a unifying view: iPKSs are rarely "alone"—their chain length, oxidation state, macrocyclization mode and even the decision between productive turnover and editing are dictated by a surrounding network of *trans*-acting TEs, hydrolases, cAT and MβL-TE domains, which together constitute an additional programmable layer that must be considered when designing or refactoring fungal polyketide pathways.

Beyond standalone PKSs and their *trans*-acting release/editing enzymes, a growing number of fungal pathways rely

on collaboration between two or more iterative megasynthases, which together build, hand over, and remodel polyketide backbones (Fig. 9A–C).[138,139] A classic paradigm is the aflatoxin pathway in *Aspergillus* sp., where the yFAS HexA/HexB produces hexanoyl-CoA that is transferred *via* a dedicated SAT to the nrPKS PksA; this programmed hand-off enables construction of the norsolorinic acid anthrone scaffold and illustrates how a primary-metabolism FAS can function as an upstream "PKS module" for a fungal nrPKS (Fig. 9A).[140] An even more direct division of labor is seen in dual iPKS systems, where an upstream hrPKS generates a reduced fragment that is selectively accepted by a downstream nrPKS SAT domain.[141] In the chaetoviridin/chaetomugilin azaphilone pathway of *Chaetomium globosum*, the hrPKS CazF iteratively builds two alternative triketides, but the nrPKS CazM SAT domain recognizes only the highly reduced (*S*,*E*)-4-methyl-hex-2-enoyl triketide and ignores the more oxidized variant, thereby enforcing branch-specific channeling toward the benzaldehyde core of the azaphilones (Fig. 9B).[88,142] Analogous hrPKS–nrPKS "quasi-modular" pairs underlie the biosynthesis of resorcylic acid lactone-type benzenediol lactones (BDLs) such as monocillin II,[28,143] and recent work in *S. cerevisiae* has shown that simply rebalancing the expression levels of the two collaborating PKS subunits by plasmid copy-number engineering can improve BDL titers by up to 10-fold and unlock otherwise silent genome-mined pathways.[44] Related hrPKS–nrPKS ensembles have been uncovered in other fungal scaffolds, including zearalenone and radicicol, where domain-resolved studies highlight the central role of the receiving SAT and PT domains in dictating which upstream intermediates are accepted and how they are cyclized.[92,144,145]

Cooperative architectures are not limited to hrPKS–nrPKS pairs. In the terrein pathway of *A. terreus*, the nrPKS TerA only reaches full catalytic efficiency when co-expressed with the PKS-like partner TerB, whose reductive and scaffolding functions tune chain processing and facilitate turnover of a key 6-hydroxymellein-type intermediate.[146,147] Even more elaborate polyketide–polyketide hybrids arise when two independent clusters cross-talk. The immunosuppressants dalmanol A and acetodalmanol A in *Daldinia eschscholzii* emerge from the coupling of a prPKS/*trans*-KR module (ChrA/ChrB) that builds a chromane-type pentaketide with an nrPKS (PksTL) that supplies a naphthalene fragment; a promiscuous monooxygenase then triggers oxidative coupling between the two polyketide halves, and co-expression of pksTL, chrA and chrB in *A. oryzae* or even co-culture of strains expressing each cluster separately is sufficient to reconstitute these hybrids (Fig. 9C).[148] Together with recent synthetic-biology studies that systematically shuffle hrPKS–nrPKS pairs or mix-and-match collaborating BDL synthases in yeast to generate panels of new scaffolds,[44] these systems illustrate a general principle: iterative PKSs can behave as semi-modular units whose productive cooperation depends on finely tuned domain recognition and matched expression levels, offering powerful yet non-trivial levers for pathway engineering.

Beyond cooperative assemblies of multiple standalone PKSs, evolution of C-terminal fusions between hrPKS and NRPS modules gives rise to hybrid PKS–NRPS megasynthases, in which an iterative hrPKS installs a tailored polyketide chain that is immediately channelled into a non-iterative NRPS module for aminoacylation, Dieckmann-type cyclization and product release (Fig. 9D).[149] A prototypical example is the HIV-1 integrase inhibitor equisetin, whose biosynthesis in *Fusarium* sp. is directed by the hybrid enzyme EquiS: an N-terminal hrPKS iteratively assembles a reduced octaketide, which is transferred to a C-terminal NRPS module (condensation–adenylation–thiolation/peptidyl carrier protein(PCP)–reductase domain, C–A–T–R) that selects a specific amino acid, performs amide bond formation, and catalyzes reductive Dieckmann cyclization to generate the tetramic acid core (Fig. 9D).[150,151] Genome-wide mapping further shows that equisetin-type PKS–NRPS loci are widely distributed across *Fusarium* and *Alternaria* sections, underscoring that such hrPKS–NRPS dual modules represent a broadly used solution for coupling polyketide and peptide logic.[152,153]

A second, mechanistically distinct adaptation is represented by truncated PKS–NRPS (PKS-C) hybrids, in which the PKS is fused only to a single C-terminal C domain. In *Talaromyces wortmanii*, the cryptic PKS-C enzyme TwmB was shown to iteratively build long-chain reduced polyketides and then use its solitary C domain to amide-couple these chains to the ω-amino acid 5-aminopentanoic acid (5PA), yielding a family of long-chain *N*-acyl amides (wortmanamides) that resemble lipid signalling molecules.[154] Structural and mutational analysis indicate that the noncanonical C domain behaves as a bona fide condensation catalyst with strict specificity for 5PA, effectively acting as a built-in "release and tailoring" module that replaces the usual TE/R-mediated off-loading.[154] Recent work has expanded this concept of noncanonical PKS–NRPS hybrids: Ji and co-workers identified a PKS–NRPS megasynthase that participates in the biosynthesis of the sterol-C4-methyl oxidase inhibitor PF1163A, showing that atypical domain architectures and release chemistries can be harnessed to generate pharmacologically relevant scaffolds.[74] In parallel, genome-mining and pathway reconstruction studies have uncovered additional fungal PKS–NRPS hybrids that assemble phytotoxic *N*-acyl amino acids and other hybrid metabolites, highlighting how subtle changes in C-terminal domain composition (C *vs.* C–R *vs.* C–TE) and docking interfaces rewire the fate of hrPKS-derived chains.[155–158]

In even more complex cases, iPKSs collaborate with NRPS and PKS–NRPS assemblies and even with entire partner clusters, creating higher-order biosynthetic networks that underpin many architecturally elaborate fungal metabolites (Fig. 9C).[159] A striking example is the azaphilone system in *A. terreus*, where Huang and co-workers showed that four core enzymes—two nrPKSs, one hrPKS and one NRPS-like enzyme—residing in two physically separate BGCs cooperate to build a family of azaphilones bearing four fused six-membered rings; transcriptional and deletion analyses demonstrated that the two clusters are connected by transcription factor-mediated crosstalk, and that removal of any one of the four core synthases abolishes azaphilone production.[160] Similar dual-cluster azaphilone systems are being uncovered in *A. niger* and related genera,

 

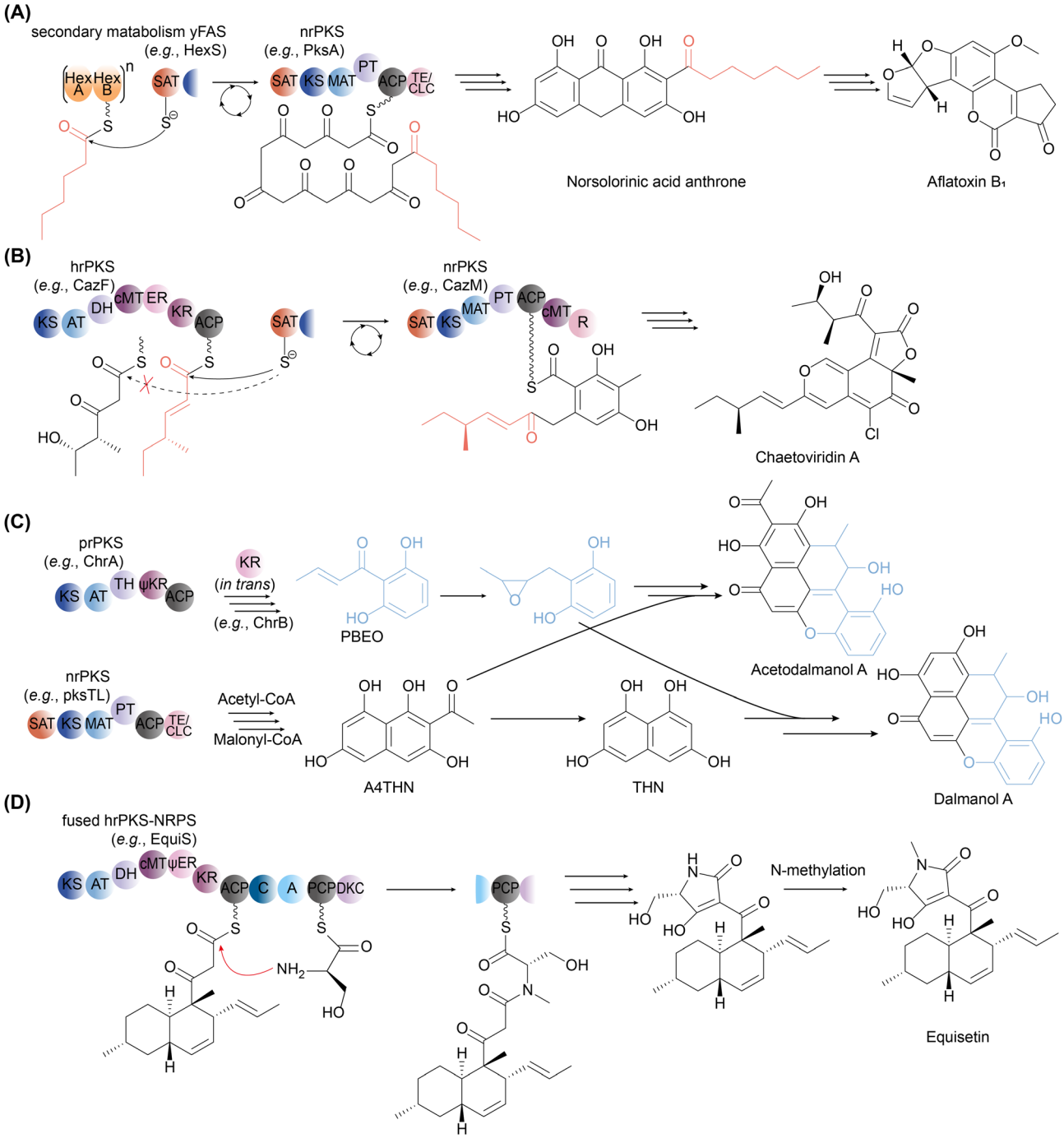


Fig. 9 Assembly-line strategies involving collaborating iPKSs. (A) In aflatoxin biosynthesis, a secondary-metabolic yFAS (yeast FAS) system (HexA/HexB) synthesizes a fatty-acid-derived chain that is transferred onto nrPKS PksA, where polyketide extension and cyclization occur; the red carbon chain indicates the portion originating from yFAS. Adapted from ref. 140. (B) Chaetoviridin A formation requires the cooperation of hrPKS CazF and nrPKS CazM: the red X marks oxidized hrPKS-derived intermediates that are not accepted by the CazM SAT domain, whereas the red polyketide chain denotes the (*S*,*E*)-4-methyl-hex-2-enoyl triketide starter unit selectively recognized by CazM. Adapted from ref. 142. (C) Dalmanol A and acetodalmanol A arise from coupling between a prPKS/*trans*-KR module (ChrA/ChrB), which produces a chromane-type pentaketide, and the nrPKS PksTL, which furnishes a naphthalene-derived fragment; a downstream monooxygenase initiates oxidative coupling between the two halves. A4THN, 2-acetyl-1,3,6,8-tetrahydroxynaphthalene. The blue substructure represents the ChrA/ChrB-derived fragment. Adapted from ref. 148. (D) A prototypical fusion-megasynthase example is equisetin, assembled by the hybrid enzyme EquiS: an N-terminal hrPKS iteratively constructs a reduced octaketide on ACP, which is then transferred to the C-terminal NRPS module (Domain abbreviations: C, condensation; A, adenylation; PCP, peptidyl-carrier protein; DKC, Diekmann cyclase) for amino-acid selection, amide bond formation, and Dieckmann-type cyclization to generate the tetramic-acid core. Red arrows trace the transfer of the fully reduced octaketide intermediate from hrPKS to the NRPS PCP domain. Adapted from ref. 150 and 151.

reinforcing the idea that inter-cluster communication is an encoded feature of some fungal polyketide networks rather than a rare curiosity.[161,162]

Conversely, hrPKSs can function as *trans* partners to PKS–NRPS assembly lines, providing tailor-made amino-acid-like building blocks that are then incorporated and rearranged by the hybrid enzyme.[163] The oxaleimide pathway in *Penicillium* species defines a prototypical model: Sato and co-workers showed that a standalone hrPKS synthesizes an olefin-containing non-proteinogenic amino acid, which is released and then activated by the A domain of a PKS–NRPS; after amide bond formation, intramolecular cyclisation and oxidative tailoring yield maleimide- and succinimide-containing natural products, illustrating a bidirectional communication in which the PKS–NRPS both receives and remodels hrPKS products.[163] More recent work on NRPS–PKS hybrids, such as the naringenin synthetase FnsA from *Pestalotiopsis fici*, further broadens this picture: here, an NRPS-like module activates and loads tyrosine, and a downstream PKS module extends and cyclizes the tethered amino acid into a flavanone scaffold, demonstrating that PKS and NRPS domains can be arranged in either orientation to create hybrid "mini-assembly lines" for polyketide–peptide scaffolds.[164,165] Across these systems, structural and biochemical studies consistently highlight the central role of docking domains and transient protein–protein interfaces between PKS and NRPS modules in mediating intermediate transfer,[166] and recent analysis have begun to correlate specific linker architectures and interface motifs with the efficiency and directionality of handover—information that is now being exploited in combinatorial engineering of fungal PKS–NRPS systems.[167,168] Together with the multi-PKS collaborations described above, these higher-order PKS–NRPS and multi-cluster networks underscore that fungal "PKS programming rules" extend beyond single megasynthases to encompass inter-enzyme, inter-module and even inter-cluster communication, providing both rich opportunities and non-trivial constraints for the design of hybrid polyketide platforms.

## 3. Combinatorial biosynthesis enabling chemical diversity

The discovery of new therapeutics still relies on navigating a vast and sparsely sampled chemical space, with individual drug candidates typically requiring more than a decade of development and median research and development investments approaching US$ 1–1.5 billion before approval.[169–171] In this context, small-molecule natural products occupy a disproportionate share of successful drugs: analyses of approvals between 1981 and 2019 indicate that roughly one quarter of all new chemical entities, and an even higher fraction of anti-infective and anticancer agents, are either natural products, semi-synthetic derivatives, or synthetic compounds bearing natural-product pharmacophores (506 of 1881 approvals).[4] Such success is rooted in the way biosynthetic pathways assemble densely functionalized, stereochemically rich scaffolds that are difficult to access by purely synthetic means. However, this very complexity also limits classical medicinal chemistry: for many fungal polyketides, multi-step derivatization or scaffold remodeling is technically challenging, low throughput, and hard to scale, so systematic structure–activity relationship (SAR) exploration remains constrained.[172,173]

At the same time, the clinical need for new molecules continues to intensify. The spread of multi-drug resistance in bacterial and fungal pathogens, reduced efficacy of long-used chemotherapeutics, and emerging indications such as immune modulation and microbiome-targeted therapies all demand scaffolds with new modes of action and tunable physicochemical properties.[174] Recent genome-mining efforts reveal that filamentous fungi encode a large number of cryptic polyketide BGCs whose products remain uncharacterized, underscoring the untapped potential of fungal secondary metabolism.[42,175] Iterative hrPKSs and nrPKSs are central to this hidden chemical space, and the mechanistic "programming rules" underlying their chain-length control, redox tailoring, and cyclization logic summarized in the previous chapter provide a rational foundation for engineering these assembly lines rather than relying on random discovery.[176] Against this backdrop, combinatorial biosynthesis has emerged as a powerful strategy to generate new-to-nature polyketides by recombining and rewiring the enzymatic components of fungal pathways instead of solely optimizing downstream chemistry.[177] In fungal systems, this encompasses three interlocking layers that we will focus on in this chapter (Fig. 10). First, precursor-directed biosynthesis modifies the supply and identity of starter and extender units feeding iPKSs, enabling programmed variation in chain length, oxidation state, and branching patterns while keeping the core megasynthase architecture intact.[178] Second, the modular logic of hrPKSs, nrPKSs, and their hybrids can be exploited through domain, linker, and subunit engineering, reshuffling PT-controlled cyclization patterns, SAT/KS interfaces, and PKS–NRPS couplings to access alternative backbone topologies and substitution patterns, as demonstrated by recent large-scale PKS recombination platforms that systematically map success rates and identify gatekeeping constraints.[33,179] Finally, combinatorial tailoring leverages the intrinsic promiscuity and engineerability of oxidases, transferases, and other peripheral enzymes to decorate both native and engineered backbones with diverse functional groups, with recent work showing that genome-guided recruitment of glycosyltransferases, P450 monooxygenases, and related enzymes can systematically expand glycosylated and oxidized natural product families.[29,180,181]

In the following sections, we therefore treat combinatorial biosynthesis as an extension of the programming logic discussed above into a design framework for fungal cell factories. Rather than merely cataloguing case studies, we organize the field by strategy—precursor-directed biosynthesis, domain and linker engineering of PKSs, subunit shuffling in polyketides and related systems, tailoring enzymes on non-native scaffolds, and enzyme engineering including directed evolution and machine-learning-guided design—and emphasize how each approach reshapes the accessible polyketide chemical space in practice

 

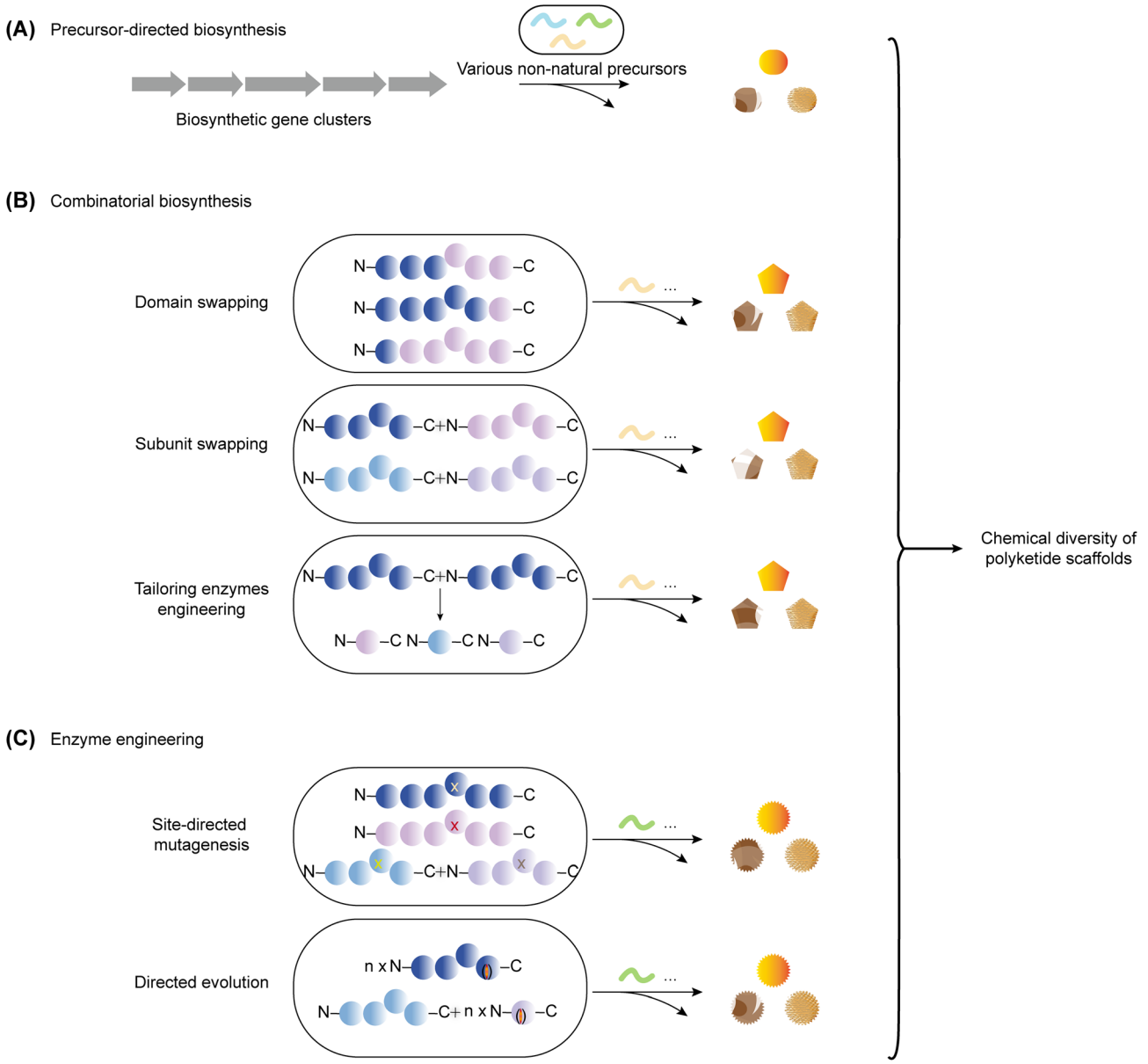


Fig. 10 Strategies for generating structurally diversified non-natural polyketide analogues. (A) Precursor-directed biosynthesis, in which engineered PKSs or associated enzymes are supplied with tailored starter or extender units (*e.g.*, modified acyl-CoAs or malonyl-CoA analogues) to expand chemical space beyond native substrates. This strategy enables incorporation of non-natural building blocks while maintaining the programmed chain-extension logic of the native megasynthase. (B) Combinatorial biosynthesis, encompassing domain swapping, subunit swapping, and post-PKS tailoring–enzyme recombination, allows the construction of hybrid assembly lines with altered reduction patterns, modified cyclization trajectories, or newly installed oxidative decorations. This includes exchanging KS–AT–DH–cMT–ER–KR–ACP modules among homologous iPKSs, merging hrPKS/prPKS/nrPKS partners, or mixing PT/TE selectivity rules to reshape backbone scaffolds and ring topologies. (C) Enzyme engineering, including structure-guided site-directed mutagenesis, interface reprogramming, and directed evolution, tunes substrate specificity, redox selectivity, and chain-length control. These methods enable rational rewiring of active sites or protein–protein interaction surfaces to create PKS variants capable of generating non-natural scaffolds with improved catalytic efficiency or novel pharmacophore features.

(Fig. 10). Where possible, we highlight not only successful examples but also quantitative lessons from large libraries and partially successful or failed constructs, which collectively begin to reveal general design rules and bottlenecks for programming fungal polyketide diversity in a predictable, cell-factory-compatible manner.

### 3.1. Precursor-directed biosynthesis

Precursor-directed biosynthesis diversifies fungal polyketides at the level of building blocks by exploiting the intrinsic substrate plasticity of biosynthetic enzymes. Instead of re-engineering the megasynthase architecture, native or heterologously expressed pathways are supplied with non-native starter or extender

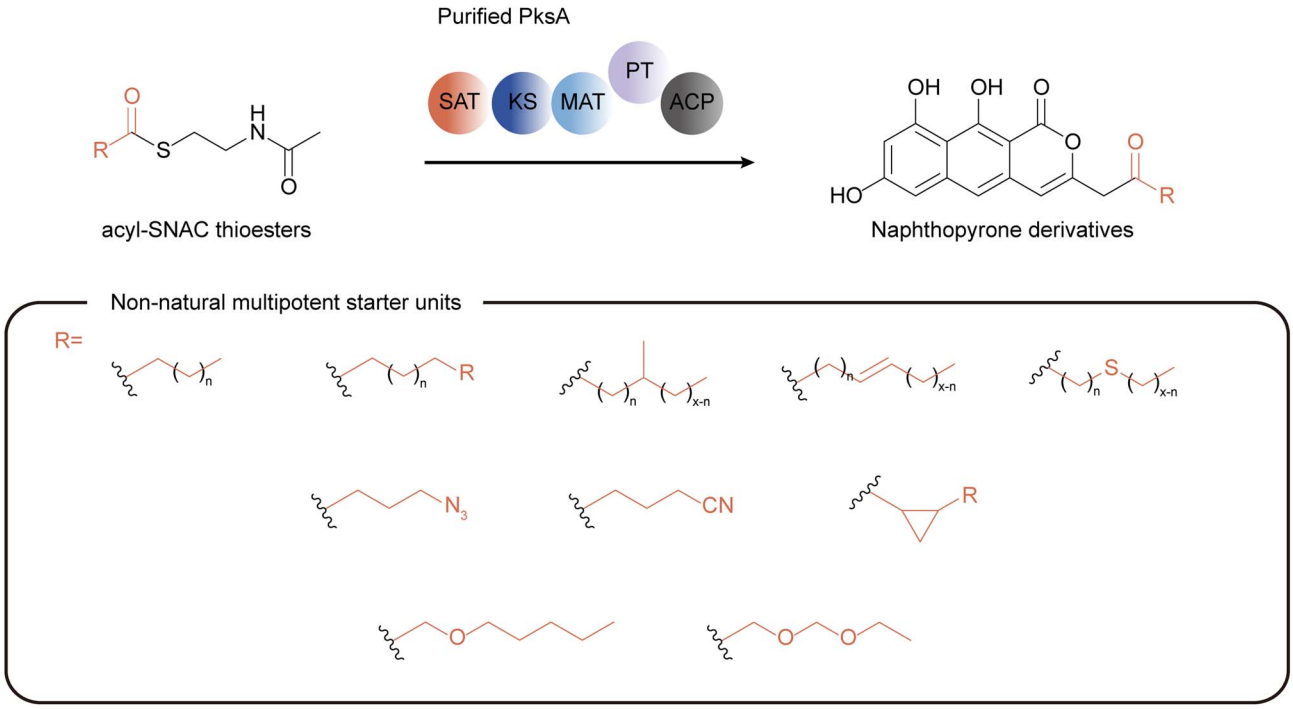


Fig. 11 Starter-unit flexibility of the TE-free nrPKS PksA revealed by precursor-directed biosynthetic assays. Purified PksA was supplied with a focused panel of non-native acyl-SNAC starter units, demonstrating that its SAT domain can accommodate substrates with diverse chain lengths and distal substituents while still directing assembly toward naphthopyrone scaffolds. Most alternative acyl-SNAC thioesters were efficiently elongated, folded, and cyclized according to the native PksA programming logic, producing on-target naphthopyrone analogues with only minor shifts in derailment product profiles. Adapted from ref. 185.

analogues (typically as CoA or *N*-acetylcysteamine (SNAC) thioesters), or with multipotent advanced intermediates, so that the iPKS machinery channels them into "pseudo-natural" scaffolds (Fig. 10A).[182] In fungal systems this strategy is particularly attractive because many hrPKSs and nrPKSs already tolerate variation in chain length, oxidation state and β-substituents; precursor engineering therefore reads out directly as new ring systems, substitution patterns and handles for downstream diversification, without the need to rewire domain–domain interfaces.

A seminal fungal example is the *C. indicum* nrPKS pksCH-2, whose heterologous expression in *A. oryzae* first revealed a chaetophenol scaffold and then a multipotent isochromene intermediate that can branch into multiple product families. Epigenetic activation and heterologous expression of pksCH-2 in *A. oryzae* enabled access to chaetophenol A and related metabolites, establishing this nrPKS as the core enzyme of the pathway.[183,184] Building on this, Asai and co-workers combined heterologous production of the isochromene intermediate with a semi-synthetic diversification campaign, using its intrinsic ortho-quinone methide reactivity to generate a large panel of pseudo-natural polyketides, including oligomeric naphthopyrones, azaphilone-type structures, isoquinoline-like compounds and indole–polyketide hybrids.[183] This chemobiosynthetic workflow—biosynthetic generation of a multipotent intermediate followed by non-enzymatic remodeling—illustrates how precursor-directed strategies can translate the promiscuity of fungal nrPKSs into densely populated local regions of chemical space while keeping the underlying gene cluster architecture unchanged.

Studies on aflatoxin biosynthesis further underscore how iPKS programming can be leveraged at the starter-unit level. The aflatoxin $B_1$ nrPKS PksA normally receives a specific hexanoyl starter from the upstream FAS, but *in vitro* assays with purified PksA and a focused panel of acyl-SNAC thioesters showed that the SAT domain can accept a surprisingly broad set of starter units with altered chain length and distal substituents while still delivering on-target naphthopyrone products (Fig. 11).[185] Most tested acyl-SNACs were elongated and cyclized according to the native programming rules, with only modest changes in derailment products, revealing that gatekeeping occurs mainly at the level of global geometry rather than fine chemical detail.[185] Related work on collaborating hrPKS–nrPKS systems, such as the Hpm8/Hpm3 pair from hypothemycin biosynthesis, demonstrated that hrPKSs can also accept β-ketoacyl-SNAC intermediates and process them through multiple extension and redox cycles, again highlighting that iterative PKSs can be treated as chemoenzymatic reactors for pre-formed intermediates rather than only *de novo* acyl-CoA starters.[186] Together with earlier chain-length control studies on dual iPKS systems that fed tailored acyl-SNAC mimics to partner reductases, these experiments begin to quantitatively map which positions along the starter unit and growing chain are tolerant to modification, and which are tightly constrained by the catalytic cavities of SAT, KS and downstream tailoring domains.[22]

More recent work has extended these principles towards scalable discovery and functionalization. In yeast systems, increasing the copy number of engineered polyketide BGCs has been used to boost titers and to facilitate detection of low-abundance "unnatural" analogues arising from intrinsic precursor promiscuity, illustrating how pathway-level engineering alone can amplify the readout of these effects even without external precursor feeding.[44] Beyond fungi, chemobiosynthetic campaigns on complex bacterial polyketides such as FK506 have used domain-specific knowledge of extender-unit selection to introduce clickable propargyl groups *via* precursor-directed routes, affording high-titer FK506 analogues that are directly compatible with bioorthogonal chemistry.[178] Likewise, precursor-directed access to odd-chain polyunsaturated fatty acids and other polyketide-like lipids is emerging as a way to generate standards and probe biological function.[187] Similar strategies that expand malonyl- or methylmalonyl-CoA supply, or introduce synthetic routes to non-native acyl-CoAs, have been shown to increase titers and diversify products in engineered polyketide pathways, underscoring that "endogenous" precursor perturbation and chemobiosynthetic feeding represent two complementary modes of precursor-directed biosynthesis rather than distinct categories.[188] These examples reinforce a general design logic: once the tolerance window of each iPKS domain to starter or extender analogues is quantitatively defined, precursor pools can be rationally perturbed to install handles (for example alkynes, halogens or photo-crosslinkers) and to probe structure–activity relationships without reconfiguring the underlying assembly line. In the context of fungal polyketides, precursor-directed biosynthesis therefore represents a conceptually simple yet powerful first layer of combinatorial design that complements the domain, subunit and tailoring strategies discussed in the following sections.

### 3.2. Combinatorial biosynthesis

**3.2.1. Domain swapping.** At the level of the megasynthase architecture, domain swapping in iPKSs aims to rewire programming by splitting the enzyme into structurally coherent fragments and recombining them with non-cognate partners, often in combination with rational linker design (Fig. 10B).[189] In fungal nrPKSs, a common strategy is to fix a single N-terminal loading/elongation cassette (typically SAT–KS–MAT) that defines the chain-extension regime, and then systematically pair it with alternative PT, ACP and TE domains to read out how each downstream module shapes cyclization and product release.[190] Early combinatorial experiments with the cercosporin synthase CTB1 and the atrochrysone synthase ACAS exemplified this logic: CTB1 SAT–KS–MAT was treated as a generic $C_{14}$ chain-builder and fused *in vitro* with heterologous PT/ACP/TE cassettes, revealing that ACAS PT could redirect the same $C_{14}$ intermediate into a pannorin-type α-pyrone scaffold, while other PT/TE combinations yielded alternative shunt products or stalled intermediates.[106,191,192] These chimeric assemblies showed that, once a SAT–KS–MAT block is chosen, domain swaps downstream predominantly reprogram first-ring topology and release chemistry rather than chain length, and that viable non-natural scaffolds only emerge when PT and TE can both accommodate the geometry of the same growing intermediate.[91] Subsequent work has extended this modular view to intact fungal nrPKSs expressed *in vivo*. In *A. nidulans*, swapping the C-terminal domains of the *A. niger* DtbA PKS with phylogenetically related PT/TE cassettes produced distinct benzaldehyde *versus* carboxylate-terminated products, again highlighting that altered domain combinations can uncover cryptic release modes and access non-native aromatic frameworks without changing the core SAT–KS–MAT engine.[193] Collectively, these fungal studies define the "classical" domain swapping paradigm: maintain one iterative condensing region to preserve the basic chain-building logic, while permuting cyclization and release domains to diversify polyketide ring systems. At the same time, their variable success rates also exposed a recurring bottleneck that will recur throughout this chapter—namely, that the precise placement of domain boundaries and linkers is as critical as the choice of domains themselves (Fig. 12).

Recent advances in modular PKS engineering provide a complementary, technology-driven perspective that is directly relevant for refining domain and linker design in iterative systems. Biosensor-guided screens of hundreds of AT-swapped type I PKS chimeras with randomized junctions showed that only a small fraction of naive boundary choices preserve both solubility and wild-type production levels, and that "good" boundaries cluster near structurally conserved helices and loop regions.[189] Likewise, AlphaFold-assisted design of chimeric modular PKSs, combined with systematic testing of docking geometries, demonstrated that computationally selected junctions can yield active synthases that integrate seamlessly into engineered pathways and produce diverse non-natural polyketides.[139] These studies underlying design principles—choosing boundaries that respect local secondary structure, preserving key inter-domain contacts, and using high-throughput readouts to refine linker placement—are directly transferable (Fig. 12).

Although conceptual and technical advances from modular PKS engineering provide valuable guidance, important mechanistic differences distinguish bacterial modular systems from fungal iPKSs. In modular PKSs, each module is typically used once per elongation cycle, and domain boundaries often correspond to naturally separable units. In contrast, fungal iPKSs reuse the same catalytic domains across multiple iterations, and ACP must repeatedly shuttle among competing catalytic sites within a confined megasynthase architecture.[16,17] As a result, swapping a single cassette in an iterative system can propagate ripple effects across multiple rounds of extension, altering reduction timing, cyclization trajectory, and release logic in ways not typically observed in modular assembly lines. Thus, while boundary conservation, docking-face compatibility, and structural modeling are broadly transferable principles, the iterative reuse of domains and dynamic ACP routing impose additional layers of constraint unique to fungal iPKSs. Appreciating these distinctions is essential to avoid overgeneralizing modular assumptions to iterative systems. Together with

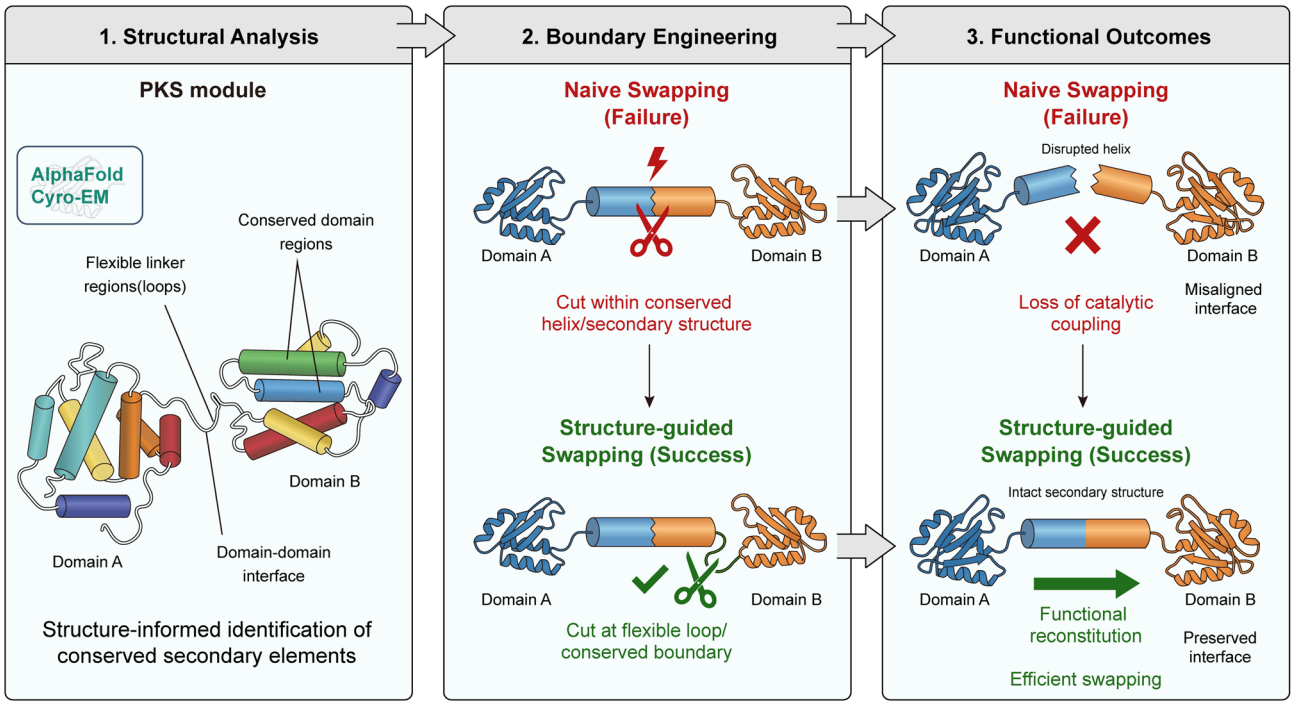


Fig. 12 Structural basis of naive *versus* structure-guided domain swapping in fungal iPKS. (1) Structural analysis. Experimentally determined or predicted PKS structures obtained by cryo-electron microscopy (cryo-EM) or AlphaFold are used to define domain organization, linker regions, and inter-domain interfaces. (2) Boundary engineering. In naive domain swapping, exchange boundaries between the N-terminal domain (domain A, blue) from one PKS and the C-terminal domain (domain B, orange) from another PKS are selected based on approximate sequence annotations, often cutting through critical linker or interface regions, leading to disrupted domain alignment. In contrast, structure-guided swapping defines boundaries using structural models or interface predictions, preserving essential linker segments and inter-domain interactions. (3) Functional outcomes. Naive swapping typically produces misassembled or poorly active chimeric PKSs due to loss of structural coupling, whereas structure-guided swapping maintains architectural integrity and enables functional recombinant enzymes capable of productive polyketide biosynthesis. Adapted from ref. 139 and 189.

emerging structural dissection of fungal condensing regions that pinpoints how SAT–KS interfaces select acyl groups and control initiation,[23] these advances set the stage for the following sections, where we discuss how domain and linker engineering of SAT–KS–MAT, KR, PT and TE can systematically reshape chain length, cyclization patterns and release modes in iterative fungal PKSs.[194]

Domain and linker engineering experiments on starter-unit selection have clarified how much of chain length control is "hard-wired" into the KS domain *versus* upstream SAT choice. In the asperfuranone pathway of *A. nidulans*, the nrPKS AfoE was first established as the backbone synthase for a $C_{14}$ aromatic scaffold.[195] Building on this, Liu and co-workers developed an *in vivo* swapping platform in *A. nidulans* in which the SAT domain of AfoE was replaced by SAT domains from ten other nrPKSs, including the isoquinoline-forming AN3386.[196] The AfoE–AN3386 chimera accepted a longer, AN3386-type starter unit and produced a new $C_{14}$ aromatic polyketide *in vivo*, demonstrating that SAT exchange can redirect which acyl unit is loaded onto the ACP (Fig. 13).[196] However, when larger N-terminal fragments such as SAT–KS–MAT or SAT–KS–MAT–PT were swapped, the dominant products shifted to $C_{16}$ scaffolds, revealing that the KS cavity, rather than the SAT domain, sets the upper limit of chain length that can be accommodated before cyclization (Fig. 13).[196] Together with earlier "unnatural" asperfuranone hybrids created by installing the AfoE SAT into the sterigmatocystin synthase StcA,[197] these studies support a general design rule already hinted at by CTB1/ACAS chimeras in the previous section: SAT swaps are a powerful way to alter starter identity and thereby tune substituents at one end of the backbone, but the KS active site remains the principal gatekeeper for overall chain length and cannot be bypassed simply by changing the loading domain. Recent work on other iPKSs reinforces and extends this picture. Systematic starter-unit feeding to the aflatoxin nrPKS PksA showed that a wide panel of acyl-SNAC primers could be elongated and cyclized to the same naphthopyrone framework, with derailment occurring only when starter length or branching exceeded the geometric tolerance of the KS–ACP chamber.[185] In basidiomycete nrPKSs, mutational analysis and chimeric constructs demonstrated that exchanging closely related KS domains alone can shift product chain length, even when SAT domains are deleted or held constant, again pinpointing the KS as the decisive chain-length determinant.[16,51] For collaborating hrPKS–nrPKS pairs from *Rhytidhysteron rufulum*, Wang and co-workers further showed that altering KS active-site residues and interface geometry reshapes the distribution of S-type benzenediol macrolactones, whereas changing upstream loading pathways primarily affects

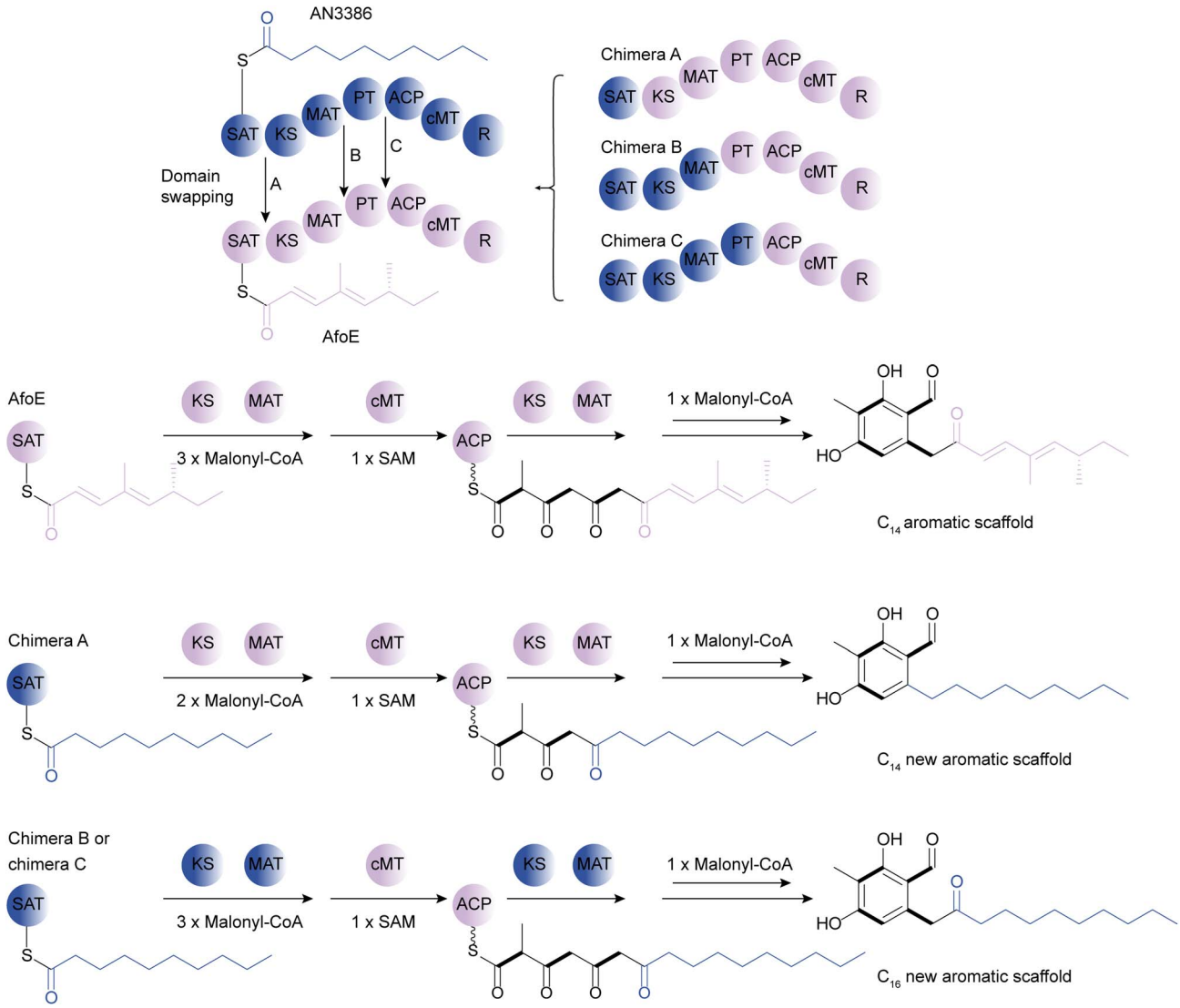


Fig. 13 Domain organization and SAT-domain swapping between the iPKSs AN3386 and AfoE. The native nrPKS AfoE synthesizes a $C_{14}$ aromatic scaffold, whereas the isoquinoline-type PKS AN3386 initiates polyketide assembly with a longer starter unit. *In vivo* domain-exchange experiments showed that replacing the AfoE SAT domain with that of AN3386 redirects the loading step, enabling incorporation of a longer AN3386-type starter unit and yielding a new $C_{14}$ aromatic polyketide. Starter units introduced by different SAT domains are highlighted in blue or pink. In contrast, swapping larger N-terminal fragments (*e.g.*, SAT–KS–MAT or SAT–KS–MAT–PT) shifted the major products to $C_{16}$ scaffolds, demonstrating that the KS active-site cavity determines the maximum elongation length that can be accommodated before cyclization. This KS-governed chain-length constraint is indicated by bold black bonds marking the accepted extender-unit span. Adapted from ref. 196.

flux into the system rather than the intrinsic chain-length preference of the nrPKS.[198] Complementary structural and evolution-guided studies in modular bacterial PKSs,[33] where conserved KS-boundary motifs were identified as safe fusion points that preserve chain-length control, suggest that respecting the local architecture around KS active sites will be equally critical when designing fungal chimeras. Altogether, these results frame domain and linker engineering of SAT–KS–MAT cassettes as a way to decouple "which starter enters" from "how far the chain is extended": SAT swapping and precursor engineering provide handle-like perturbations at the initiation step, while KS-centered design defines the chain-length window within which the downstream PT, reductive domains and TE can further sculpt cyclization patterns and release modes.

Once the SAT–KS–MAT cassette has fixed the chain-length window, a second layer of programming is imposed by the KR and cMT domains, which decide at which iterations β-keto groups are reduced or methylated. Domain and motif swaps in these regions have therefore been used to rewire methylation patterns and oxidation states without altering the underlying backbone length.[23] In the tenellin–desmethylbassianin–militarinone family of hrPKS-NRPS hybrids, exchanging subfragments of the cMT, ψKR and KR domains between TENS, DMBS and MILS leads to mixtures of penta-, hexa- and hepta-ketide pyridones with altered *C*-methylation patterns, directly linking subtle changes in the reductive module to shifts in both chain length and methylation "dosing" during the programmed iterations.[58,199] Recent AlphaFold2-guided engineering of the

TENS KR domain has sharpened this picture: swapping a 15-residue "substrate-binding helix" from the hexaketide synthase DMBS into TENS, or re-installing smaller DMBS- or MILS-derived motifs, reproducibly increases the fraction of hexaketide products at the expense of the native pentaketide, whereas single-site mutations in the same region have only marginal effects.[32] Similar principles are now being explored in modular PKSs, where Keiser and co-workers systematically exchanged KR domains to probe and re-engineer stereocenter formation along bacterial assembly lines, underscoring that precise editing of gatekeeping elements—rather than indiscriminate domain swapping—is a broadly applicable route to combinatorial diversification across both iterative and modular systems.[200] These experiments reinforce two practical lessons for combinatorial biosynthesis with iPKSs: (i) methylation and reduction can indeed be reprogrammed by transplanting cMT/KR substructures from cognate systems, but (ii) productive changes usually require swapping whole motifs or domains, with boundaries chosen to preserve local secondary structure and inter-domain packing, rather than isolated point mutations.[201]

Complementary studies in stand-alone fungal hrPKSs converge on the same design logic. Using the lovastatin nonaketide synthase LovB as a model, Cacho and co-workers showed that the embedded MT domain is catalytically competent on multiple β-ketoacyl substrates but is kinetically tuned to act with highest efficiency on its native tetraketide intermediate, thereby enforcing stage-specific methylation during the iteration cycle.[56] Follow-up biochemical and structural work on the PksCT cMT domain from citrinin biosynthesis, including domain dissection and reconstitution with chimeric partners, demonstrated that inserting or removing cMT from otherwise identical nrPKSs can slow extension and introduce new methylation events, consistent with direct competition between KS and cMT for the same ACP-bound intermediates.[94] More recently, methyltransferase-focused genome mining has begun to identify PKSs with unusual cMT motifs and to validate them as sources of non-canonical methylation patterns, providing a forward-engineering route to "dial in" atypical *C*-methylation on fungal backbones.[194,202] Together with KR-helix swaps in TENS and related systems,[32] these results position reductive and methyltransferase domains as programmable "fine-tuning knobs" layered on top of KS-defined chain length: by carefully choosing domain or motif donors and respecting structurally informed junctions, combinatorial biosynthesis can systematically reshape oxidation state and *C*-methylation patterns of iterative fungal polyketides, setting the stage for the PT and TE engineering strategies.

Once chain length and oxidation state have been set by the SAT–KS–MAT and reductive modules, PT domain imposes a third layer of programming by dictating how the linear poly-β-keto chain is folded and which carbons are joined in the first aldol cyclization. In fungal nrPKSs, PT domains channel identical or closely related ACP-tethered intermediates into distinct aromatic and macrolactone scaffolds, and are therefore natural levers for combinatorial control of ring topology.[98] Recent work on basidiomycete nrPKSs, where swapping or deleting PT domains leads to wholesale shifts in cyclization outcome and accumulation of off-pathway shunt products, reinforced that PTs act as strict gatekeepers for the regioselective aldol reaction and must be co-optimized with KS and TE when building chimeras.[16] Structural and mechanistic studies have begun to resolve the basis for this gatekeeping: the dissected PksA PT adopts a double-hot-dog fold with a deep, two-part reaction chamber that enforces C4–C9 cyclization geometry,[97] while more recent crystallographic and computational analyses of a bacterial PT domain controlling C2–C7 orsellinic acid cyclization highlight how subtle rearrangements in the binding pocket and phosphopantetheine channel can switch between different aldol modes.[102,203] These insights provide a structural context for interpreting PT domain swaps in fungal combinatorial biosynthesis.

BDL macrolides illustrate how PT exchanges can be used to redirect first-ring topology and generate new scaffolds. Resorcylic acid lactone (RAL)- and dihydroxyphenylacetic acid lactone (DAL)-type BDLs differ only in how the benzenediol ring is connected to the macrolactone (C2–C7 *versus* C3–C8), yet they are produced by closely related hrPKS–nrPKS pairs whose PT domains encode distinct cyclization rules.[198] By swapping the PT domains of the monocillin II nrPKS CcRadS2 and the 10,11-dehydrocurvularin nrPKS AtCurS2, Xu and co-workers converted the native C2–C7 (RAL-type) condensation into a C3–C8 (DAL-type) cyclization and accessed the non-natural macrolactone radilarin, while otherwise preserving the upstream programming of chain length and reduction pattern.[204] Complementary "first-ring reprogramming" studies, in which a handful of active-site residues in the bikaverin and aflatoxin PT domains were mutated or transplanted, showed that altering key pocket-lining positions can flip between C2–C7, C4–C9 and C6–C11 aldol modes and output different aromatic frameworks from the same linear precursor.[204] Together with emerging PT-focused engineering in newly characterized nrPKSs that couple mutagenesis with *in vivo* chimera libraries,[35] these examples position PT domains as modular "cyclization switches": when domain and linker boundaries are chosen to preserve the KS–PT–ACP interface, swapping or subtly redesigning PTs allows combinatorial biosynthesis to systematically remap first-ring topology on a KS-defined backbone.

As the last step in the iPKS assembly line, TE or R domains impose a decisive layer of programming by dictating how the PT-shaped intermediate is released—as a macrolactone, pyrone, hydrolyzed acid or reduced aldehyde.[198] In fungal nrPKSs that make BDL macrolides, O–C bond-forming TEs from AtCurS2 and CcRadS2 catalyze macrocyclization of benzenediol–polyene intermediates to distinct ring sizes and substitution patterns, and swapping these closely related TEs alters the balance between macrocycles and pyrone shunt products, demonstrating that even subtle changes in the TE pocket reshape the accessible scaffold set.[205] Heterologous expression and domain swapping in the *A. niger* nrPKS DtbA further underscore this gatekeeping role: replacing the native R domain, which normally performs NAD(P)H-dependent reductive release to benzaldehydes, with TE domains from AusA or ANID_06448 produced new polyketides in which the

 

corresponding positions are liberated as carboxylic acids, whereas other TE choices failed to give detectable products.[206] More systematic dissection of nrPKS TEs has shown that their intrinsic programming—whether they favor macrolactonization, hydrolysis or pyrone formation—is tightly coupled to both chain length and the geometry of the first ring installed by SAT–KS–PT, such that small perturbations in intermediate shape can flip the outcome between productive macrocycles and stalled, off-pathway species.[198] Furthermore, high-resolution structures of modular polyene macrolide TEs have revealed how active-site tunnels and transient dimer interfaces choreograph macrocycle closure, and how mutating gatekeeping residues can redirect release towards alternative macrocycles or linear acids.[43] Together, these studies frame TE and R domains as context-dependent "final filters" in domain-swapped PKSs: they can unlock new release modes and functional groups, but only when their active-site geometry is compatible with the KS-defined chain length and PT-defined ring topology, a constraint that strongly shapes the success rate of combinatorial TE/R engineering.

Domain swapping at the junction between PKS and NRPS modules presents a related, and often even stricter, set of constraints. In a landmark combinatorialization of fungal PKS-NRPS hybrids, five enzymes (PsoA, CpaS, LovB, EqxS and FsdS) responsible for chemically diverse natural products were fused in 57 different module combinations, yet only six chimeras produced detectable polyketide–peptide hybrids, and four of these corresponded to known scaffolds.[207] The low productivity rate in this large-scale recombination experiment (~10%) provides one of the clearest semi-quantitative illustrations of the intrinsic constraints governing domain recombination in fungal PKS–NRPS systems. Detailed comparison between productive and non-productive constructs suggested that most failures arose not from catalytic incompetence of individual domains, but from mis-matched inter-domain interfaces at the ACP–C junction, incompatible trajectory of the tethered phosphopantetheine arm, or steric conflicts between the incoming polyketide intermediate and the NRPS condensation pocket.[207] These results underscore that interface geometry, rather than primary sequence homology alone, is a dominant determinant of chimera viability. More recent structural and biochemical work on NRPS elongation modules, including minimal C domain docking elements and extended T–C interfaces, has provided a physical basis for these observations by mapping how specific helices and loop surfaces mediate productive ACP/T-domain engagement and *trans*-thioesterification.[121,208] In parallel, engineering of PKSs with synthetic docking domains and orthogonal coiled-coil or SpyTag/SpyCatcher interfaces has illustrated that artificial connector motifs can, in principle, overcome some native incompatibilities at PKS–PKS and PKS–NRPS junctions, but only when the designed interface preserves the spatial orientation of the catalytic domains.[209]

Taken together, lessons from both successful and failed engineering attempts allow failure modes in fungal iPKS domain swapping to be categorized into several recurring classes: (i) mis-matched inter-domain interfaces that disrupt catalytic handoffs; (ii) incompatibility in ACP trajectory or phosphopantetheine reach; (iii) substrate tunnel or cavity mismatch at the KS or TE level; (iv) TE or R release chemistry misalignment with upstream cyclization geometry; and (v) expression and solubility deficiencies of large chimeric mega-synthases. Importantly, many unsuccessful constructs fail for geometric rather than catalytic reasons, emphasizing that spatial and conformational logic—rather than mere domain identity—governs iPKS programming. Recognizing and classifying these bottlenecks elevates domain swapping from empirical recombination toward structurally informed design (Fig. 12).

**3.2.2. Subunit swapping.** Beyond intra-enzyme domain swaps, collaborating hrPKS–nrPKS pairs themselves can be treated as exchangeable modules (Fig. 10B). In BDL pathways, each scaffold is assembled by a dedicated hrPKS "priming" subunit followed by a partner nrPKS "tailoring" subunit, and subunit swapping between homologous pairs has been used to diversify macrolactone architectures without changing the underlying iterative logic.[210] In a seminal study, Xu and co-workers rebuilt four BDL synthase pairs (CcRadS1–CcRadS2, AzResS1–AzResS2, LtLasS1–LtLasS2 and AtCurS1–AtCurS2) in *S. cerevisiae* and combinatorially co-expressed all 16 possible hrPKS–nrPKS combinations; 14 of these produced isolable macrolactone products, many of which were non-cognate frameworks not observed in nature (Fig. 14A).[143] In most cases the hrPKS could be swapped wholesale without loss of activity, and the nrPKS faithfully imposed its native PT- and TE-controlled ring topology on the incoming benzenediol side chain, indicating a high degree of modular compatibility at the subunit level.[143] However, certain hrPKS–nrPKS combinations only became productive when the nrPKS SAT domain was replaced with a more promiscuous counterpart, underscoring that even in this relatively "friendly" homologous space, the *trans*-acting loading preference of the nrPKS can become a bottleneck for subunit-level recombination (Fig. 14A).[198] From a design perspective, these results complement the domain-level engineering described above: rather than rewiring SAT–KS–PT–TE inside a single PKS, subunit swapping treats the entire hrPKS or nrPKS as a plug-and-play unit, while still relying on SAT and TE as key gating elements that must be matched appropriately across subunits.

Subunit shuffling between cryptic and well-characterized BDL synthases has revealed additional programming layers that are only apparent when hrPKS and nrPKS subunits from different pathways are recombined.[211] Genome mining of the dothideomycete *Rhytidhysteron rufulum* uncovered a collaborating hrPKS–nrPKS pair that, when expressed alone in *S. cerevisiae*, produced only trace levels of rare S-type BDLs with a phenylacetate core.[198] By systematically pairing this "cryptic" hrPKS (RrDalS1) and nrPKS (RrDalS2) with non-cognate partners from the four canonical BDL families, and combining subunit swaps with targeted SAT and TE domain exchanges, Wang and co-workers generated a panel of DAL and acyl dihydroxyphenylacetic acid ester (ADAE) scaffolds that extended the S-type BDL chemical space by 20+ new congeners.[198] Mechanistic analysis showed that the chain length of the hrPKS product is strongly influenced in *trans* by the off-loading

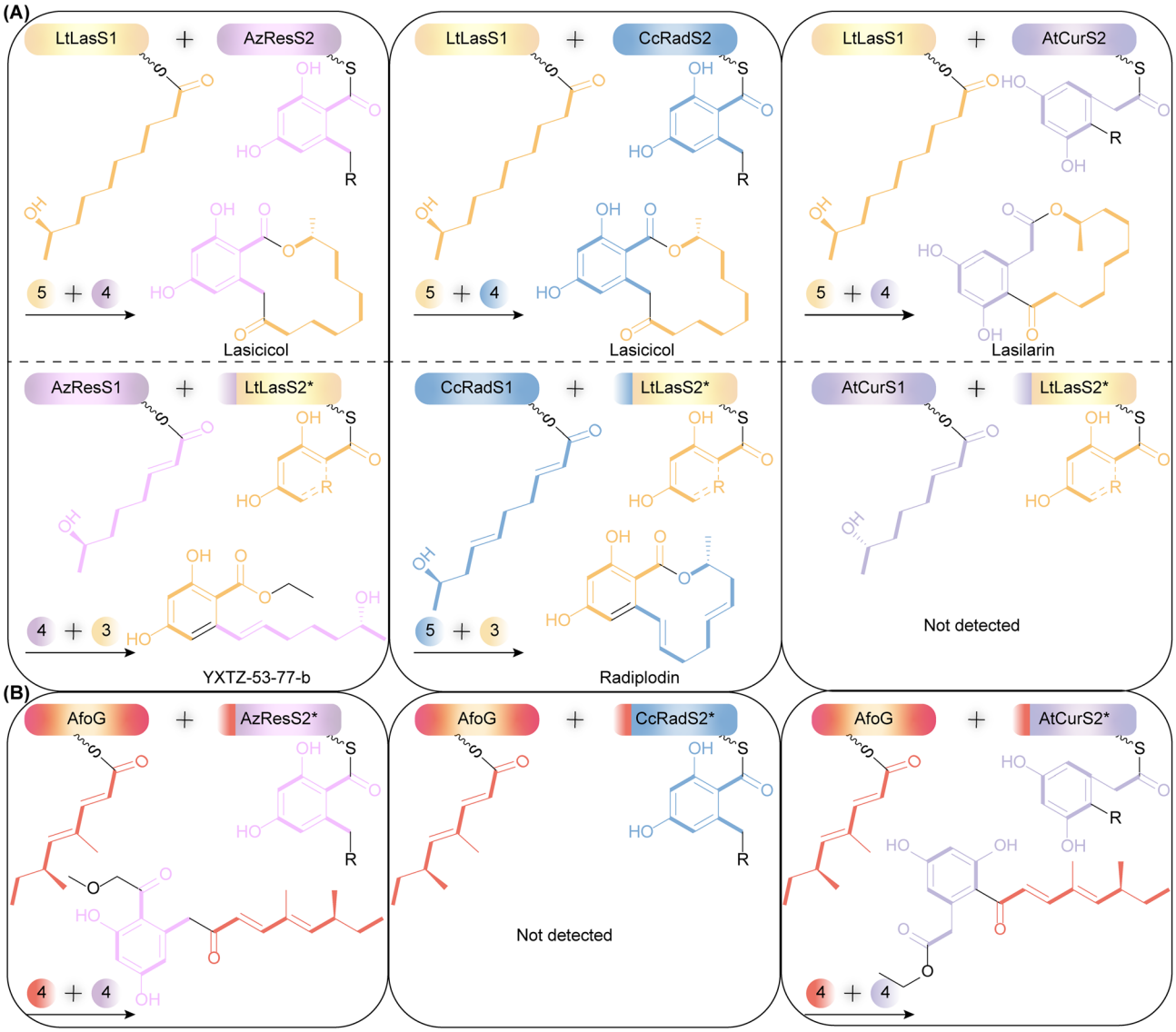


Fig. 14 Subunit-swapping strategies in iPKS assembly lines involving hrPKS–nrPKS pairs. (A) Heterologous recombination of matched subunits from four homologous benzenediol lactone (BDL) synthase pairs—CcRadS1–CcRadS2, AzResS1–AzResS2, LtLasS1–LtLasS2, and AtCurS1–AtCurS2—demonstrates that exchanging cognate S1 (hrPKS) and S2 (nrPKS) partners can reconstitute functional hybrids that preserve native programming features while altering the resulting lactone scaffolds. Adapted from ref. 143 and 198. (B) Cross-family subunit swaps between non-homologous BDL nrPKSs (AzResS2, CcRadS2, AtCurS2) and the asperfuranone-pathway hrPKS AfoG reveal broader programmability: hybrid hrPKS–nrPKS combinations generate chimeric scaffolds incorporating mixed biosynthetic synthons from both partners. Product backbones are color-coded according to the hrPKS- and nrPKS-derived segments. Product structures are colored to indicate their subunit origin, and numbered spheres denote the count of $C_2$ extender units incorporated by each PKS component. Split-color boxes mark constructs in which SAT domains were replaced by hrPKS-derived SAT modules to restore compatibility at the loading interface. Adapted from ref. 213 and 214.

preferences of the downstream nrPKS SAT domain, which can selectively intercept shorter or longer priming units, while the TE domain of the nrPKS acts as a size- and shape-selective filter that decides whether a given priming unit is released as a macrocycle (DAL) or diverted into linear ester products (ADAE).[198] In this view, KS and PT define the intrinsic chain and ring logic of each subunit, whereas SAT and TE belong to an "extrinsic" programming layer that emerges only when hrPKS and nrPKS are combined. More recently, this subunit-centric design has been extended to enhance the visibility of low-abundance chimeras while exploiting intrinsic precursor promiscuity to generate additional "unnatural" congeners. In *S. cerevisiae*, Li and co-workers co-expressed multiple BDL-type hrPKS–nrPKS pairs together with non-cognate subunit combinations, systematically probing which pairings could still cooperate without disrupting their intrinsic programming, and used mild plasmid copy-number tuning to balance the expression of the two subunits so that several previously barely detectable non-cognate products could be isolated and structurally characterized.[44] More importantly, their work shows that even without external precursor feeding, simply activating and amplifying the endogenous precursor heterogeneity and cross-

subunit transfer tolerance of hrPKS–nrPKS pairs allows subunit shuffling to perturb the internal precursor pool and yield series of subtly different, but potentially functionally divergent, BDL-type "unnatural" natural products.[44] Taken together, these BDL-focused examples position subunit shuffling as a powerful tool not only to revive cryptic iPKS pairs and generate structurally diverse macrolactones, but also to deconvolute how intrinsic chain-building rules (encoded by KS, KR and PT) are modulated by extrinsic filters (SAT and TE) imposed by partner subunits.

Although subunit shuffling within homologous BDL families with cooperative iPKS pairs is a relatively straightforward way to obtain structurally diverse macrolactones, there are far fewer examples where non-homologous iPKS pairs from distinct polyketide families are merged to create entirely new biosynthetic logics.[212] A representative case is the interface between BDLs and azaphilones such as asperfuranone. Azaphilones constitute a structurally diverse class of fungal polyketides with prominent bioactivities, and the asperfuranone pathway in *A. nidulans* uses a collaborating hrPKS AfoG and nrPKS AfoE to build a benzaldehyde-type intermediate (pre-asperfuranone) that underpins this family (Fig. 14B).[195,213] By exploiting this shared logic, Bai and co-workers used iPKS subunit shuffling to merge the BDL and asperfuranone families: the asperfuranone hrPKS AfoG was combined with several BDL nrPKSs, and replacement of the recipient nrPKS SAT domains enabled loading of the AfoG-derived benzaldehyde starter, yielding three productive chimeras that produced four hybrid scaffolds bearing both BDL macrolactone and azaphilone-like features (Fig. 14B).[214] In these hybrids, both partners largely retained their intrinsic programming—AfoG still constructed the highly reduced benzaldehyde starter unit, while the BDL nrPKSs imposed their native PT/TE-controlled cyclization and release patterns—so that subunit rearrangement effectively created a composite program rather than scrambling each individual step. This example encapsulates the design principles for non-homologous subunit swapping: success depends on installing a compatible SAT–ACP interface, ensuring that kinetic competition for the shared intermediate favors productive transfer, and respecting the "hard-wired" chain-length and cyclization preferences embedded in each synthase.[198,214] Continued dissection of how iPKS domains interact across subunit boundaries and partition reactive intermediates will be crucial to move from semi-empirical subunit shuffling toward rational cross-family recombination, thereby accelerating the discovery of new fungal polyketide scaffolds and guiding the engineering of iPKSs to produce truly "non-natural" natural products.

**3.2.3. Post-PKS diversification by promiscuous tailoring enzymes.** Beyond engineering the PKS assembly line itself by subunit swapping and domain recombination, fungal polyketide chemical space can be expanded along an orthogonal axis by "bolt-on" tailoring enzyme modules (Fig. 10B). These enzymes—most prominently CYPs, FMOs, multicopper oxidases (laccases), sulfotransferases, *O*-methyltransferases (OMT), and (methyl)glycosyltransferases—are typically co-localized with PKSs in biosynthetic gene clusters and install oxidative, charged, and sugar decorations on pre-assembled backbones.[215,216] Many of them display a useful combination of substrate promiscuity (tolerating diverse native and engineered scaffolds) and position selectivity (controlling the exact site and stereochemistry of modification), which makes them ideal building blocks for combinatorial biosynthesis on both native and non-native polyketide skeletons.[217,218] In this section, we focus on how such promiscuous tailoring enzymes have been redeployed as modular catalysts for late-stage diversification, complementing the backbone engineering strategies discussed above and enabling libraries of "non-natural" natural products to be assembled *in vivo*.

A first class of tailoring modules exploits oxidative phenol coupling to convert monomeric polyketides into axis-chiral dimers with defined regio- and atroposelectivity. In addition to CYPs and FMOs that catalyze intramolecular and intermolecular C–C bond formation on aromatic polyketides,[219] fungal multicopper oxidases (laccases) have emerged as surprisingly selective catalysts for intermolecular coupling.[220] Fürtges and co-workers demonstrated that the heterologously expressed laccase *Av*-VirL from *A. viridinutans* regioselectively converts the non-natural substrate (*R*)-semivioxanthin into its 6,6′-homodimer, establishing that a single laccase can program phenol coupling without auxiliary proteins and that closely related homologues are embedded in multiple dimeric naphthopyrone and perylenequinone BGCs (*e.g.* vioxanthin, xanthoepocin, hypocrellin A).[215] Subsequent mechanistic work on the viriditoxin pathway showed that a dedicated dirigent-like protein (VdtD) can further control the stereochemical outcome of multicopper oxidase VdtB, biasing the ratio of atropisomeric dimers and illustrating how auxiliary proteins can be layered onto laccase cores to tune stereoselectivity.[221,222] A complementary and more stringent example of such modular control is provided by sporandol biosynthesis in *Chrysosporium merdarium*.[221] In this pathway, a nrPKS generates a monomeric naphthopyrone backbone that is released by a *trans*-acting MβL-TE and subsequently *O*-methylated to form torachrysone, which then serves as the substrate for oxidative dimerization. Strikingly, the laccase alone is catalytically inactive toward productive coupling; only the co-expression of a fasciclin domain-containing (fas) accessory protein enables regio- and atroposelective phenol coupling to yield sporandol (Fig. 15).[221] This system highlights an important design principle for post-PKS diversification: oxidative phenol coupling can be programmed not only by the laccase core itself, but by modular auxiliary proteins that gate enzyme–substrate recognition and enforce productive dimerization geometries. Such accessory-controlled laccase modules act as transferable "decision layers" operating on pre-assembled scaffolds, allowing identical monomers to be routed toward distinct dimeric outcomes without modifying the upstream PKS assembly line. This modularity is particularly attractive for combinatorial biosynthesis, as it enables late-stage diversification of both native and engineered polyketide scaffolds while preserving the upstream assembly line intact.

Orthogonal to such oxidative dimerization, negatively charged modifications offer a way to modulate solubility and target engagement without altering the aromatic core.[223] A

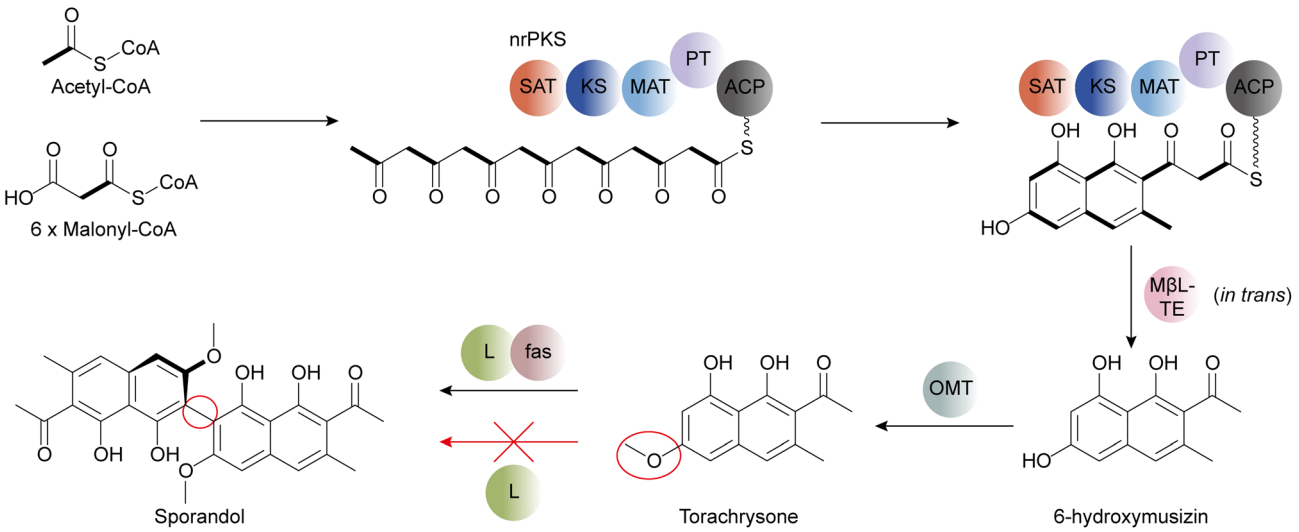


Fig. 15 Post-PKS diversification through modular oxidative tailoring in sporandol biosynthesis. A representative example illustrating how post-PKS tailoring enzymes expand fungal polyketide chemical diversity without re-engineering the upstream assembly line. In the sporandol pathway, a PKS-derived monomeric polyketide scaffold is first modified by *O*-methylation and subsequently subjected to oxidative phenol coupling. The multicopper oxidase (laccase) alone is insufficient to catalyze productive dimerization, whereas co-expression with a fas accessory protein enables regio- and atroposelective dimer formation. This system exemplifies how tailoring enzyme modules, rather than PKS engineering, can act as transferable post-assembly "decision layers" to program late-stage diversification of polyketide scaffolds. Red circles indicate sites of chemical modification introduced by tailoring enzymes; red arrows and crossed symbols denote inactive coupling in the absence of accessory proteins. Abbreviations: OMT, *O*-methyltransferase; L, laccase; fas, fasciclin domain-containing accessory protein. Adapted from ref. 221.

prominent example is phenolic sulfation of BDLs, where a fungal sulfotransferase is recruited as a broad-specificity tailoring module. Guided by genome mining of *F. graminearum* PH-1, Xie and co-workers identified FgSULT1 as a phenolic sulfotransferase that forms a distinct fungal/bacterial-family clade rather than clustering with canonical mammalian enzymes.[224] When FgSULT1 was co-expressed with a panel of BDL and non-macrocyclic BDL homologues in *S. cerevisiae*, the enzyme cleanly installed sulfate groups on multiple phenolic substrates, yielding a library of non-natural BDL sulfates with improved aqueous solubility and distinct bioactivity profiles relevant to human and veterinary drug discovery as well as crop protection.[224] Importantly, this work shows that a single promiscuous sulfotransferase can be combined with different native or engineered PKS pairs to generate sulfated analogues without re-optimizing the core assembly line, provided that cofactor 3′-phosphoadenosine-5′-phosphosulfate (PAPS) supply and compartmentalization are appropriately managed.[224,225] As more fungal sulfotransferases and their associated PAPS-regeneration systems are uncovered by BGC-centered genome mining and functional screens, this type of charged "sulfation cassette" is likely to become a generalizable module for orthogonal late-stage diversification of complex polyketide scaffolds in yeast and filamentous-fungal hosts.

Complementary to these charged decorations, neutral but polarity-tuning modifications such as *O*-methylation are powerful for reshaping physicochemical and pharmacological properties without dramatically altering scaffold topology.[226] The BDL system nicely illustrates how OMTs can function as programmable tailoring modules. In the lasiodiplodin/hypothemycin pathways, two orthologous OMTs (LtOMT and HsOMT) install methoxy groups at distinct positions on the same BDL core, yielding orthogonal regioisomers from a common scaffold.[210] Structure-guided engineering of their active-site cavities revealed that a small set of amino acid substitutions is sufficient to "swap" the preferred methylation site, while retaining broad acceptance of BDL analogues generated by PKS subunit shuffling.[210] This work established a generalizable design rule: OMT active sites are sufficiently plastic that regioselectivity, rather than substrate scope, can be rationally reprogrammed, enabling late-stage installation of complementary methoxy patterns on families of native and non-native polyketide backbones.[210,227] Building on this concept, Zhang and co-workers recently used BGC-centered genome mining to systematically expand the accessible toolbox of fungal methyltransferases, combining sequence similarity networks and *in vivo* assays to identify new OMTs with distinct positional preferences and donor usage.[29] Their study highlights how tailoring-enzyme families can be prospected at scale to populate a modular "methylation palette" for combinatorial design, rather than relying on one or two canonical OMTs.[29,228]

An even more dramatic increase in diversity is achieved when sugar-based tailoring modules are layered onto polyketide scaffolds. A key example is the glycosyltransferase–methyltransferase (GT–MT) pair from the entomopathogenic fungus *Beauveria bassiana*, which defines a methylglucosylation functional unit.[229] Xie and co-workers identified a founding GT family member that is not orthologous to previously characterized fungal GTs and showed that this enzyme can glucosylate a broad panel of drug-like substrates—including polyketides,

 

anthraquinones, flavonoids and naphthalenes—to give both *O*- and *N*-glucosides with remarkable regio- and stereospecificity.[230] These glucosides are then faithfully processed by a dedicated MT to provide 4-*O*-methylglucosides, effectively bundling glucosylation and methylation into a single, portable tailoring cassette.[230] When co-expressed with native or non-native BDL PKS pairs such as LtLasS1–LtLasS2 in yeast, this GT–MT module decorates both natural and engineered BDL scaffolds with 4-*O*-methylglucosides, producing a panel of "non-natural" natural products that exhibit greatly enhanced aqueous solubility and, for selected members, pronounced antiproliferative or matrix-adhesion inhibitory activities.[230] Recent work has extended this logic beyond single-pathway case studies and toward tailoring-guided discovery and deployment. Chen and co-workers developed a tailoring enzyme-guided genome-mining and MS-based metabolomics workflow that uses specific GT motifs as beacons to prioritize fungal BGCs likely to encode glucosylated natural products.[180] By heterologously expressing selected GTs and their cognate PKSs, they uncovered multiple previously unknown glucosides that would have been difficult to predict from core PKS architecture alone.[180] This study underscores a central theme of this section: tailoring enzymes not only diversify known scaffolds but also direct us to new polyketide families when used as genomic markers. In parallel, *B. bassiana* has been repeatedly exploited as a whole-cell biocatalyst to convert exogenous aromatic scaffolds into methylglucosides; for instance, Peng and co-workers used *B. bassiana* to transform resveratrol and piceatannol into a set of stilbene methylglucosides, one of which displayed promising GPR119 agonism and insulin-secretion activity relevant to type 2 diabetes therapy.[231] These transformations emphasize how promiscuous fungal GT–MT machineries can be applied directly to non-native, xenobiotic-like scaffolds to generate medicinally relevant analogues without rebuilding the upstream PKS.

Beyond these pathway-embedded modules, stand-alone fungal OGTs with broad aglycone and donor spectra further expand the combinatorial space. A recent Mycology study characterized MrOGT2 from *Metarhizium robertsii* that accepts at least four UDP-sugar donors and 17 structurally diverse acceptors, including multiple flavonols and aromatic polyketide-like compounds.[232] MrOGT2 thus exemplifies a "plug-and-play" GT that can be wired into engineered PKS pathways or used in whole-cell biotransformation to append different sugar moieties—including non-native donors—onto a given backbone.[232] Combined with chassis-level strategies such as deleting endogenous glycosidases to prevent product hydrolysis and boosting UDP-sugar biosynthesis in *S. cerevisiae*,[233] these advances point toward glycodiversification platforms where PKS-derived aglycones and sugar-tailoring modules can be mixed and matched in a semi-orthogonal fashion. Taken together, these studies illustrate how promiscuous tailoring enzymes—OMTs with reprogrammable regioselectivity, sulfotransferases, and (methyl)glucosylation cassettes—transform backbone-engineered fungal polyketides into rich libraries of non-native analogues with tunable polarity, charge, and three-dimensional topology. Rather than repeatedly redesigning the PKS itself, combinatorial biosynthesis increasingly relies on assembling small sets of well-characterized tailoring modules on both native and hybrid scaffolds, guided by genome mining, structural modelling, and high-throughput metabolomics.

### 3.3. Enzyme engineering

Beyond swapping or recombining whole domains, a complementary and often more tractable strategy is to engineer the catalytic "gatekeepers" within iterative PKSs themselves. In these systems, the shape and electrostatics of active-site pockets in product template (PT), enoyl reductase (ER), and other reductive domains dictate cyclization topology, chain length, and reduction pattern, thereby hard-wiring the accessible chemical space.[24,106] Structure-guided point mutations at a small number of residues can therefore retune these intrinsic programming rules while preserving the native protein–protein interfaces and dynamic choreography of the megasynthase—an advantage over wholesale domain or subunit swapping, where mis-matched linkers or docking surfaces frequently cause aggregation or loss of activity (Fig. 10C).[96,198] PT domains of fungal nrPKSs provide a clear example of how subtle sequence changes redirect first-ring cyclization. RALs and BDLs such as monocillin II and 10,11-dehydrocurvularin are assembled by hrPKS–nrPKS pairs, where the nrPKS PT domain channels a highly reactive poly-β-keto chain into either C2–C7 or C8–C3 F-mode aldol cyclization, giving rise to distinct aromatic frameworks.[204] Homology modelling based on the aflatoxin PT structure, combined with large-scale sequence analysis of >600 fungal PT domains, revealed that a small set of cavity-lining residues shapes the cyclization chamber and correlates with the observed ring-closure modes across PT clades.[96,98] Guided by these models, Xu and co-workers introduced three mutations (F1455Y, Y1576F, W1584L) into a BDL-type PT domain and successfully redirected its regioselectivity from a native C8–C3 to a C2–C7 cyclization pattern, yielding the non-natural RAL YXTZ-3-16-2 from the same upstream hrPKS product (Fig. 16).[204] Intriguingly, the reverse mutational path did not convert a C2–C7 PT into a robust C8–C3 catalyst, highlighting that PT programming is not simply encoded by a few "toggle residues" but emerges from more global conformational and trajectory constraints in the cyclization chamber.[41,98,204] This asymmetric mutational landscape is an important lesson for combinatorial design: PT domains can be pushed into new regions of chemical space, but achieving fully reversible switching between distinct ring-closure logics remains challenging. Taken together, the backbone diversification of combinatorial libraries is achieved not only by swapping modules, but by rationally editing the intrinsic selectivity of individual domains.

Recent work has reinforced the idea that modest sequence changes in hrPKSs can rewire more global features such as chain length. Using the tenellin highly reducing PKS as a model, Schmidt and Cox combined sequence analysis, alanine scanning, and multi-site mutagenesis to identify four residues that influence when the iterative cycle terminates.[32] Introducing these mutations led to minor, but reproducible, production of

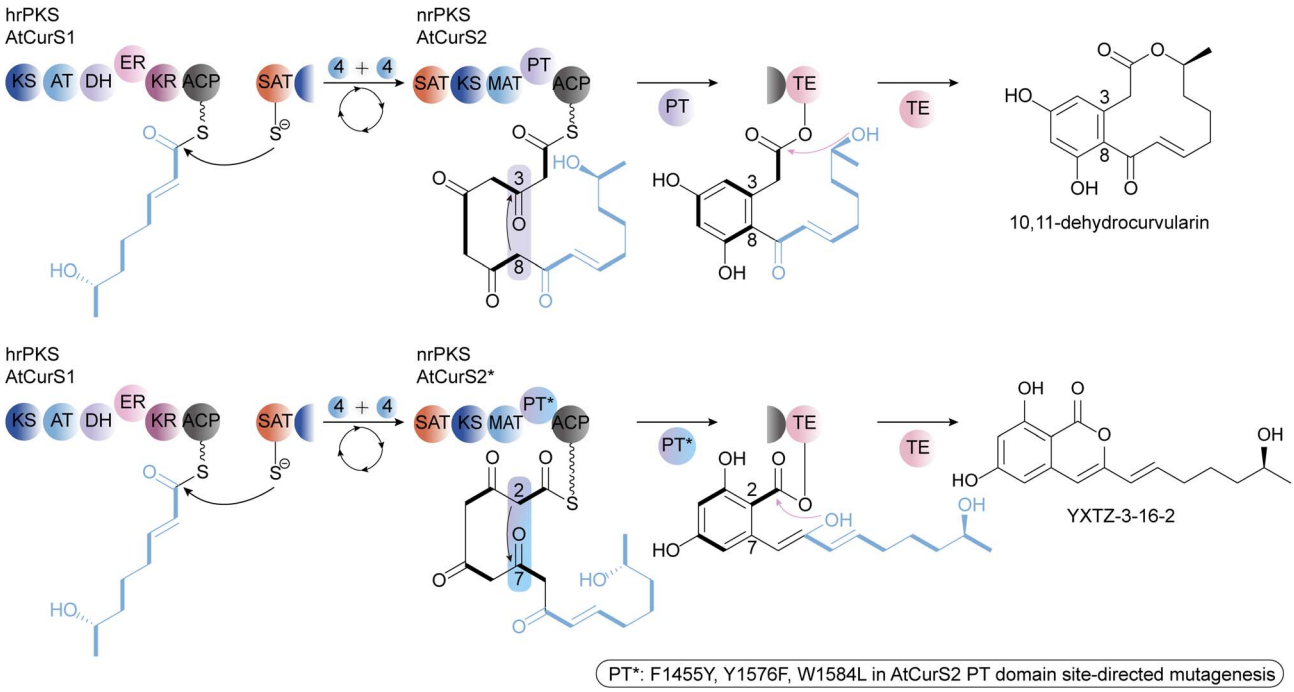


Fig. 16 PT domain engineering redirects aromatic ring cyclization in synergistic hrPKS–nrPKS systems. In the native BDL pathway, the PT domain of nrPKS AtCurS2 promotes a C8–C3 first-ring cyclization, converting the hrPKS-derived intermediate into 10,11-dehydrocurvularin. *In vivo* mutational analysis revealed that introducing the substitutions F1455Y, Y1576F, and W1584L within the PT domain (PT*) remodels the active-site geometry, switching the cyclization trajectory to a C2–C7 mode and yielding the non-natural product YXTZ-3-16-2. The blue structures represent the hrPKS-generated polyketide chains (with bold bonds indicating the number of extender units incorporated), whereas the black structures denote the nrPKS-extended backbones (bold bonds marking additional elongation steps). Blue and purple boxed regions highlight the distinct aromatic ring-forming positions specified by PT* and the wild-type PT domain, respectively. Adapted from ref. 204.

hexaketide products in addition to the native pentaketides, thereby directly linking a small set of amino acids to chain-length selection.[32] Although the shift was incomplete, this study provides rare, quantitative evidence that hrPKS chain-length programming can be tuned by minimal sequence edits, complementing earlier bioinformatic analyses that had inferred such relationships from natural diversity alone.[24,32]

ER domains in hrPKSs represent another crucial gatekeeper layer, controlling which β-keto intermediates are reduced and thus shaping both oxidation state patterns and the timing of chain termination.[234] The ER from the squalestatin tetraketide synthase (SQTKS) was the first *cis*-acting ER domain to be isolated and biochemically characterized *in vitro*, where it forms a discrete dimer and shows broad activity toward a panel of di- and triketide enoyl substrates but fails to reduce a tetraketide intermediate, which instead acts as a competitive inhibitor.[57] Docking of natural and non-natural substrate mimics into homology models of the SQTKS ER active site, followed by targeted mutagenesis, pinpointed Phe1941 and Phe2157 as steric gatekeepers that restrict both chain length and methylation pattern.[64] In particular, the F1941A mutation converted the tetraketide from an inhibitor into a true substrate, while F2157A enlarged the pocket sufficiently to accommodate longer and more heavily methylated intermediates.[64,235] These engineered ER variants displayed significantly altered programming *in vitro*, reducing substrates that are completely excluded by the wild-type enzyme, and thereby demonstrating that a handful of point mutations can relax strict gatekeeping without compromising overall catalytic competence. Taken together, the backbone diversification of combinatorial libraries is achieved not only by swapping modules, but by rationally editing the intrinsic selectivity of individual domains.

In parallel with editing core PT and ER domains, accessory and tailoring enzymes that act "downstream" or in *trans* to iterative PKSs can also be engineered into powerful, broadly reusable modules. A classic paradigm is provided by *trans*-acting AT LovD decorates the hrPKS product of LovF with an α-methylbutyryl side chain in lovastatin biosynthesis. In its native context, LovD is strongly dependent on direct interaction with the LovF ACP and efficiently accepts only the natural ACP-bound thioester.[130,236] Through multiple rounds of laboratory evolution, Jiménez-Osés and co-workers converted LovD into variants with dramatically improved catalytic efficiency, solubility, and stability for simvastatin semisynthesis, culminating in the industrial biocatalyst LovD9, which carries 29 amino-acid substitutions and exhibits ~$10^3$-fold higher activity on the non-native acyl donor α-dimethylbutyryl-*S*-methyl-mercaptopropionate (DMB–SMMP) while becoming essentially independent of the LovF–ACP partner.[237,238] Subsequent structural and microsecond-scale molecular dynamics (MD) simulations showed that these distant mutations reshape the active-site dynamics and narrow the substrate channel in a way that

favors binding and turnover of the free thioester, rather than the native ACP-bound intermediate (Fig. 10C).[237] Conceptually, LovD evolution demonstrates how a PKS-associated AT—functionally very similar to many fungal tailoring enzymes that rely on ACP-bound intermediates—can be reprogrammed into a stand-alone biocatalyst that accepts non-native donors, thereby decoupling tailoring from tight protein–protein recognition and enabling late-stage diversification of polyketide scaffolds.

This logic is increasingly being extended to genuine tailoring enzymes that install oxygenation or glycosidic decorations on polyketide scaffolds. Fungal and bacterial CYP monooxygenases have been engineered to alter regio- and chemoselectivity for C–H activation, allowing access to new hydroxylated analogues that would be difficult to obtain by chemistry alone. For example, Renata and co-workers have introduced catalytically self-sufficient P450 fusions with tuned redox-partner linkers, enabling efficient, site-selective oxidations *in vitro* and in whole cells, while maintaining or even enhancing catalytic turnover on complex natural-product-like substrates.[239] More recently, Yong *et al.* used structure-guided mutagenesis to reprogramme the fungal-like P450revI, shifting its preferred C–H activation site and generating a novel hydroxylated polyketide derivative with improved bioactivity, thereby showcasing how semi-rational engineering can redirect late-stage oxidation patterns without sacrificing overall scaffold recognition.[240] In parallel, GTs are being re-designed to broaden or retune their donor and acceptor repertoires, often starting from promiscuous enzymes identified by genome mining. Lu and co-workers, for example, mined and comprehensively engineered the plant UGT75AJ2, using mutagenesis and structural analysis to generate variants capable of glycosylating multiple phenolic and heterocyclic scaffolds with distinct UDP-sugar donors;[241] such workflows are directly translatable to fungal GTs that act on polyketide aglycones, and complement fungal methylglucosylation modules discussed in the previous section. Collectively, these studies support a general design principle: tailoring enzymes, like LovD, can be "lifted" from their native assembly lines and reshaped into modular catalysts whose substrate and position selectivity are tuned to serve as plug-and-play tools for polyketide diversification.

Beyond individual case studies, recent advances in high-throughput screening and machine learning (ML) are beginning to systematize tailoring-enzyme engineering in a way that is highly compatible with fungal combinatorial biosynthesis. Biosensor-guided evolution has emerged as a particularly powerful strategy: d'Oelsnitz and co-workers developed a transcription-factor-based biosensor for a key intermediate and used it, together with ML-assisted library design, to evolve pathway enzymes and increase branch flux.[242,243] More broadly, researchers have highlighted how ML-guided sequence design, together with droplet- and cell-based ultrahigh-throughput screening, can accelerate both discovery and optimization of biocatalysts across diverse enzyme families, including oxygenases and GTs relevant to natural-product tailoring.[244,245] Although these technology stacks have so far been applied mainly to plant and bacterial enzymes, they provide a clear blueprint for how fungal tailoring enzymes—P450s, FMOs, GTs, MTs—could be engineered in chassis such as *S. cerevisiae* to favor desired modifications on native and non-natural polyketide backbones.

At the same time, the practical scope of enzyme engineering is being reshaped by genome-editing and structure-prediction tools that make it possible to generate targeted PKS and tailoring-enzyme libraries *in situ* rather than relying solely on heterologous refactoring. CRISPR/Cas systems are now routinely established in non-model filamentous fungi that natively produce complex polyketides. In *Edenia gomezpompae*, Zhai and co-workers recently developed a CRISPR/Cas9 platform using the endogenous U6 promoter and showed that deletion of a single iPKS gene (*Egpks*) abolishes production of the spiroketal naphthoquinones preussomerins, thereby validating cluster boundaries and assigning function to the core enzyme.[246] Although this first study focused on knockout, the same toolkit is directly applicable to site-specific mutagenesis of active-site and gatekeeper residues in EgPKS and its associated tailoring enzymes to generate panels of non-native preussomerin analogues.[246] In *A. niger*, Yuan and co-workers compared Cas9- and Cas12a-based systems at the albA PKS locus and demonstrated efficient, programmable editing of the polyketide backbone gene with distinct indel profiles,[247] providing a practical route to multiplexed mutagenesis of catalytic residues or whole domains in native producers. Together with earlier CRISPR/Cas9 systems established in *Fusarium* and *A. terreus* for PKS genes such as *fum1* (fumonisins) and lovastatin-pathway components,[248–250] these studies make it increasingly realistic to move from "one-off" deletions toward saturation mutagenesis of key domains, combinatorial editing of tailoring-gene sets, and ultimately in-fungus evolution of enzyme variants that furnish non-natural polyketide chemotypes. Complementing these genetic tools, deep-learning-based structure prediction and coevolution analysis are beginning to bring rationality to a space where combinatorial swapping has historically suffered from very low success rates. In a landmark study on modular PKSs, Englund and co-workers used AlphaFold2 models of the KS–AT linker region to interpret why most AT-domain exchanges disrupt structure, then built a fluorescence-based solubility biosensor to screen hundreds of AT-swapped hybrids and identify a narrow set of domain boundaries that maintain polyketide production.[189] Nava *et al.* reviewed AlphaFold2-guided module boundary selection with systematic recombination of stambomycin-like modules, generating *de novo* macrolactone products and establishing a "module-based" engineering strategy that respects the natural architecture of the assembly line.[176] Even more strikingly, Mabesoone and co-workers analyzed amino-acid coevolution patterns in *trans*-AT PKSs to pinpoint a single, evolutionarily privileged recombination site; inserting or deleting modules at this position yielded 22 engineered assembly lines across multiple pathways with a markedly higher fraction of fully functional hybrids that still produced complex non-natural polyketides.[33] These studies collectively highlight general principles—respecting evolutionarily conserved cut sites, preserving docking-face complementarity, and using AlphaFold2/co-

evolution maps to avoid disruptive linkers—that are directly applicable to iterative fungal PKSs and their associated tailoring enzymes. In this sense, enzyme engineering—supported by these new tools—provides a realistic and increasingly high-success-rate route to expand non-natural polyketide diversity.

## 4. Engineering fungal and yeast cell factories

Having outlined how iPKSs and their tailoring enzymes can be rationally rewired at the enzyme level to generate new scaffolds, we now turn to the cellular context in which these machineries operate. Early studies on fungal polyketide biosynthesis largely relied on native producers and classical fermentation, combined with gene-by-gene reconstruction of pathways and analysis of accumulated intermediates.[230] With the advent of genome sequencing, comparative genomics, and synthetic biology, hundreds of putative polyketide BGCs can now be rapidly predicted and transplanted into tractable fungal hosts such as *Aspergillus* and *Saccharomyces* for systematic interrogation (Fig. 17).[251] However, many of these pathways remain transcriptionally silent or very weakly expressed, leading to low titers that hinder both scalable production and the detection of minor shunt products that often encode new chemotypes.

In this section, we organize fungal and yeast cell-factory engineering along a progressive design logic: first, activating and refactoring silent BGCs in their native chromosomal context; second, deploying genetically tractable chassis to decouple pathways from native regulation and enable modular recombination; third, rewiring central metabolism to support acetyl- and malonyl-CoA-intensive biosynthesis; and finally, leveraging compartmentalization and spatial organization to coordinate precursor supply, trafficking and self-protection (Fig. 17), across non-reducing, partially reducing and highly reducing iterative PKS systems and their hybrid assemblies. Together, these layers define a cellular framework in which fungal polyketide biosynthesis can move beyond opportunistic discovery toward programmable and scalable platform engineering.

### 4.1. Activating silent BGCs in native fungi

A first layer of strain engineering targets transcriptionally silent or weakly expressed BGCs directly in their native hosts, using pathway-specific transcription factors (PSTFs), promoter engineering, CRISPR-based transcriptional activation, and

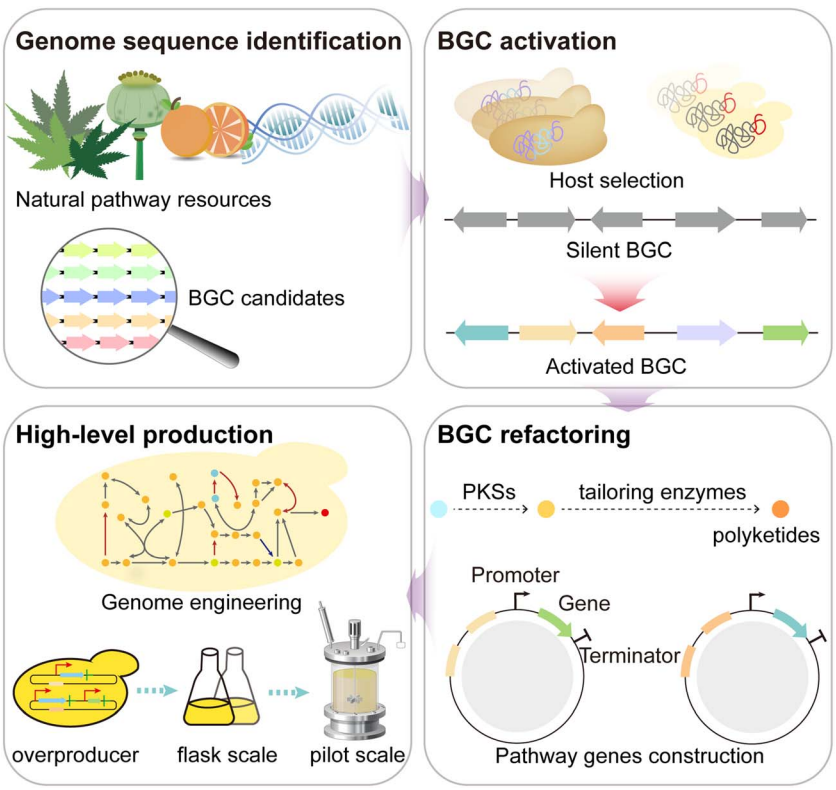


Fig. 17 Workflow for developing microbial cell factories to activate, reconstruct, and optimize biosynthetic gene clusters (BGCs) for efficient polyketide production. Advances in fungal genome sequencing enable systematic identification of BGC candidates from native producers, followed by activation of silent or weakly expressed clusters either in the original host or in a heterologous chassis. Reconstituted pathways are then refactored and optimized through promoter engineering, modular reconstruction, and pathway balancing to enhance flux through key enzymatic steps. Subsequent rounds of genome-scale engineering, strain refinement, and AI-assisted design yield improved production hosts suitable for shake-flask evaluation and pilot-scale fermentation, accelerating the discovery and scalable manufacture of polyketide natural products.

epigenetic modulation to convert cryptic loci into productive pathways (Fig. 17).[252] Many polyketide clusters reside in heterochromatic regions or carry promoters that are barely active under laboratory conditions, such that the encoded iPKSs and tailoring enzymes remain silent even though the genetic capacity is present.[253] In *A. nidulans*, systematic promoter replacement of nrPKS genes and key tailoring genes with strong inducible promoters enabled product assignment for eight nrPKSs, including seven previously unknown aromatic polyketides and the identification of the nrPKS genes responsible for alternariol and cichorine biosynthesis, illustrating how in masse promoter engineering in the native genome can rapidly unlock the endogenous polyketide repertoire.[254]

PSTFs provide a complementary handle to turn up individual polyketide pathways without disturbing surrounding loci. In *A. nidulans*, overexpression of PSTFs has repeatedly been shown to induce otherwise cryptic clusters: for example, regulatory crosstalk between a NRPS cluster and a silent polyketide cluster activated the asperfuranone pathway, with the upstream TF *scpR* driving expression of the asperfuranone activator *afoA* and thereby switching on the entire cluster in its native chromosomal context.[255] Complementing cluster-local PSTFs, Seo and co-workers recently constructed a gene regulatory network resource for *A. fumigatus* that predicts *trans*-acting regulators of multiple BGCs; targeted deletion or overexpression of TFs such as *rogA*, *hsfA*, *skn7* and *rofA* led to pronounced changes in the production of gliotoxin, helvolic acid and fumitremorgin, showing how systems-level TF maps can guide rational activation or attenuation of native polyketide and alkaloid pathways.[256] Together with large-scale analyses of PSTFs across *Aspergillus* genomes, these studies establish PSTF overexpression, rational TF selection and targeted promoter substitution as general strategies to "de-repress" native iPKSs and map their associated tailoring networks.[257]

More recently, CRISPR-mediated transcriptional activation (CRISPRa) has extended this logic to programmable activation of silent clusters *in situ*.[258] In *A. nidulans*, a dLbCas12a-VPR system was used to target the promoter of the native NRPS-like gene *micA*, resulting in strong up-regulation of the mic cluster and markedly increased production of the polyketide-like metabolite microperfuranone and its oxidized analogue dehydromicroperfuranone.[259] A related dCas9-VPR CRISPRa tool in *P. rubens* targeted the promoter of the cluster-resident TF *macR* and successfully activated the transcriptionally silent native macrophorin BGC, yielding antimicrobial macrophorins directly from the industrial penicillin producer background.[260] These examples show that CRISPRa can be applied in diverse filamentous fungi to enhance expression of native polyketide clusters without integrating extra copies or relocating the pathway.

In parallel, epigenetic reprogramming has emerged as a complementary approach to awaken multiple clusters at once.[261] Deletion or inhibition of histone-modifying enzymes can relax chromatin around otherwise silent BGCs and uncover new polyketides.[253] In the endophytic fungus *C. olivaceum*, deletion of a class I histone deacetylase (HDAC) led to the activation of several secondary metabolite gene clusters and the discovery of new aromatic polyketide-derived compounds that were undetectable in the wild-type strain.[262] More broadly, systematic treatment of native fungi with small-molecule epigenetic modifiers has been shown to trigger expression of otherwise silent nrPKS clusters and yield structurally diverse polyketides, underscoring chromatin engineering as a powerful, cluster-agnostic lever for expanding chemical space directly in native producers.[253,263]

### 4.2. *Aspergillus* as a chassis for fungal polyketides

Beyond editing native producers, *Aspergillus* species—most prominently *A. nidulans* and *A. niger*—have emerged as programmable chassis for fungal BGCs. Their fast growth, well-developed genetics, and relatively well-annotated secondary metabolomes make them ideal "workhorse" hosts to refactor polyketide clusters from diverse fungi, decouple them from native regulation, and systematically map both core iPKS products and downstream tailoring logic.[264] Rather than serving only as titer-boosting hosts, these *Aspergillus* platforms increasingly function as discovery engines that generate series of analogues suitable for combinatorial biosynthesis and designer-structure exploration.[265,266]

In *A. nidulans*, several complementary chassis tools now coexist. A key development is the use of genetic dereplication strains, in which major endogenous BGCs are deleted to simplify the metabolite background.[267,268] Lin and co-workers combined such a dereplication strain with a modular cloning and expression workflow to refactor the cryptic *spy* BGC from the human pathogen *A. fumigatus*; expression of the six-gene cluster in *A. nidulans* revealed the sartorypyrone pathway and delivered twelve products, seven of which were previously unknown, including a triacetic acid lactone – producing PKS that doubles as a biorenewable platform catalyst.[269] In parallel, the fungal artificial chromosome-mass spectrometry (FAC-MS) platform enables high-throughput capture of intact BGCs from genomic DNA into self-replicating *A. nidulans* – compatible chromosomes; expression of 56 *A. terreus* clusters in *A. nidulans* uncovered 15 new metabolites, including polyketide–NRPS hybrids, underscoring how a single *Aspergillus* chassis can be used to systematically mine the secondary metabolome of another fungus.[270,271]

Building on these chromosome-based systems, episomal AMA1-based pYFAC vectors provide a more flexible route to cluster expression and recombination.[272] Roux and Chooi described multi-marker AMA1 plasmids for episomal BGC expression in *A. nidulans*, which support high transformation efficiency, elevated compound titers, and convenient shuffling of pathway combinations to probe intermediate formation and tailoring steps.[273] Next-generation AMA1 plasmids further improve copy number control and stability and have been adapted not only for pathway assembly but also for CRISPR/Cas delivery in filamentous fungi, making *A. nidulans* a versatile chassis for iPKSs and accessory enzymes alike.[274] These tools collectively shift *A. nidulans* from "one cluster per study" to a modular, recombinable platform on which multiple polyketide pathways, domain- or tailoring-enzyme variants, and hybrid clusters can be tested in parallel—directly serving the goal of programmable polyketide diversification.

The same chassis has also proven effective for expressing BGCs from phylogenetically distant fungi and exploiting host-pathway cross-chemistry. Yu and co-workers activated the silent nrPKS SlPKS4 from the marine-derived fungus *Simplicillium lamellicola* HDN13-430 by cloning a 9.5 kb genomic fragment into *A. nidulans* A1145; the heterologous host produced the C7-methyl isocoumarin similanpyrone B together with pestapyrone A, an oxidized derivative formed by endogenous *A. nidulans* enzymes.[275] This example illustrates two important aspects of the *Aspergillus* chassis: first, it can faithfully support non-native iPKSs from ecologically and taxonomically distant donors; second, its native tailoring network can further "decorate" the imported scaffold, spontaneously generating non-natural analogues that enrich the accessible chemical space for subsequent design. Similar logic has been applied to other BGCs—for instance, expression of the *bue* PKS cluster from *A. burnettii* in *A. nidulans*, coupled with transcription-factor overexpression, yielded improved access to the target metabolite and pathway intermediates for structure–activity studies.[276]

*Aspergillus* chassis engineering is not restricted to *A. nidulans*. In *A. niger*, ATNT and related systems combine strong heterologous promoters and regulatory elements from the *A. terreus* terrein cluster to enable high-level expression of polycistronic secondary metabolites gene clusters.[277] Kirchgaessner and co-workers recently introduced a TetON-based expression system in *A. niger* that can stably express very long PKS and NRPS genes and BGCs from both Basidiomycota and early-diverging fungi, providing an inducible platform for complex megasynthases that are difficult to handle in yeast or bacteria.[278] These developments effectively position *A. niger* as a complementary chassis where long, intron-rich PKSs and their accessory genes can be expressed under precise temporal control, enabling time-resolved analysis of product formation and shunt pathways.

Finally, recent systematic TF-overexpression efforts in *A. nidulans* further blur the line between native and heterologous use of this chassis. Guo *et al.* constructed a panel of 51 strains in which secondary-metabolism-associated TFs—cluster-resident regulators, global secondary metabolite TFs, and candidates inferred from large-scale transcriptomics—were individually placed under the strong xylose-inducible *xylP* promoter at the neutral *yA* locus.[279] Induction triggered distinct metabolite profiles and unveiled multiple bioactive compounds, including benzaldehyde derivatives and polyketide–alkaloid hybrids with selective anticancer or antimicrobial activity.[279] Taken together, these *Aspergillus* platforms—chromosomal and episomal expression in dereplicated *A. nidulans* strains, cross-chemistry with imported PKSs, and inducible long-gene expression in *A. niger*—provide a fungal chassis toolkit. They allow not only higher titers but, more importantly, systematic exploration of new scaffolds, tailoring patterns, and hybrid pathways, turning fungal polyketide biosynthesis into a practical platform for building and testing designer natural products.

### 4.3. Yeast and non-conventional yeasts as programmable platforms

Compared to filamentous fungi, yeasts offer a more standardized genetic and fermentation toolkit, making them attractive plug-and-play chassis for fungal BGCs.[280] In the context of designer polyketides, the key question is not simply whether a yeast host can produce a given metabolite at high titer, but whether it can be systematically programmed to read diverse PKS pathways, tolerate their products, and support combinatorial pathway design (Fig. 17).

In *S. cerevisiae*, this idea is embodied by the HEx (Heterologous EXpression) platform, which couples curated genome mining with a unified expression architecture and engineered host strains.[281] By repairing mitochondrial defects in a laboratory strain and implementing a family of *adh2*-like, glucose-repressed promoters, Harvey and co-workers built a panel of *S. cerevisiae* strains expressing 41 cryptic fungal BGCs and detected new metabolites from 22 of them, including multiple polyketide and meroterpenoid scaffolds that had not been observed in the native producers.[281] Conceptually, HEx treats *S. cerevisiae* as a BGC screening and diversification engine: clusters from taxonomically distant fungi are standardized into yeast-friendly parts, expressed under a common regulatory regime, and then systematically surveyed for their intrinsic capacity to generate novel scaffolds and tailoring patterns.

Beyond "on/off" expression of whole clusters, more recent work has tuned *S. cerevisiae* as a chassis for unnatural and analog-generating polyketide pathways. For example, Li *et al.* used plasmid copy number engineering to separately vary the dosage of two collaborating PKSs (hrPKS and nrPKS), thereby accelerating the identification of expression regimes that favored non-native extender units and shunt products.[44] This strategy effectively turns copy number and promoter strength into quantitative knobs for redistributing flux across PKS subunits and tailoring steps, resulting in non-natural polyketide variants that would be difficult to access by domain swapping alone.[44] Similar logic underlies modular reconstructions of fungal bikaverin and bostrycoidin pathways in yeast, where enzyme fusions and stepwise assembly are used not only to boost titers but also to reveal alternative tailoring sequences and identify branch points that can be repurposed for analogue generation.[282,283] Together, these works position *S. cerevisiae* less as a generic workhorse and more as a programmable reader of fungal BGC logic, in which pathway balancing and modular constructs are deliberately used to expose new scaffold space.

Complementing *S. cerevisiae*, *Komagataella phaffii* (syn. *Pichia pastoris*) brings a different design space: strong, tightly inducible promoters (*e.g. AOX1*), efficient secretion, and a methylotrophic metabolism that is orthogonal to most polyketide pathways.[284] Kong *et al.* reconstructed the terreic acid pathway in *K. phaffii* by stepwise introduction of biosynthetic genes, using heterologous expression to deconvolute individual monooxygenation and cyclization steps and to identify intermediates that could serve as branching points for analogue formation.[83] More broadly, Qian and co-workers outlined a general workflow in which *K. phaffii* is used as a chassis to functionally annotate fungal BGCs, leveraging its scalable fermentation and simple background metabolome to support comparative analysis of multiple PKS variants and tailoring modules within the same host.[285] These case studies are supported by a rapidly expanding synthetic-biology toolbox in *K.*

 

*phaffii*—including multi-locus CRISPR–Cas9 integration, piggyBac-based mutagenesis and genome-scale metabolic models—which collectively position this yeast as a promising chassis for future combinatorial expression of fungal PKSs, systematic testing of tailoring networks, and ultimately diversification of designer polyketide scaffolds.[286,287]

A recent and conceptually important advance has been the introduction of black yeasts as broad-spectrum heterologous hosts for fungal polyketides. In a 2025 study, Cruz-Morales and co-workers established *Exophiala viscosa* and *Knufia petricola* as tractable chassis, assembling a panel of fungal PKSs including 6MSAS, YWA1 and bikaverin synthases, and several benzenediol lactone-type systems.[288] Despite their evolutionary distance from conventional yeasts, these black yeasts supported correct folding and activation of multiple large iPKSs and produced structurally diverse polyketides, often with fewer endogenous side products than *S. cerevisiae*.[289] Importantly, the authors emphasized that *Exophiala* and *Knufia* combine yeast-like genetic tractability with a richer native secondary metabolism and extremotolerance, traits that should facilitate future efforts to mix heterologous PKSs with endogenous tailoring networks and explore non-natural scaffolds under stress or unusual growth conditions.[288] This work points toward a "portfolio chassis" view, where different yeasts are chosen not only for their engineering tools but for how their intrinsic biology shapes accessible polyketide diversity.

The oleaginous yeast *Y. lipolytica* offers yet another angle by naturally supporting high acetyl-/malonyl-CoA flux and tolerating hydrophobic metabolites.[290] In a recent demonstration, Bejenari *et al.* simultaneously integrated the type I PKS genes for 6-MSA and the aza-anthraquinone pigment bostrycoidin, together with a cognate phosphopantetheinyl transferase (PPTase), using CRISPR–Cas9-mediated, markerless genome editing in *Y. lipolytica*.[80] The resulting strains produced up to 403 mg per L 6-MSA and 35 mg per L bostrycoidin, the latter >10-fold higher than in an analogous *S. cerevisiae* system, and established *Y. lipolytica* as a dual-PKS chassis for complex fungal polyketides.[80] While these studies focused primarily on titer, its combination of multiple PKSs and an activating PPTase in a single oleaginous host suggests clear routes toward library-style expression of PKS variants and tailored co-expression of decorating enzymes.[80,291] Together with broader advances in *Y. lipolytica* synthetic biology—expanded promoter sets, efficient CRISPR toolkits, and organelle-targeted engineering—this work underlines the potential of oleaginous yeasts as platforms where flux, compartmentalization, and PKS diversity can be co-optimized.[292] Collectively, these yeast and non-conventional yeast chassis illustrate a shift from "one host, one product" toward programmable, multi-host platforms for fungal polyketide diversification.

### 4.4. Metabolic rewiring for malonyl-CoA and acetyl-CoA supply

For iterative fungal PKSs—including non-reducing, partially reducing and highly reducing systems—the availability and partitioning of malonyl-CoA and acetyl-CoA not only limit titers but also constrain which non-native extender units and starter acyl-CoAs can realistically be explored (Fig. 18).[188] Early work in fungal and yeast platforms therefore relied on relatively coarse interventions, such as overexpressing acetyl-CoA carboxylase encoding gene (*ACC1*), relieving Snf1-mediated phosphorylation of Acc1, or attenuating competing fatty-acid synthesis, which enabled the first heterologous production of fungal-type polyketides (such as 6-MSA and bikaverin) in *S. cerevisiae* and related hosts.[135,291,293,294] While these strategies demonstrated that malonyl-CoA supply could be strengthened sufficiently to support heterologous PKSs, they often came at the cost of growth defects, lipid imbalance and poor control over carbon flux, making them sub-optimal for systematically exploring non-natural polyketide space (Fig. 16).[295,296]

To move beyond static overexpression, genetically encoded malonyl-CoA sensors have emerged as a central tool to couple flux rewiring with high-throughput screening. A widely used design is the flaviolin colorimetric reporter based on bacterial type III PKS RppA, whose flaviolin output correlates with intracellular malonyl-CoA and has been repeatedly deployed to identify pathway bottlenecks and beneficial mutations in malonyl-CoA-derived pathways, including polyketides.[297] In parallel, fungal-focused studies are also beginning to exploit biosensor-specific acyl-CoA pools, exemplified by direct utilization of flaviolin for the characterization of peroxisomal acetyl-CoA in *S. cerevisiae*.[298] Complementarily, Li and co-workers re-engineered the bacterial transcription factor FapR and its operator *fapO* into *S. cerevisiae* to build a malonyl-CoA biosensor that converts intracellular malonyl levels into fluorescence, enabling genome-wide overexpression screening and uncovering new targets that raise malonyl-CoA and downstream 3-hydroxypropionic acid titers.[299,300] Subsequent work has ported and optimized similar sensor architectures in oleaginous yeasts such as *Y. lipolytica*, where malonyl-responsive circuits have been used to enrich high-flux mutants for malonyl-derived products and to guide rational pathway balancing.[301] Recent work has further refined malonyl-CoA sensors in reconstituted and *in vivo* systems to detect acetyl-CoA carboxylase activity with high sensitivity.[302] Although most of these sensor systems were initially developed for commodity chemicals rather than fungal polyketides, the same designs can in principle be wired to iPKS or tailoring-enzyme outputs (for example *via* colorimetric reporters or growth-coupled selection), providing a route to screen large combinatorial PKS/tailoring libraries under malonyl-CoA limitation.

More recently, several studies have shifted from "pushing" the native acetyl-CoA carboxylase route towards designing orthogonal or artificial malonyl-CoA pathways that decouple malonyl supply from central carbon metabolism. Li and co-workers established a non-carboxylative malonyl-CoA (NCM) pathway that bypasses acetyl-CoA altogether and instead converts 3-oxopropanoate into malonyl-CoA, thereby avoiding ATP-costly carboxylation, carbon loss and tight native regulation.[303] Introducing this pathway dramatically increased production of malonyl-derived families, including phenolic, quinone, alkene, aminoglycoside and macrolide polyketides, underscoring how orthogonal malonyl-CoA circuits can unlock

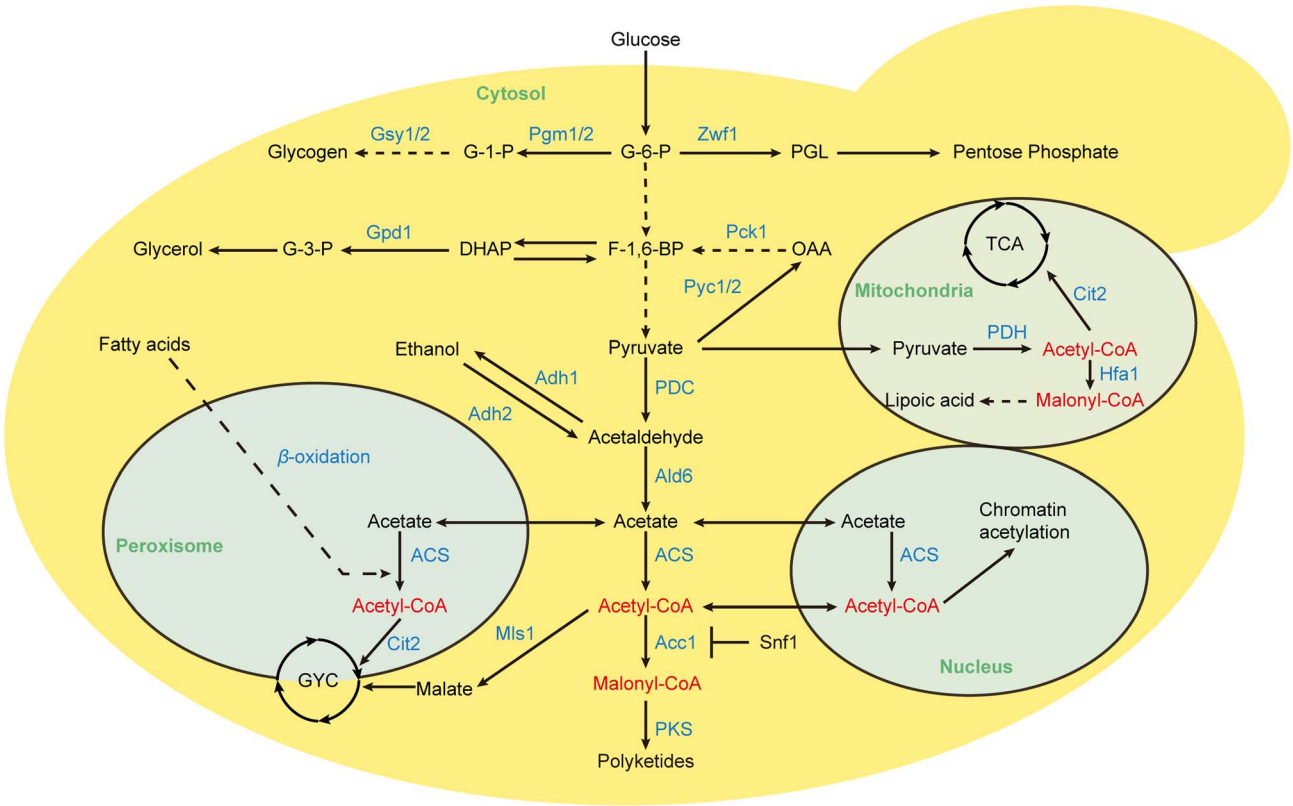


Fig. 18 Compartmentalized acetyl-CoA and malonyl-CoA metabolism in heterologous host and metabolic rewiring strategies to enhance precursor supply for polyketide biosynthesis. Yeast distributes acetyl-CoA metabolism across the cytosol, mitochondria, peroxisomes, and nucleus, generating multiple partially insulated cofactor pools that collectively determine the availability of building blocks for polyketide assembly. Cytosolic acetyl-CoA—derived from glycolysis (*via* pyruvate decarboxylation, acetaldehyde/ethanol conversion, or acetate activation), mitochondrial export, and peroxisomal β-oxidation—is converted into malonyl-CoA by acetyl-CoA carboxylase (Acc1). Activation of the AMP-activated protein kinase (AMPK) homolog Snf1 suppresses malonyl-CoA formation through phosphorylation-dependent inhibition of Acc1, creating a major regulatory node that influences PKS extender-unit flux. In parallel, the mitochondrial acetyl-CoA carboxylase Hfa1 provides an additional malonyl-CoA source, linking organelle-specific acetyl-CoA pools to global precursor availability. Metabolic engineering strategies therefore focus on rewiring cofactor and acyl-CoA metabolism to increase cytosolic acetyl-CoA generation, channel organelle-specific acetyl-CoA pools toward malonyl-CoA formation, alleviate Acc1/Snf1 regulation, and rebalance central pathways (glycolysis, TCA cycle, glyoxylate shunt, ethanol metabolism). In the schematic, enzymes are highlighted in blue, organelle compartments in green, and the production routes of acetyl-CoA and malonyl-CoA in red. Abbreviations: G-6-P, glucose-6-phosphate; G-1-P, glucose-1-phosphate; PGL, 6-phosphogluconolactone; F-1,6-BP, fructose-1,6-bisphosphate; DHAP, dihydroxyacetone phosphate; G-3-P, glyceraldehyde-3-phosphate; OAA, oxaloacetate; TCA, tricarboxylic acid cycle; GYC, glyoxylate cycle. Enzymes: Pgm1/2, phosphoglucose mutase; Gsy1/2, glycogen synthase; Zwf1, glucose-6-phosphate dehydrogenase; Gpd1, glycerol-3-phosphate dehydrogenase; Pyc1/2, pyruvate carboxylase; Pck1, PEP carboxykinase; PDH, pyruvate dehydrogenase complex; Cit2, citrate synthase; PDC, pyruvate decarboxylase; Adh1/2, alcohol dehydrogenase; Ald6, aldehyde dehydrogenase; ACS, acetyl-CoA synthase; Mls1, malate synthase; Acc1, acetyl-CoA carboxylase; Snf1, AMPK homolog; Hfa1, mitochondrial acetyl-CoA carboxylase.

broad polyketide chemical space rather than just boosting a single product.[303,304] In parallel, Klass *et al.* disrupted the native malonyl-CoA pathway and installed an orthogonal malonate transporter/ligase module, then used adaptive laboratory evolution (ALE) to identify regulatory mutations that further elevated malonyl-CoA and polyketide titers while suppressing off-target acyl-CoA utilization.[305] Conceptually, both studies illustrate a shift from incremental tuning of Acc1 towards modular malonyl-CoA "plug-ins" whose flux can be externally controlled (for example by malonate feeding) and whose architecture is less entangled with host lipid homeostasis—an attractive blueprint for constructing fungal or yeast chassis that can tolerate high malonyl-CoA levels while feeding diverse PKS libraries.

An orthogonal strategy is to route carbon into malonyl-CoA *via* amino acid-derived or β-alanine-based pathways, which can be thermodynamically favorable and avoid the kinetic and regulatory constraints of acetyl-CoA carboxylation. In *Y. lipolytica*, two malonyl-CoA pathways derived from L-glutamate and L-aspartate were recently engineered to enhance malonyl-CoA supply and support high-titer production of malonyl-derived compounds.[306] Complementary work in *Corynebacterium glutamicum* has combined β-alanine-based malonyl-CoA pathways with hybrid biological–chemical strategies to minimize carbon loss and expand the usable diacid feedstocks, thereby improving access to malonyl- and methylmalonyl-derived extender units for downstream polyketide synthases.[304] These examples highlight a broader design principle

 

that is equally relevant to fungal polyketides: building auxiliary malonyl-generating modules that can be switched on only when needed (for example during library production), reducing the burden on central metabolism while still enabling extensive exploration of non-native PKS building blocks.[304,306,307] Together, these developments suggest that future "designer" fungal polyketide platforms will rely less on simple *ACC1* overexpression and more on programmable precursor modules that can be dialed to support diverse PKS architectures and combinatorial tailoring, while maintaining host viability and providing built-in selection handles for library exploration.

### 4.5. Compartmentalization engineering

Beyond pathway refactoring and precursor rewiring, many fungal type I polyketide pathways are inherently partitioned across organelles such as the cytosol, endoplasmic reticulum (ER), Golgi, peroxisomes, vacuoles and toxin-associated vesicles (Fig. 18).[308] Systematic imaging and genetics have revealed that iPKSs and their tailoring enzymes often assemble into spatially confined "microfactories", which shape precursor access, constrain reactive intermediates, and couple product formation to self-protection.[38] For designer fungal polyketides, this spatial layer is not just a curiosity: it offers an additional handle to program which precursors are available, where β-oxidation-like editing occurs, and how toxic scaffolds are sequestered or exported.

A well-resolved example is the mycophenolic acid (MPA), where an nrPKS (MpaC') produces the 5-methylorsellinic acid core in the cytosol, while a P450–hydrolase fusion (MpaDE') and an oxidase (MpaB') are anchored on the ER, and the prenyltransferase MpaA' resides at the Golgi.[309] The pathway is completed by a β-oxidation-like cascade and a dedicated acyl-CoA hydrolase (MpaH') in peroxisomes, which iteratively shorten and release the side chain to give MPA.[310] This multi-organelle layout, elucidated by GFP tagging and organelle markers, shows how a fungal nrPKS core is functionally wired to peroxisomal lipid metabolism and ER/Golgi trafficking.[309] Recent work further optimizes the β-oxidation-like steps for improved MPA titers and suggests that tuning peroxisomal chain-shortening can, in principle, be used to generate non-natural analogues with modified side chains.[311]

Subcellular mapping of other mycotoxin pathways supports a similar design logic. In the viriditoxin pathway, the nrPKS VdtA and associated tailoring enzymes localize to punctate structures consistent with peroxisome-like compartments, and a membrane transporter VdtG is required for efficient dimer formation and export, pointing to a confined, transporter-gated assembly line.[220] For the *Alternaria* AK toxin, several enzymes in the polyketide-derived portion of the pathway carry canonical C-terminal peroxisomal targeting sequences; mutational removal of these tripeptides relocalizes the proteins to the cytosol and disrupts toxin formation, directly demonstrating that peroxisomal import is necessary for productive polyketide assembly.[312] In aflatoxin and sterigmatocystin biosynthesis, peroxisomes again contribute acetyl-CoA *via* β-oxidation, while enzymes that act later in the pathway relocalize from the cytosol to ER-derived "aflatoxisomes" and other toxin-associated vesicles as biosynthesis is induced, linking flux control and self-resistance to the formation of dedicated vesicular compartments.[313]

Together, these studies outline a set of design principles that are directly relevant for engineering fungal platforms for designer polyketides. First, short peroxisomal targeting signals and ER/Golgi anchor motifs can be used to deliberately co-localize iPKSs with β-oxidation modules or redox-intense tailoring enzymes, as exemplified by MPA, AK toxin and aflatoxin pathways.[309,314] Second, transporter positioning at organelle membranes (such as VdtG in viriditoxin biosynthesis) can be exploited to gate intermediate export and to separate toxic end products from sensitive cellular targets.[220,315] Finally, the emergence of toxisome-like vesicles shows that fungal cells can build inducible, ER-connected reaction chambers around polyketide pathways; analogous "synthetic toxisomes" in engineered strains could host highly reactive halogenases, P450 cascades or dimerizing laccases discussed in previous sections.[313]

Early proof-of-concept work in yeast cell factories already mirrors parts of this strategy: peroxisomal acetyl-CoA has been tapped directly for polyketide synthesis by co-targeting Acc and model PKSs to the peroxisome,[298] and compartmentalizing toxic enzymes into peroxisomes has been shown to alleviate cytotoxicity while maintaining flux through specialized pathways.[316,317] Although these examples mainly involve non-fungal or type III systems, they reinforce the notion that organelles can be repurposed as programmable microreactors. Looking forward, combining such compartmentalization strategies with the dynamic control and biosensor frameworks outlined above—ideally using compartment-specific sensors or inducible targeting tags—should enable fungal hosts in which iPKSs and tailoring enzymes are not only sequence-programmed but also spatially orchestrated, completing the platform vision of fungal polyketide biosynthesis as a chassis for designer natural products (Fig. 18).

## 5. Perspectives

In the coming years, we anticipate that fungal iPKSs will increasingly be treated as programmable molecular machines rather than idiosyncratic "black boxes". Structural biology has now illuminated several recurring "programming rules" – including domain competition for shared intermediates (for example between MT, KR and NRPS loading domains),[23] SAT-mediated starter and chain-length filtering,[16,51] and TE-gated decisions that determine whether a given intermediate is edited, cyclized or hydrolyzed.[198] Cryo-EM structures of full or partial megasynthases, combined with biochemical dissection of condensed regions and isolated tailoring domains, have started to reveal how conformational dynamics and domain–domain interfaces encode these rules in three dimensions.[33] At the same time, high-throughput mutagenesis and screening, together with AI-based structure prediction and molecular docking, are beginning to convert qualitative mechanistic models into quantitative design tools.[318]

It is important, however, to recognize the current practical boundaries of these approaches. AlphaFold-class models are highly reliable for predicting static folds and stable domain interfaces, but fungal iPKSs operate through dynamic conformational transitions, and catalytically relevant states may be transient and only partially captured in single-structure predictions.[31] Similarly, docking simulations of ACP-tethered intermediates are often weakly constrained, as the flexible phosphopantetheine arm and iterative substrate repositioning introduce degrees of freedom that are difficult to model without complementary crosslinking data or cryo-EM state trapping.[102,203] In addition, many fungal PKSs function within multiprotein assemblies or engage *trans*-acting partners, where predicted interfaces should be interpreted as testable hypotheses rather than definitive solutions.[31,130] Addressing these limitations—through integration of structural ensembles, experimental state stabilization and iterative model validation—will be essential for transforming AI-assisted predictions from suggestive models into genuinely predictive engineering tools. We expect that expanding structural coverage across hrPKS, prPKS, nrPKS and hybrid PKS-NRPS families, particularly for transient states and *trans*-acting partners, will be essential to move from *post hoc* explanation toward truly predictive control of chain length, reduction pattern and cyclization outcomes.

For combinatorial biosynthesis, the accumulated "successes and failures" now point to several practical design principles. First, random domain swapping is unlikely to be productive; instead, exchanges should be aligned with natural interface boundaries and respect native docking interactions, especially around SAT–KS, ACP–partner and TE/CLC gates that act as context-dependent filters for chain length and ring topology.[209] Second, TE, SAT and PT domains should be treated as coupled decision nodes: TE specificity often determines whether a chimeric enzyme produces a macrocycle, a linear shunt product or nothing at all, while SAT and PT impose upstream constraints on accessible intermediates.[35] Third, computation should precede construction: sequence co-evolution analysis, AlphaFold-class interface models and MD-based conformational sampling can be used to pre-screen domain pairings, identify incompatible surfaces and prioritise a smaller set of rational chimeras for experimental testing.[189] Finally, combinatorial PKS engineering needs to be embedded in high-throughput design-build–test–learn loops, where barcoded libraries, miniaturised cultivation and multiplexed LC-MS readouts are coupled to machine-learning models that update design rules based on both positive and negative outcomes.[319,320] In this framework, the goal is no longer to find isolated "lucky" non-natural products, but to establish programmable PKS platforms that can be steered toward defined regions of chemical space with quantifiable success rates.

On the cell-factory side, fungal polyketides are ideally positioned to benefit from integrated chassis and pathway engineering. The past decade has demonstrated that supply of acetyl-CoA, malonyl-CoA and redox cofactors can be substantially improved by combining precursor pathway rewiring, cofactor balancing and biosensor-guided dynamic control; yet for fungal polyketides this has so far been explored only in a limited set of chassis and pathways.[297,321,322] Building on this work, a key future direction will be to treat dynamic regulation engineering, subcellular compartmentalization and cofactor management as a unified design problem. For example, targeting PKSs and accessory enzymes to peroxisomes, mitochondria or engineered micro-compartments could decouple polyketide biosynthesis from central carbon flux, enrich hydrophobic intermediates and enable local CoA recycling, while parallel engineering of cytosolic acetyl-CoA and malonyl-CoA pools maintains robust growth. In parallel, malonyl-CoA- and polyketide-responsive biosensors, RNA-based switches and tunable feedback controllers will be needed to implement closed-loop regulation that adapts enzyme expression to precursor availability and alleviates toxicity in real time.[323]

Looking ahead, we foresee at least three interlinked challenges and opportunities. First, there is a pressing need to close the gap between sequence and function by integrating high-resolution structures, AI-based prediction and systematic mutational data into unified models that can forecast iterative programming outcomes for uncharacterized PKSs. Second, combinatorial biosynthesis must evolve from semi-empirical domain swapping to rational, AI-assisted exploration of design space, where interface-aware chimeras, engineered tailoring enzymes and precursor-directed strategies are designed and evaluated in a data-driven manner across entire families of PKSs and tailoring networks. Third, fungal and yeast cell factories should be developed as versatile platforms that can host multiple polyketide families, combining genome mining, modular BGC integration, organelle and membrane engineering, and automated DBTL cycles for rapid strain optimisation.[324] Finally, translating these advances into drug discovery, agrochemicals and sustainable materials will require closer coupling between cheminformatics, bioactivity profiling and process engineering so that "designer" polyketides can be prioritized not only for structural novelty but also for manufacturability and application relevance. We envisage that integrating programmable PKS modules with versatile fungal and yeast cell factories will transform fungal polyketides from sporadic natural products into systematically accessible molecular platforms for future medicines and renewable functional materials.

## 6. Author contributions

Sang Yup Lee, Yeo Joon Yoon, and Ye Li conceived and supervised the manuscript. Pingxin Lin, Zhenhao Fu, Ye Li, Yeo Joon Yoon, and Sang Yup Lee wrote the manuscript. All authors proofread the entire manuscript and provided suggestions for improvement on all sections.

## 7. Conflicts of interest

There are no conflicts to declare.

## 8. Data availability

No primary research results, software or code have been included and no new data were generated or analysed as part of this review.

## 9. Acknowledgements

This research was supported by the Bio & Medical Technology Development Program of the National Research Foundation funded by the Ministry of Science and ICT (No. RS-2025-02263193). The authors thank OpenAI for providing access to ChatGPT, which was used after manuscript completion for grammar checking and language refinement. All conceptual development and final content of the manuscript were conceived, written, and verified by the authors.

## 10. References

1 H. Hussain, A. M. Al-Sadi, B. Schulz, M. Steinert, A. Khan, I. R. Green and I. Ahmed, *Future Med. Chem.*, 2017, **9**, 1631–1648.
2 L. Katz, *J. Ind. Microbiol. Biotechnol.*, 2016, **43**, 155–176.
3 D. J. Newman and G. M. Cragg, *J. Nat. Prod.*, 2016, **79**, 629–661.
4 D. J. Newman and G. M. Cragg, *J. Nat. Prod.*, 2020, **83**, 770–803.
5 D. J. Newman, *Natl. Sci. Rev.*, 2022, **9**, nwac206.
6 M. C. Stroe, J. Gao, M. Pitz and R. Fischer, *Mol. Microbiol.*, 2024, **121**, 18–25.
7 Y. H. Chooi and Y. Tang, *J. Org. Chem.*, 2012, **77**, 9933–9953.
8 J. Huffman, R. Gerber and L. Du, *Biopolymers*, 2010, **93**, 764–776.
9 D.-S. Tian, X. Zhang and R. J. Cox, *Nat. Prod. Rep.*, 2025, **42**, 720–738.
10 K. Wadhwa, N. Kapoor, H. Kaur, E. A. Abu-Seer, M. Tariq, S. Siddiqui, V. K. Yadav, P. Niazi, P. Kumar and S. Alghamdi, *Mycobiology*, 2024, **52**, 335–387.
11 S. Kushwaha, H. Soni, S. Tandon, G. Singh, Y. Gandhi, V. Kumar, C. Jagtap, C. V. Narasimhaji, S. Mathapati, N. Srikanth and R. Acharya, *Food Nutr.*, 2025, **1**, 100005.
12 C. K. Anumudu, C. T. Ekwueme, C. C. Uhegwu, C. Ejileugha, J. Augustine, C. A. Okolo and H. Onyeaka, *Int. J. Mol. Sci.*, 2025, **26**, 184.
13 M. Liu, X. Zhang, H. Luan, Y. Zhang, W. Xu, W. Feng and P. Song, *Front. Microbiol.*, 2024, **15**, 1434987.
14 S. Yuan, J. V. Gopal, S. Ren, L. Chen, L. Liu and Z. Gao, *Eur. J. Med. Chem.*, 2020, **202**, 112502.
15 J. Wang, Z. Deng, J. Liang and Z. Wang, *Nat. Prod. Rep.*, 2023, **40**, 1498–1520.
16 N. A. Löhr, M. Rakhmanov, J. M. Wurlitzer, G. Lackner, M. Gressler and D. Hoffmeister, *Fungal Biol. Biotechnol.*, 2023, **10**, 17.
17 E. M. Musiol-Kroll, F. Zubeil, T. Schafhauser, T. Härtner, A. Kulik, J. McArthur, I. Koryakina, W. Wohlleben, S. Grond, G. J. Williams, S. Y. Lee and T. Weber, *ACS Synth. Biol.*, 2017, **6**, 421–427.
18 J. E. Kim, I. S. Jang, S. H. Son, Y. J. Ko, B. K. Cho, S. C. Kim and J. Y. Lee, *Metab. Eng.*, 2019, **56**, 50–59.
19 H. Chen and L. Du, *Appl. Microbiol. Biotechnol.*, 2016, **100**, 541–557.
20 H. Jenke-Kodama, A. Sandmann, R. Müller and E. Dittmann, *Mol. Biol. Evol.*, 2005, **22**, 2027–2039.
21 B. Wang, F. Guo, C. Huang and H. Zhao, *Proc. Natl. Acad. Sci. U. S. A.*, 2020, **117**, 8449–8454.
22 A. O. Zabala, Y. H. Chooi, M. S. Choi, H. C. Lin and Y. Tang, *ACS Chem. Biol.*, 2014, **9**, 1576–1586.
23 M. E. Foran, N. B. Auckloo, Y. T. C. Ho, S. Liu, Y. Hai and M. Jenner, *Chem. Sci.*, 2025, **16**, 13173–13182.
24 R. J. Cox, *Nat. Prod. Rep.*, 2023, **40**, 9–27.
25 R. P. P. Neves, P. Ferreira, F. E. Medina, P. Paiva, J. P. M. Sousa, M. F. Viegas, P. A. Fernandes and M. J. Ramos, *Top. Catal.*, 2022, **65**, 544–562.
26 S. C. Tsai, *Annu. Rev. Biochem.*, 2018, **87**, 503–531.
27 J. C. Frisvad, T. Isbrandt and T. O. Larsen, in *Comprehensive Natural Products III*, ed. H.-W. Liu and T. P. Begley, Elsevier, Oxford, 2020, vol. 1, pp. 313–332.
28 G. W. Heberlig, M. Wirz, M. Wang and C. N. Boddy, *Org. Lett.*, 2014, **16**, 5858–5861.
29 L. Zhang, Y. Liu, K. Chen, Q. Yue, C. Wang, L. Xie, I. Molnár and Y. Xu, *Metab. Eng.*, 2025, **92**, 125–135.
30 D. A. Herbst, C. A. Townsend and T. Maier, *Nat. Prod. Rep.*, 2018, **35**, 1046–1069.
31 J. Wang, J. Liang, L. Chen, W. Zhang, L. Kong, C. Peng, C. Su, Y. Tang, Z. Deng and Z. Wang, *Nat. Commun.*, 2021, **12**, 867.
32 K. Schmidt and R. J. Cox, *RSC Adv.*, 2024, **14**, 8963–8970.
33 M. F. J. Mabesoone, S. Leopold-Messer, H. A. Minas, C. Chepkirui, P. Chawengrum, S. Reiter, R. A. Meoded, S. Wolf, F. Genz, N. Magnus, B. Piechulla, A. S. Walker and J. Piel, *Science*, 2024, **383**, 1312–1317.
34 E. Skellam, *Trends Biotechnol.*, 2019, **37**, 416–427.
35 E. Skellam, S. Rajendran and L. Li, *Commun. Chem.*, 2024, **7**, 89.
36 F. Alberti, G. D. Foster and A. M. Bailey, *Appl. Microbiol. Biotechnol.*, 2017, **101**, 493–500.
37 J.-Y. Shen, Q. Zhao and Q.-L. He, *ACS Synth. Biol.*, 2023, **12**, 1908–1923.
38 X. Meng, Y. Fang, M. Ding, Y. Zhang, K. Jia, Z. Li, J. Collemare and W. Liu, *Biotechnol. Adv.*, 2022, **54**, 107866–107886.
39 H. Liu, M. Marsafari, F. Wang, L. Deng and P. Xu, *Metab. Eng.*, 2019, **56**, 60–68.
40 C. M. Palmer, K. K. Miller, A. Nguyen and H. S. Alper, *Metab. Eng.*, 2020, **57**, 174–181.
41 M. Klaus, E. Rossini, A. Linden, K. S. Paithankar, M. Zeug, Z. Ignatova, H. Urlaub, C. Khosla, J. Köfinger, G. Hummer and M. Grininger, *JACS Au*, 2021, **1**, 2162–2171.
42 J. I. Massawe, J. M. Madede, C. P. Mrina, C. B. Mpinda and F. N. Mpenda, *Discover Life*, 2025, **55**, 25.
43 Y. Zhou, W. Tao, Z. Qi, J. Wei, T. Shi, Q. Kang, J. Zheng, Y. Zhao and L. Bai, *ACS Catal.*, 2022, **12**, 762–776.
44 Y. Li, P. Lin, X. Lu, H. Yan, H. Wei, C. Liu, X. Liu, Y. Yang, I. Molnár and Z. Bai, *ACS Synth. Biol.*, 2023, **12**, 2226–2235.
45 E. B. Go and Y. Tang, in *Comprehensive Natural Products III*, ed. H.-W. Liu and T. P. Begley, Elsevier, Oxford, 2020, vol. 1, pp. 333–364.
46 R. J. Cox and E. J. Skellam, in *Comprehensive Natural Products III*, ed. H.-W. Liu and T. P. Begley, Elsevier, Oxford, 2020, vol. 1, pp. 266–312.

47 L. Hang, N. Liu and Y. Tang, *ACS Catal.*, 2016, **6**, 5935–5945.
48 L. Liu, Z. Zhang, C.-L. Shao and C.-Y. Wang, *Front. Microbiol.*, 2017, **8**, 1685.
49 Y. Zhang, J. Bai, L. Zhang, C. Zhang, B. Liu and Y. Hu, *Angew. Chem., Int. Ed.*, 2021, **60**, 6639–6645.
50 D.-W. Gao, C. S. Jamieson, G. Wang, Y. Yan, J. Zhou, K. N. Houk and Y. Tang, *J. Am. Chem. Soc.*, 2021, **143**, 80–84.
51 N. A. Löhr, M. C. Urban, F. Eisen, L. Platz, W. Hüttel, M. Gressler, M. Müller and D. Hoffmeister, *ChemBioChem*, 2023, **24**, e202200649.
52 E. Skellam, *Nat. Prod. Rep.*, 2022, **39**, 754–783.
53 S. Poust, R. M. Phelan, K. Deng, L. Katz, C. J. Petzold and J. D. Keasling, *Angew. Chem., Int. Ed.*, 2015, **54**, 2370–2373.
54 T. M. McCullough, A. Dhar, D. L. Akey, J. R. Konwerski, D. H. Sherman and J. L. Smith, *Structure*, 2023, **31**, 1109–1120.
55 J. Takino, A. Kotani, T. Ozaki, W. Peng, J. Yu, Y. Guo, S. Mochizuki, K. Akimitsu, M. Hashimoto, T. Ye, A. Minami and H. Oikawa, *Angew. Chem., Int. Ed.*, 2021, **60**, 23403–23411.
56 R. A. Cacho, J. Thuss, W. Xu, R. Sanichar, Z. Gao, A. Nguyen, J. C. Vederas and Y. Tang, *J. Am. Chem. Soc.*, 2015, **137**, 15688–15691.
57 D. M. Roberts, C. Bartel, A. Scott, D. Ivison, T. J. Simpson and R. J. Cox, *Chem. Sci.*, 2017, **8**, 1116–1126.
58 X. L. Yang, S. Friedrich, S. Yin, O. Piech, K. Williams, T. J. Simpson and R. J. Cox, *Chem. Sci.*, 2019, **10**, 8478–8489.
59 Y. Tsunematsu, M. Fukutomi, T. Saruwatari, H. Noguchi, K. Hotta, Y. Tang and K. Watanabe, *Angew. Chem., Int. Ed.*, 2014, **53**, 8475–8479.
60 T. Yamamoto, Y. Tsunematsu, K. Hara, T. Suzuki, S. Kishimoto, H. Kawagishi, H. Noguchi, H. Hashimoto, Y. Tang, K. Hotta and K. Watanabe, *Angew. Chem., Int. Ed.*, 2016, **55**, 6207–6210.
61 H. Na, Y.-y. Zheng, Y. Jia, J. Feng, J. Huang, J. Huang, C.-Y. Wang and G. Yao, *Microb. Cell Fact.*, 2024, **23**, 134.
62 B. D. Ames, C. Nguyen, J. Bruegger, P. Smith, W. Xu, S. Ma, E. Wong, S. Wong, X. Xie, J. W. H. Li, J. C. Vederas, Y. Tang and S.-C. Tsai, *Proc. Natl. Acad. Sci. U. S. A.*, 2012, **109**, 11144–11149.
63 K. C. Mulder, F. Mulinari, O. L. Franco, M. S. Soares, B. S. Magalhaes and N. S. Parachin, *Biotechnol. Adv.*, 2015, **33**, 648–665.
64 O. Piech and R. J. Cox, *RSC Adv.*, 2020, **10**, 18469–18476.
65 J. Kuo, S. R. Lynch, C. W. Liu, X. Xiao and C. Khosla, *ACS Chem. Biol.*, 2016, **11**, 2636–2641.
66 D. Kong, Q. He, D.-M. Lin, H. Zhang, L. Chen, Y. Fan, M.-C. Tang and Y. Zou, *J. Am. Chem. Soc.*, 2025, **147**, 4701–4706.
67 Y. Feng, Y. Wang, J. Liu, Y. Liu, X. Cao and S. Xue, *ACS Chem. Biol.*, 2017, **12**, 2830–2836.
68 H. Tao, T. Mori, X. Wei, Y. Matsuda and I. Abe, *Angew. Chem., Int. Ed.*, 2021, **60**, 8851–8858.
69 S. Kishimoto, Y. Tsunematsu, T. Matsushita, K. Hara, H. Hashimoto, Y. Tang and K. Watanabe, *Biochemistry*, 2019, **58**, 3933–3937.
70 L. Hang, M. C. Tang, C. J. B. Harvey, C. G. Page, J. Li, Y. S. Hung, N. Liu, M. E. Hillenmeyer and Y. Tang, *Angew. Chem., Int. Ed.*, 2017, **56**, 9556–9560.
71 F. Jiang, A. Liu, Q. Wei and Y. Hu, *Chin. Chem. Lett.*, 2024, **35**, 109504.
72 W.-G. Wang, H. Wang, L.-Q. Du, M. Li, L. Chen, J. Yu, G.-G. Cheng, M.-T. Zhan, Q.-F. Hu, L. Zhang, M. Yao and Y. Matsuda, *J. Am. Chem. Soc.*, 2020, **142**, 8464–8472.
73 Y. Takekawa, J. Takino, S. Sato, H. Oikawa, T. Ose and A. Minami, *Biochem. Biophys. Res. Commun.*, 2025, **761**, 151737.
74 Q. Ji, X. Wei, S. Liu and Y. Matsuda, *Org. Lett.*, 2025, **27**, 36–40.
75 H. Kage, E. Riva, J. S. Parascandolo, M. F. Kreutzer, M. Tosin and M. Nett, *Org. Biomol. Chem.*, 2015, **13**, 11414–11417.
76 Y. H. Chooi, C. Krill, R. A. Barrow, S. Chen, R. Trengove, R. P. Oliver and P. S. Solomon, *Appl. Environ. Microbiol.*, 2015, **81**, 177–186.
77 J. Wei, L. Liu, X. Yuan, D. Wang, X. Wang, W. Bi, Y. Yang and Y. Wang, *Mycobiology*, 2023, **51**, 360–371.
78 M. Garello, E. Piombo, F. Buonsenso, S. Prencipe, S. Valente, G. R. Meloni, M. Marcet-Houben, T. Gabaldón and D. Spadaro, *Food Microbiol.*, 2024, **122**, 104532.
79 J. Punya, P. Swangmaneecharern, S. Pinsupa, P. Nitistaporn, S. Phonghanpot, V. Kunathigan, S. Cheevadhanarak, M. Tanticharoen and A. Amnuaykanjanasin, *Fungal Biol.*, 2015, **119**, 538–550.
80 M. Bejenari, E. M. L. Spedtsberg, J. Mathiesen, A. C. Jeppesen, L. Cernat, A. Toussaint, C. Apostol, V. Stoianov, T. B. Pedersen, M. R. Nielsen and J. L. Sørensen, *Front. Fungal Biol.*, 2024, **5**, 1327777.
81 H. Wang, C. Peng, X.-X. Chen, H.-Y. Wang, R. Yang, H. Xiang, Q.-F. Hu, L. Liu, L. W. Chung, Y. Matsuda and W.-G. Wang, *ACS Catal.*, 2024, **14**, 10796–10805.
82 B. Li, Y. Chen, Y. Zong, Y. Shang, Z. Zhang, X. Xu, X. Wang, M. Long and S. Tian, *Environ. Microbiol.*, 2019, **21**, 1124–1139.
83 C. Kong, H. Huang, Y. Xue, Y. Liu, Q. Peng, Q. Liu, Q. Xu, Q. Zhu, Y. Yin, X. Zhou, Y. Zhang and M. Cai, *Sci. Rep.*, 2018, **8**, 2116.
84 L. M. Petersen, D. K. Holm, P. B. Knudsen, K. F. Nielsen, C. H. Gotfredsen, U. H. Mortensen and T. O. Larsen, *J. Antibiot.*, 2015, **68**, 201–205.
85 P. Reveglia, M. Masi and A. Evidente, *Biomolecules*, 2020, **10**, 772.
86 L. Liu, M. C. Tang and Y. Tang, *J. Am. Chem. Soc.*, 2019, **141**, 19538–19541.
87 J. M. Crawford, A. L. Vagstad, K. P. Whitworth, K. C. Ehrlich and C. A. Townsend, *ChemBioChem*, 2008, **9**, 1019–1023.
88 J. M. Winter, D. Cascio, D. Dietrich, M. Sato, K. Watanabe, M. R. Sawaya, J. C. Vederas and Y. Tang, *J. Am. Chem. Soc.*, 2015, **137**, 9885–9893.
89 A. Nivina, K. P. Yuet, J. Hsu and C. Khosla, *Chem. Rev.*, 2019, **119**, 12524–12547.
90 M. Choquer, K. L. Dekkers, H. Q. Chen, L. Cao, P. P. Ueng, M. E. Daub and K. R. Chung, *Mol. Plant-Microbe Interact.*, 2005, **18**, 468–476.

 

91 D. A. Herbst, C. R. Huitt-Roehl, R. P. Jakob, J. M. Kravetz, P. A. Storm, J. R. Alley, C. A. Townsend and T. Maier, *Nat. Chem. Biol.*, 2018, **14**, 474–479.
92 P. Chattopadhyay and G. Banerjee, *J. Fungi*, 2025, **11**, 641.
93 F. Li, Z. Lin, J. P. Torres, E. A. Hill, D. Li, C. A. Townsend and E. W. Schmidt, *J. Am. Chem. Soc.*, 2022, **144**, 9363–9371.
94 P. A. Storm, D. A. Herbst, T. Maier and C. A. Townsend, *Cell Chem. Biol.*, 2017, **24**, 316–325.
95 D. Yan and Y. Matsuda, *Small Methods*, 2024, **8**, 2400107.
96 J. F. Barajas, G. Shakya, G. Moreno, H. Rivera Jr, D. R. Jackson, C. L. Topper, A. L. Vagstad, J. J. La Clair, C. A. Townsend, M. D. Burkart and S. C. Tsai, *Proc. Natl. Acad. Sci. U. S. A.*, 2017, **114**, E4142–E4148.
97 J. M. Crawford, T. P. Korman, J. W. Labonte, A. L. Vagstad, E. A. Hill, O. Kamari-Bidkorpeh, S. C. Tsai and C. A. Townsend, *Nature*, 2009, **461**, 1139–1143.
98 L. Liu, Z. Zhang, C. L. Shao, J. L. Wang, H. Bai and C. Y. Wang, *Sci. Rep.*, 2015, **5**, 10463.
99 V. Schroeckh, K. Scherlach, H.-W. Nützmann, E. Shelest, W. Schmidt-Heck, J. Schuemann, K. Martin, C. Hertweck and A. Brakhage Axel, *Proc. Natl. Acad. Sci. U. S. A.*, 2009, **106**, 14558–14563.
100 E. Szewczyk, Y. M. Chiang, C. E. Oakley, A. D. Davidson, C. C. Wang and B. R. Oakley, *Appl. Environ. Microbiol.*, 2008, **74**, 7607–7612.
101 Y. Li, W. Xu and Y. Tang, *J. Biol. Chem.*, 2010, **285**, 22764–22773.
102 Y. Feng, X. Yang, H. Ji, Z. Deng, S. Lin and J. Zheng, *Commun. Biol.*, 2022, **5**, 508.
103 S. S. Gao, A. Duan, W. Xu, P. Yu, L. Hang, K. N. Houk and Y. Tang, *J. Am. Chem. Soc.*, 2016, **138**, 4249–4259.
104 M. R. Nielsen, T. Sørensen, T. B. Pedersen, K. R. Westphal, L. Díaz Fernández De Quincoces, T. E. Sondergaard, R. Wimmer, D. W. Brown and J. L. Sørensen, *Fungal Genet. Biol.*, 2024, **174**, 103912.
105 N. A. Löhr, L. Platz, D. Hoffmeister and M. Müller, *Curr. Opin. Chem. Biol.*, 2024, **82**, 102510.
106 A. L. Vagstad, A. G. Newman, P. A. Storm, K. Belecki, J. M. Crawford and C. A. Townsend, *Angew. Chem., Int. Ed.*, 2013, **52**, 1718–1721.
107 Z. C. Litman, Y. Chen and D. H. Sherman, *J. Am. Chem. Soc.*, 2025, **147**, 40305–40318.
108 T. P. Korman, J. M. Crawford, J. W. Labonte, A. G. Newman, J. Wong, C. A. Townsend and S. C. Tsai, *Proc. Natl. Acad. Sci. U. S. A.*, 2010, **107**, 6246–6251.
109 J. M. Crawford, P. M. Thomas, J. R. Scheerer, A. L. Vagstad, N. L. Kelleher and C. A. Townsend, *Science*, 2008, **320**, 243–246.
110 K. D. Patel, F. B. d'Andrea, N. M. Gaudelli, A. R. Buller, C. A. Townsend and A. M. Gulick, *Nat. Commun.*, 2019, **10**, 3868.
111 A. L. Vagstad, E. A. Hill, J. W. Labonte and C. A. Townsend, *Chem. Biol.*, 2012, **19**, 1525–1534.
112 Q. Liu, D. Zhang, S. Gao, X. Cai, M. Yao, Y. Xu, Y. Gong, K. Zheng, Y. Mao, L. Yang, D. Yang, I. Molnár and X. Yang, *Angew. Chem., Int. Ed.*, 2023, **62**, e202214379.
113 X. Zhang, L. Liu, J. Huang, X. Ren, G. Zhang, Q. Che, D. Li and T. Zhu, *Mar. Drugs*, 2025, **23**, 130.
114 N. Sbaraini, A. Crombie, J. A. Kalaitzis, D. Vuong, J. Bracegirdle, F. Windsor, A. Lau, R. Chen, Y. P. Tan, A. Lacey, E. Lacey, A. M. Piggott and Y.-H. Chooi, *Chem. Sci.*, 2024, **15**, 18872–18880.
115 C. W. Johnson, L. Nuniz, B. Perlatti, G. F. Bills and Y. Tang, *ChemBioChem*, 2025, **26**, e202500003.
116 C.-Y. Chiang, M. Ohashi and Y. Tang, *Nat. Prod. Rep.*, 2023, **40**, 89–127.
117 G. Lackner, M. Misiek, J. Braesel and D. Hoffmeister, *Fungal Genet. Biol.*, 2012, **49**, 996–1003.
118 Y. Li, Y.-H. Chooi, Y. Sheng, J. S. Valentine and Y. Tang, *J. Am. Chem. Soc.*, 2011, **133**, 15773–15785.
119 D. Jiang, Y. Li, W. Wu, H. Zhang, R. Xu, H. Xu, R. Zhan and L. Sun, *Biotechnol. Bioeng.*, 2021, **118**, 4623–4634.
120 A. L. Vagstad, S. B. Bumpus, K. Belecki, N. L. Kelleher and C. A. Townsend, *J. Am. Chem. Soc.*, 2012, **134**, 6865–6877.
121 S. Hwang, N. Lee, S. Cho, B. Palsson and B.-K. Cho, *Front. Mol. Biosci.*, 2020, **7**, 87.
122 F. Xie, A. F. Kiefer, A. K. H. Hirsch, O. V. Kalinina, C. Fu and R. Müller, *Cell Rep. Phys. Sci.*, 2023, **4**, 101394.
123 M. C. Tang, C. R. Fischer, J. V. Chari, D. Tan, S. Suresh, A. Chu, M. Miranda, J. Smith, Z. Zhang, N. K. Garg, R. P. St Onge and Y. Tang, *J. Am. Chem. Soc.*, 2019, **141**, 8198–8206.
124 G. Jogl and L. Tong, *Cell*, 2003, **112**, 113–122.
125 F. Ozhelvaci and K. Steczkiewicz, *Proteins:Struct., Funct., Bioinf.*, 2025, **93**, 855–870.
126 Y. Ding, X. Long, J. Zhang, C. Qu, P. Wang, X. Yang, P.-T. Puno and J. Deng, *Chem. Sci.*, 2025, **16**, 8302–8308.
127 A. A. Stierle, D. B. Stierle, J. Alverson and N. Gibson, *J. Nat. Prod.*, 2021, **84**, 3064–3070.
128 Y. Morishita, H. Zhang, T. Taniguchi, K. Mori and T. Asai, *Org. Lett.*, 2019, **21**, 4788–4792.
129 F. Trenti, K. E. Lebe, E. Adelin, J. Ouazzani, C. Schotte and R. J. Cox, *RSC Adv.*, 2020, **10**, 27369–27376.
130 W. Xu, Y. H. Chooi, J. W. Choi, S. Li, J. C. Vederas, N. A. Da Silva and Y. Tang, *Angew. Chem., Int. Ed.*, 2013, **52**, 6472–6475.
131 G. Kim, D. Lee, J. H. Kim, S. D. Kim, H. Kim, J. H. Kim, S. S. Yim, S.-J. Yeom, J. D. Keasling and B.-K. Cho, *Nat. Prod. Rep.*, 2025, **42**, 1489–1506.
132 P. A. Storm and C. A. Townsend, *Chem. Commun.*, 2018, **54**, 50–53.
133 M. Sasseville, H. D. T. Nguyen, S. Drouin and A. Bahadoor, *ACS Omega*, 2024, **9**, 20368–20377.
134 K. K. Nagasawa, K. M. Yost, Z. Sun and Y. Tang, *ChemBioChem*, 2025, **26**, e202400846.
135 L. Sun, G. Liu, Y. Li, D. Jiang, W. Guo, H. Xu and R. Zhan, *Metab. Eng.*, 2019, **54**, 212–221.
136 N. Choudhary, T. E. Collignon, D. Tewari and A. Bishayee, *Phytomedicine*, 2022, **105**, 154356.
137 P. A. Baldera-Aguayo, A. Lee and V. W. Cornish, *ACS Synth. Biol.*, 2022, **11**, 2429–2444.
138 L. Kahlert, M. Villanueva, R. J. Cox and E. J. Skellam, *Angew. Chem., Int. Ed.*, 2021, **60**, 11423–11429.

139 Y. Chainani, J. Diaz, M. Guilarte-Silva, V. Blay, Q. Zhang, W. Sprague, K. E. J. Tyo, L. J. Broadbelt, A. Mukhopadhyay, J. D. Keasling, H. G. Martin and T. W. H. Backman, *Nat. Commun.*, 2025, **16**, 5787.
140 J. Yuan, D. Li, L. Qin, J. Shen, X. Guo, E. Tumukunde, M. Li and S. Wang, *BMC Mol. Biol.*, 2019, **20**, 4.
141 M. Hauser, J. Pang, D. Lai, Y. Sun, H. Yao and R. Cox, *ChemRxiv*, 2025, preprint, DOI: 10.26434/chemrxiv-2025-lmg8x-v2.
142 K. Williams, C. Greco, A. M. Bailey and C. L. Willis, *ChemBioChem*, 2021, **22**, 3027–3036.
143 Y. Q. Xu, T. Zhou, S. W. Zhang, P. Espinosa-Artiles, L. Y. Wang, W. Zhang, M. Lin, A. A. L. Gunatilaka, J. X. Zhan and I. Molnár, *Proc. Natl. Acad. Sci. U. S. A.*, 2014, **111**, 12354–12359.
144 S. J. Hoogstra, K. N. Hendricks, D. R. McMullin, J. B. Renaud, J. Bora, M. W. Sumarah and C. P. Garnham, *Toxins*, 2024, **16**, 404.
145 H. Zhou, K. Qiao, Z. Gao, J. C. Vederas and Y. Tang, *J. Biol. Chem.*, 2010, **285**, 41412–41421.
146 G. Yao, X. Bai, B. Zhang, L. Wang, S. Chen and Z. Wang, *Microb. Cell Fact.*, 2022, **21**, 136.
147 L. Kahlert, D. Bernardi, M. Hauser, L. P. Ióca, R. G. S. Berlinck, E. J. Skellam and R. J. Cox, *Chem.–Eur. J.*, 2021, **27**, 11895–11903.
148 Z. Z. Zhou, H. J. Zhu, L. P. Lin, X. Zhang, H. M. Ge, R. H. Jiao and R. X. Tan, *Chem. Sci.*, 2019, **10**, 73–82.
149 L. Feng, M. T. Gordon, Y. Liu, K. B. Basso and R. A. Butcher, *Nat. Commun.*, 2021, **12**, 4912.
150 C. D. Campbell and J. C. Vederas, *Biopolymers*, 2010, **93**, 755–763.
151 F.-Q. Guo, K.-W. Xu, J.-S. Wu, Z.-X. Peng, X.-L. Yuan, Y. Yuan, J.-T. Shi, Y.-Q. Li, C.-S. Zhang and D.-L. Zhao, *Ind. Crops Prod.*, 2025, **232**, 121295.
152 Z. Huang, W. Zhu, Y. Bai, X. Bai and H. Zhang, *Microb. Cell Fact.*, 2024, **23**, 93.
153 N. E. Kim and J. R. Dettman, *BMC Genomics*, 2025, **26**, 678.
154 Y. Hai and Y. Tang, *J. Am. Chem. Soc.*, 2018, **140**, 1271–1274.
155 S. Bonhomme, C. Contreras-Martel, A. Dessen and P. Macheboeuf, *Structure*, 2023, **31**, 700–712.
156 L. Chen, X. Wang, Y. Zou and M.-C. Tang, *Org. Lett.*, 2024, **26**, 3597–3601.
157 Y. Jiao, J. Ling, R. A. A. Khan, N. Luo, Z. Li, Z. Li, Y. Yang, J. Zhao, Z. Mao, G. F. Bills, B. Xie and Y. Li, *J. Agric. Food Chem.*, 2025, **73**, 226–236.
158 K. A. J. Bozhüyük, L. Präve, C. Kegler, L. Schenk, S. Kaiser, C. Schelhas, Y.-N. Shi, W. Kuttenlochner, M. Schreiber, J. Kandler, M. Alanjary, T. M. Mohiuddin, M. Groll, G. K. A. Hochberg and H. B. Bode, *Science*, 2024, **383**, eadg4320.
159 T. Awakawa, T. Fujioka, L. Zhang, S. Hoshino, Z. Hu, J. Hashimoto, I. Kozone, H. Ikeda, K. Shin-Ya, W. Liu and I. Abe, *Nat. Commun.*, 2018, **9**, 3534.
160 X. Huang, W. Zhang, S. Tang, S. Wei and X. Lu, *Angew. Chem., Int. Ed.*, 2020, **59**, 4349–4353.
161 A. O. Zabala, W. Xu, Y.-H. Chooi and Y. Tang, *Chem. Biol.*, 2012, **19**, 1049–1059.
162 Y. Wang, K. J. Torma, J. B. Pyser, P. M. Zimmerman and A. R. H. Narayan, *ACS Cent. Sci.*, 2024, **10**, 708–716.
163 M. Sato, J. E. Dander, C. Sato, Y. S. Hung, S. S. Gao, M. C. Tang, L. Hang, J. M. Winter, N. K. Garg, K. Watanabe and Y. Tang, *J. Am. Chem. Soc.*, 2017, **139**, 5317–5320.
164 H. Zhang, Z. Li, S. Zhou, S.-M. Li, H. Ran, Z. Song, T. Yu and W.-B. Yin, *Nat. Commun.*, 2022, **13**, 6361.
165 H. Zhang, A. Zhang, Y. Wen, J. Ji and W.-B. Yin, *J. Agric. Food Chem.*, 2025, **73**, 20810–20817.
166 J. C. Corpuz, J. O. Sanlley and M. D. Burkart, *Synth. Syst. Biotechnol.*, 2022, **7**, 677–688.
167 H. L. Schubert, F. Li, C. P. Hill and E. W. Schmidt, *Proc. Natl. Acad. Sci. U. S. A.*, 2025, **122**, e2419884122.
168 S. Furumura, T. Ozaki, A. Sugawara, Y. Morishita, K. Tsukada, T. Ikuta, A. Inoue and T. Asai, *J. Nat. Prod.*, 2023, **86**, 398–405.
169 O. J. Wouters, M. McKee and J. Luyten, *JAMA*, 2020, **323**, 844–853.
170 T. J. Hwang, J. J. Darrow and A. S. Kesselheim, *JAMA*, 2017, **318**, 2137–2138.
171 J. A. DiMasi, H. G. Grabowski and R. W. Hansen, *J. Health Econ.*, 2016, **47**, 20–33.
172 S. O. Oselusi, A. Christoffels and S. A. Egieyeh, *Molecules*, 2021, **26**, 3970–3988.
173 R. A. Shenvi, *ACS Cent. Sci.*, 2024, **10**, 519–528.
174 W. R. Miller and C. A. Arias, *Nat. Rev. Microbiol.*, 2024, **22**, 598–616.
175 C. Wieder, M. Künzer, R. Wiechert, K. Seipp, K. Andresen, P. Stark, A. Schüffler, T. Opatz and E. Thines, *Org. Lett.*, 2025, **27**, 1036–1041.
176 A. A. Nava, J. Roberts, R. W. Haushalter, Z. Wang and J. D. Keasling, *ACS Synth. Biol.*, 2023, **12**, 3148–3155.
177 H. Sun, Z. Liu, H. Zhao and E. L. Ang, *Drug Des., Dev. Ther.*, 2015, **9**, 823–833.
178 D. Goranovič, B. Jenko, B. Ramšak, A. Podgoršek Berke, L. Bedrač, J. Horvat, M. Šala, D. Makuc, G. M. Carriche, L. Silva, A. Lopez Krol, A. Pšeničnik, M. B. Durán Alonso, M. Avbelj, S. Stavber, J. Plavec, T. Sparwasser, R. Müller, G. Kosec, Š. Fujs and H. Petković, *J. Nat. Prod.*, 2025, **88**, 619–630.
179 K. A. Ray, J. D. Lutgens, R. Bista, J. Zhang, R. R. Desai, M. Hirsch, T. Miyazawa, A. Cordova and A. T. Keatinge-Clay, *Nat. Commun.*, 2024, **15**, 6485.
180 D. Chen, Z. Song, J. Han, J. Liu, H. Liu and J. Dai, *J. Am. Chem. Soc.*, 2024, **146**, 9614–9622.
181 G. Yook, J. Nam, Y. Jo, H. Yoon and D. Yang, *Microb. Cell Fact.*, 2025, **24**, 35.
182 M. Alanjary, C. Cano-Prieto, H. Gross and M. H. Medema, *Nat. Prod. Rep.*, 2019, **36**, 1249–1261.
183 T. Asai, K. Tsukada, S. Ise, N. Shirata, M. Hashimoto, I. Fujii, K. Gomi, K. Nakagawara, E. N. Kodama and Y. Oshima, *Nat. Chem.*, 2015, **7**, 737–743.
184 T. Asai, T. Yamamoto, N. Shirata, T. Taniguchi, K. Monde, I. Fujii, K. Gomi and Y. Oshima, *Org. Lett.*, 2013, **15**, 3346–3349.

 

185 C. R. Huitt-Roehl, E. A. Hill, M. M. Adams, A. L. Vagstad, J. W. Li and C. A. Townsend, *ACS Chem. Biol.*, 2015, **10**, 1443–1449.
186 Z. Gao, J. Wang, A. K. Norquay, K. Qiao, Y. Tang and J. C. Vederas, *J. Am. Chem. Soc.*, 2013, **135**, 1735–1738.
187 A. Palyzová, M. Kulišová, K. Majtán, K. Fous, I. J. Kolouchová and T. Řezanka, *Food Chem.*, 2025, **483**, 144204.
188 L. Milke and J. Marienhagen, *Appl. Microbiol. Biotechnol.*, 2020, **104**, 6057–6065.
189 E. Englund, M. Schmidt, A. A. Nava, S. Klass, L. Keiser, Q. Dan, L. Katz, S. Yuzawa and J. D. Keasling, *Nat. Commun.*, 2023, **14**, 4871.
190 U. Fatema, A. Broberg, D. F. Jensen, M. Karlsson and M. Dubey, *Sci. Rep.*, 2018, **8**, 15009.
191 N. A. Löhr, F. Eisen, W. Thiele, L. Platz, J. Motter, W. Hüttel, M. Gressler, M. Müller and D. Hoffmeister, *Angew. Chem., Int. Ed.*, 2022, **61**, e202116142.
192 A. G. Newman, A. L. Vagstad, P. A. Storm and C. A. Townsend, *J. Am. Chem. Soc.*, 2014, **136**, 7348–7362.
193 H. H. Yeh, S. L. Chang, Y. M. Chiang, K. S. Bruno, B. R. Oakley, T. K. Wu and C. C. Wang, *Org. Lett.*, 2013, **15**, 756–759.
194 P. A. Storm, P. Pal, C. R. Huitt-Roehl and C. A. Townsend, *ACS Chem. Biol.*, 2018, **13**, 3043–3048.
195 Y. M. Chiang, E. Szewczyk, A. D. Davidson, N. Keller, B. R. Oakley and C. C. Wang, *J. Am. Chem. Soc.*, 2009, **131**, 2965–2970.
196 T. Liu, J. F. Sanchez, Y. M. Chiang, B. R. Oakley and C. C. Wang, *Org. Lett.*, 2014, **16**, 1676–1679.
197 T. Liu, Y.-M. Chiang, A. D. Somoza, B. R. Oakley and C. C. C. Wang, *J. Am. Chem. Soc.*, 2011, **133**, 13314–13316.
198 C. Wang, X. Wang, L. Zhang, Q. Yue, Q. Liu, Y. M. Xu, A. A. L. Gunatilaka, X. Wei, Y. Xu and I. Molnár, *J. Am. Chem. Soc.*, 2020, **142**, 17093–17104.
199 K. M. Fisch, W. Bakeer, A. A. Yakasai, Z. Song, J. Pedrick, Z. Wasil, A. M. Bailey, C. M. Lazarus, T. J. Simpson and R. J. Cox, *J. Am. Chem. Soc.*, 2011, **133**, 16635–16641.
200 L. S. Keiser, P. P. Gatenil, Y. Zhu, K. Deng, L. Waldburger, J. W. Gin, Y. Chen, E. E. K. Baidoo, C. J. Petzold, N. Lanclos, T. R. Northen, E. Englund and J. D. Keasling, *J. Am. Chem. Soc.*, 2025, **147**, 42237–42252.
201 C. Cano-Prieto, A. Undabarrena, A. C. de Carvalho, J. D. Keasling and P. Cruz-Morales, *Annu. Rev. Biochem.*, 2024, **93**, 411–445.
202 M. A. Skiba, A. P. Sikkema, W. D. Fiers, W. H. Gerwick, D. H. Sherman, C. C. Aldrich and J. L. Smith, *ACS Chem. Biol.*, 2016, **11**, 3319–3327.
203 H. Ji, T. Shi, Y.-L. Zhao and J. Zheng, *ChemCatChem*, 2024, **16**, e202400800.
204 Y. Xu, T. Zhou, Z. Zhou, S. Su, S. A. Roberts, W. R. Montfort, J. Zeng, M. Chen, W. Zhang, M. Lin, J. Zhan and I. Molnár, *Proc. Natl. Acad. Sci. U. S. A.*, 2013, **110**, 5398–5403.
205 Y. Xu, T. Zhou, S. Zhang, L. J. Xuan, J. Zhan and I. Molnár, *J. Am. Chem. Soc.*, 2013, **135**, 10783–10791.
206 H. H. Yeh, S. L. Chang, Y. M. Chiang, K. S. Bruno, B. R. Oakley, T. K. Wu and C. C. Wang, *Org. Lett.*, 2013, **15**, 756–759.
207 T. B. Kakule, Z. Lin and E. W. Schmidt, *J. Am. Chem. Soc.*, 2014, **136**, 17882–17890.
208 J. Watzel, E. Duchardt-Ferner, S. Sarawi, H. B. Bode and J. Wöhnert, *Angew. Chem., Int. Ed.*, 2021, **60**, 14171–14178.
209 S. Collin and K. J. Weissman, *Nat. Commun.*, 2025, **16**, 6690.
210 X. J. Wang, C. Wang, L. X. Duan, L. W. Zhang, H. Liu, Y. M. Xu, Q. P. Liu, T. L. Mao, W. Zhang, M. Chen, M. Lin, A. A. L. Gunatilaka, Y. Q. Xu and I. Molnár, *J. Am. Chem. Soc.*, 2019, **141**, 4355–4364.
211 Y. Xu, T. Zhou, P. Espinosa-Artiles, Y. Tang, J. Zhan and I. Molnár, *ACS Chem. Biol.*, 2014, **9**, 1119–1127.
212 X. B. Tao, S. LaFrance, Y. Xing, A. A. Nava, H. G. Martin, J. D. Keasling and T. W. H. Backman, *Nucleic Acids Res.*, 2023, **51**, D532–D538.
213 A. D. Somoza, K. H. Lee, Y. M. Chiang, B. R. Oakley and C. C. Wang, *Org. Lett.*, 2012, **14**, 972–975.
214 J. Bai, Y. Y. Lu, Y. M. Xu, W. Zhang, M. Chen, M. Lin, A. A. L. Gunatilaka, Y. Q. Xu and I. Molnár, *Org. Lett.*, 2016, **18**, 1262–1265.
215 L. Fürtges, S. Obermaier, W. Thiele, S. Foegen and M. Müller, *ChemBioChem*, 2019, **20**, 1928–1932.
216 L. S. Mazzaferro, W. Hüttel, A. Fries and M. Müller, *J. Am. Chem. Soc.*, 2015, **137**, 12289–12295.
217 B. Tan, P. Breunig, L. Arbib, Y. Kakumu, F. Biermann, K. Hardes, J. Hefendehl and E. J. N. Helfrich, *Chem. Sci.*, 2025, **16**, 16240–16249.
218 Y. Liu, X. Li, S. Sui, J. Tang, D. Chen, Y. Kang, K. Xie, J. Liu, J. Lan, L. Wu, R. Chen, Y. Peng and J. Dai, *Acta Pharm. Sin. B*, 2023, **13**, 1771–1785.
219 Z.-H. Li, Y. Dai, J. Zhou, L. Yang and S.-M. Li, *Org. Lett.*, 2025, **27**, 2433–2437.
220 A. S. Urquhart, J. Hu, Y.-H. Chooi and A. Idnurm, *Fungal Biol. Biotechnol.*, 2019, **6**, 9.
221 W. Thiele, S. Obermaier and M. Muller, *ACS Chem. Biol.*, 2020, **15**, 844–848.
222 J. Hu, H. Li and Y.-H. Chooi, *J. Am. Chem. Soc.*, 2019, **141**, 8068–8072.
223 Y. Zheng, L. Huang, C. Song and J. Li, *Nat. Commun.*, 2025, **16**, 6920.
224 L. Xie, D. Xiao, X. Wang, C. Wang, J. Bai, Q. Yue, H. Yue, Y. Li, I. Molnár, Y. Xu and L. Zhang, *mSphere*, 2020, **5**(6), e00949.
225 D. Toth, B. Dudas, A. B. Nicot, M. A. Miteva and E. Balog, *J. Chem. Inf. Model.*, 2025, **65**, 10503–10513.
226 M. A. Skiba, M. M. Bivins, J. R. Schultz, S. M. Bernard, W. D. Fiers, Q. Dan, S. Kulkarni, P. Wipf, W. H. Gerwick, D. H. Sherman, C. C. Aldrich and J. L. Smith, *ACS Chem. Biol.*, 2018, **13**, 3221–3228.
227 P. Jetha, D. Mojzita, N. Maiorova, J. C. de Ruijter, H. Maaheimo, S. Hilditch, G. Peddinti, S. Castillo, M. Toivari, M. Penttilä and I. Molnár, *Biotechnol. Biofuels Bioprod.*, 2025, **18**, 25.
228 E. Abdelraheem, B. Thair, R. F. Varela, E. Jockmann, D. Popadić, H. C. Hailes, J. M. Ward, A. M. Iribarren, E. S. Lewkowicz, J. N. Andexer, P.-L. Hagedoorn and U. Hanefeld, *ChemBioChem*, 2022, **23**, e202200212.

229 B. Chen, Y. Sun, S. Li, Y. Yin and C. Wang, *mBio*, 2021, **12**, e03279–03221.
230 L. N. Xie, L. W. Zhang, C. Wang, X. J. Wang, Y. M. Xu, H. F. Yu, P. Wu, S. L. Li, L. D. Han, A. A. L. Gunatilaka, X. Y. Wei, M. Lin, I. Molnar and Y. Q. Xu, *Proc. Natl. Acad. Sci. U. S. A.*, 2018, **115**, E4980–E4989.
231 Y. Peng, Y. Huan, J.-J. Chen, T.-J. Chen, L. Lei, J.-L. Yang, Z.-F. Shen, T. Gong and P. Zhu, *Front. Microbiol.*, 2023, **14**, 1148513.
232 Y. Ma, J. Ren, W.-B. Yin, X. Liu and W. Li, *Mycology*, 2025, **16**, 1807–1823.
233 H. Meng, B. Huang, C. Guo, M. Zheng, T. Ye, E. He, Y. Guo and W. Wang, *Plant Stress*, 2025, **18**, 101066.
234 F. Li, Z. Lin, P. J. Krug, J. L. Catrow, J. E. Cox and E. W. Schmidt, *Proc. Natl. Acad. Sci. U. S. A.*, 2023, **120**, e2305575120.
235 K. Kudo, T. Hashimoto, J. Hashimoto, I. Kozone, N. Kagaya, R. Ueoka, T. Nishimura, M. Komatsu, H. Suenaga, H. Ikeda and K. Shin-ya, *Nat. Commun.*, 2020, **11**, 4022.
236 M. Herrera-Martell, A. Mejía, L. E. Gómez-Quiroz and J. Barrios-González, *Biosci., Biotechnol., Biochem.*, 2025, **89**, 1227–1235.
237 G. Jiménez-Osés, S. Osuna, X. Gao, M. R. Sawaya, L. Gilson, S. J. Collier, G. W. Huisman, T. O. Yeates, Y. Tang and K. N. Houk, *Nat. Chem. Biol.*, 2014, **10**, 431–436.
238 X. Gao, X. Xie, I. Pashkov, M. R. Sawaya, J. Laidman, W. Zhang, R. Cacho, T. O. Yeates and Y. Tang, *Chem. Biol.*, 2009, **16**, 1064–1074.
239 H. Renata, *Biochemistry*, 2023, **62**, 253–261.
240 Y. F. Yong, S. Liu, K. Sakai, K. Fujiyama, H. Takagi, Y. Futamura, T. Shimizu, H. Osada, E. B. B. Ong and S. Takahashi, *Chem. Sci.*, 2025, **16**, 13106–13114.
241 Y. Lu, L. Xie, J. Xie, G. Liu, J. Fu, L. Zou, Q. Lin, Y. Wang and W. Chen, *Sci. Adv.*, 2025, **11**, eadu5064.
242 S. d'Oelsnitz, D. J. Diaz, W. Kim, D. J. Acosta, T. L. Dangerfield, M. W. Schechter, M. B. Minus, J. R. Howard, H. Do, J. M. Loy, H. S. Alper, Y. J. Zhang and A. D. Ellington, *Nat. Commun.*, 2024, **15**, 2084.
243 S. d'Oelsnitz, W. Kim, N. T. Burkholder, K. Javanmardi, R. Thyer, Y. Zhang, H. S. Alper and A. D. Ellington, *Nat. Chem. Biol.*, 2022, **18**, 981–989.
244 M. Gantz, S. Neun, E. J. Medcalf, L. D. van Vliet and F. Hollfelder, *Chem. Rev.*, 2023, **123**, 5571–5611.
245 B. Markus, G. C. C, K. Andreas, K. Arkadij, L. Stefan, O. Gustav, S. Elina and S. Radka, *ACS Catal.*, 2023, **13**, 14454–14469.
246 Z. Zhai, M. Zhang, R. Yin, S. Zhao, Z. Shen, Y. Yang, X. Zhang, J. Wang, Y. Qin, D. Xu, L. Zhou and D. Lai, *World J. Microbiol. Biotechnol.*, 2025, **41**, 103.
247 G. Yuan, S. Deng, J. J. Czajka, Z. Dai, B. A. Hofstad, J. Kim and K. R. Pomraning, *Front. Bioeng. Biotechnol.*, 2024, **12**, 1452496.
248 T.-Q. Shi, G.-N. Liu, R.-Y. Ji, K. Shi, P. Song, L.-J. Ren, H. Huang and X.-J. Ji, *Appl. Microbiol. Biotechnol.*, 2017, **101**, 7435–7443.
249 S.-Y. Shih, U. H. Mortensen, F.-R. Chang and H. Tsai, *Synth. Biol.*, 2022, **7**, ysac031.
250 M. Ferrara, M. Haidukowski, A. F. Logrieco, J. F. Leslie and G. Mulè, *Sci. Rep.*, 2019, **9**, 19836.
251 A. S. A. El-Sayed, S. E. Abdel-Ghany and G. S. Ali, *Appl. Microbiol. Biotechnol.*, 2017, **101**, 3953–3976.
252 F. Guzmán-Chávez, R. D. Zwahlen, R. A. L. Bovenberg and A. J. M. Driessen, *Front. Microbiol.*, 2018, **9**, 2768.
253 Y. Wang, J. Guo, J.-J. Zhong and H. Xiao, *Process Biochem.*, 2024, **145**, 32–40.
254 M. Ahuja, Y. M. Chiang, S. L. Chang, M. B. Praseuth, R. Entwistle, J. F. Sanchez, H. C. Lo, H. H. Yeh, B. R. Oakley and C. C. Wang, *J. Am. Chem. Soc.*, 2012, **134**, 8212–8221.
255 S. Bergmann, N. Funk Alexander, K. Scherlach, V. Schroeckh, E. Shelest, U. Horn, C. Hertweck and A. Brakhage Axel, *Appl. Environ. Microbiol.*, 2010, **76**, 8143–8149.
256 H.-w. Seo, W. Bok Jin and P. Keller Nancy, *mBio*, 2025, **16**, e03874–03824.
257 W. Wang, Y. Yu, N. P. Keller and P. Wang, *Int. J. Mol. Sci.*, 2021, **22**, 8709.
258 R. Arivuselvam, K. Nagappan, P. V. Raj and R. Rajeshkumar, *Int. J. Nutr., Pharmacol., Neurol. Dis.*, 2024, **14**, 292–299.
259 I. Roux, C. Woodcraft, J. Hu, R. Wolters, C. L. M. Gilchrist and Y.-H. Chooi, *ACS Synth. Biol.*, 2020, **9**, 1843–1854.
260 L. Mózsik, M. Hoekzema, N. A. W. de Kok, R. A. L. Bovenberg, Y. Nygård and A. J. M. Driessen, *Sci. Rep.*, 2021, **11**, 1118.
261 Q. Peng, Y. Li, J. Fang and X. Yu, *Mar. Drugs*, 2023, **21**, 585.
262 P. Zhao, S. Cao, J. Wang, J. Lin, Y. Zhang, C. Liu, H. Liu, Q. Zhang, M. Wang, Y. Meng, X. Yin, J. Qi, L. Zhang and X. Xia, *Appl. Microbiol. Biotechnol.*, 2024, **108**, 332.
263 L. Yang, G. Wu, F. Meng, H. Ran, W. Yin, W. Li and X. Liu, *Int. J. Mol. Sci.*, 2022, **23**, 3686.
264 Y.-M. Chiang, T.-S. Lin and C. C. C. Wang, *J. Nat. Prod.*, 2022, **85**, 2484–2518.
265 K. A. Markham, C. M. Palmer, M. Chwatko, J. M. Wagner, C. Murray, S. Vazquez, A. Swaminathan, I. Chakravarty, N. A. Lynd and H. S. Alper, *Proc. Natl. Acad. Sci. U. S. A.*, 2018, **115**, 2096–2101.
266 H. Shi, B. Lin, M. Zheng, F. Gan, Z. Lin, X. Xin, J. Zhao, X. Qu and F. An, *Bioresour. Bioprocess.*, 2025, **12**, 2.
267 S. Galanie, K. Thodey, I. J. Trenchard, M. Filsinger Interrante and C. D. Smolke, *Science*, 2015, **349**, 1095–1100.
268 R. M. Pullen, S. R. Decker, V. Subramanian, M. J. Adler, A. V. Tobias, M. Perisin, C. J. Sund, M. D. Servinsky and M. T. Kozlowski, *ACS Synth. Biol.*, 2025, **14**, 343–362.
269 S.-Y. Lin, C. E. Oakley, C. B. Jenkinson, Y.-M. Chiang, C.-K. Lee, C. G. Jones, P. M. Seidler, H. M. Nelson, R. B. Todd, C. C. C. Wang and B. R. Oakley, *Chem. Sci.*, 2023, **14**, 11022–11032.
270 K. D. Clevenger, J. W. Bok, R. Ye, G. P. Miley, M. H. Verdan, T. Velk, C. Chen, K. Yang, M. T. Robey, P. Gao, M. Lamprecht, P. M. Thomas, M. N. Islam, J. M. Palmer, C. C. Wu, N. P. Keller and N. L. Kelleher, *Nat. Chem. Biol.*, 2017, **13**, 895–901.

 

271 J. W. Bok, R. Ye, K. D. Clevenger, D. Mead, M. Wagner, A. Krerowicz, J. C. Albright, A. W. Goering, P. M. Thomas, N. L. Kelleher, N. P. Keller and C. C. Wu, *BMC Genomics*, 2015, **16**, 343.
272 L. Mózsik, C. Pohl, V. Meyer, R. A. L. Bovenberg, Y. Nygård and A. J. M. Driessen, *ACS Synth. Biol.*, 2021, **10**, 2850–2861.
273 I. Roux and Y. H. Chooi, in *Engineering Natural Product Biosynthesis: Methods and Protocols*, ed. E. Skellam, Humana, New York, NY, 2022, vol. 2489, pp. 75–92.
274 I. Roux, C. Woodcraft, N. Sbaraini, A. Pepper, E. Wong, J. Bracegirdle and Y.-H. Chooi, *Microb. Biotechnol.*, 2024, **17**, e70010.
275 J. Yu, X. Liu, C. Ma, C. Li, Y. Zhang, Q. Che, G. Zhang, T. Zhu and D. Li, *Mar. Drugs*, 2023, **21**, 490.
276 I. Roux, S. Bowles, J. A. Kalaitzis, D. Vuong, E. Lacey, Y.-H. Chooi and A. M. Piggott, *Org. Biomol. Chem.*, 2021, **19**, 9506–9513.
277 E. Geib and M. Brock, *Fungal Biol. Biotechnol.*, 2017, **4**, 13.
278 L. Kirchgaessner, J. M. Wurlitzer, P. S. Seibold, M. Rakhmanov and M. Gressler, *Fungal Biol. Biotechnol.*, 2023, **10**, 4.
279 S. Guo, L. Pardeshi, L. Qin, C. Y. Cheung, X. Liu, L. Fan, C. C. Mok, C. Parsania, Z. Dong, B. C. B. Ko, K. Tan and K. H. Wong, *Commun. Biol.*, 2025, **8**, 1444.
280 Y. Wu, F. L. Gong and S. Li, *Curr. Opin. Plant Biol.*, 2023, **71**, 102314.
281 C. J. B. Harvey, M. Tang, U. Schlecht, J. Horecka, C. R. Fischer, H.-C. Lin, J. Li, B. Naughton, J. Cherry, M. Miranda, Y. F. Li, A. M. Chu, J. R. Hennessy, G. A. Vandova, D. Inglis, R. S. Aiyar, L. M. Steinmetz, R. W. Davis, M. H. Medema, E. Sattely, C. Khosla, R. P. St. Onge, Y. Tang and M. E. Hillenmeyer, *Sci. Adv.*, 2018, **4**, e5459–e5473.
282 M. Zhao, Y. Zhao, M. Yao, H. Iqbal, Q. Hu, H. Liu, B. Qiao, C. Li, C. A. S. Skovbjerg, J. C. Nielsen, J. Nielsen, R. J. N. Frandsen, Y. Yuan and J. D. Boeke, *Nat. Commun.*, 2020, **11**, 6197.
283 T. B. Pedersen, M. R. Nielsen, S. B. Kristensen, E. M. L. Spedtsberg, W. Yasmine, R. Matthiesen, S. E. K. Kaniki, T. Sørensen, C. Petersen, J. Muff, T. E. Sondergaard, K. L. Nielsen, R. Wimmer and J. L. Sørensen, *Int. J. Mol. Sci.*, 2020, **21**, 7601.
284 K. Ebner, N. Bernat-Camps, S. Scheipel, C. Dörner, F. Valero, A. Glieder and X. Garcia-Ortega, *Microb. Cell Fact.*, 2025, **24**, 228.
285 Z. Qian, Q. Liu and M. Cai, in *Engineering Natural Product Biosynthesis: Methods and Protocols*, ed. E. Skellam, Humana, New York, NY, 2022, vol. 2489, pp. 115–127.
286 J. Berrios, C. W. Theron, S. Steels, B. Ponce, E. Velastegui, C. Bustos, C. Altamirano and P. Fickers, *Microorganisms*, 2022, **10**, 1466.
287 K. Zhang, X. Duan, P. Cai, L. Gao, X. Wu, L. Yao and Y. J. Zhou, *Microb. Cell Fact.*, 2022, **21**, 182.
288 P. Cruz-Morales, A. Gadar-Lopez, d. A. C. Carvalho, X. Li, D. Rago, L. Ahonen, C. Gotfredsen, M. Lukassen, C. Cano-Prieto, L. Chen, S. Jayachandran, J. Brogaard, M. v. Bargen, L. Bhagavan, T. Strucko, A. Frey, D. Arsovska, E. Carr, S. Jensen, S. Harris, U. Mortensen and J. Kiesling, *Research Square*, 2025, DOI: 10.21203/rs.3.rs-6001933/v1.
289 E. C. Carr, Q. Barton, S. Grambo, M. Sullivan, C. M. Renfro, A. Kuo, J. Pangilinan, A. Lipzen, K. Keymanesh, E. Savage, K. Barry, I. V. Grigoriev, W. R. Riekhof and S. D. Harris, *G3:Genes, Genomes, Genet.*, 2023, **13**, jkad110.
290 D. Dietrich, S. Jovanovic-Gasovic, P. Cao, M. Kohlstedt and C. Wittmann, *Microb. Cell Fact.*, 2023, **22**, 199.
291 W. Wei, M. Li, G. Cai, J. Xu, P. Zhang, T. Qian, X. Chen, H. Su, Y. Zhu, X. Chu and B.-C. Ye, *J. Agric. Food Chem.*, 2025, **73**, 30380–30391.
292 C. Madzak, *J. Fungi*, 2021, **7**, 548.
293 A. Tippelt and M. Nett, *Microb. Cell Fact.*, 2021, **20**, 1–24.
294 K. R. Kildegaard, N. B. Jensen, K. Schneider, E. Czarnotta, E. Özdemir, T. Klein, J. Maury, B. E. Ebert, H. B. Christensen, Y. Chen, I.-K. Kim, M. J. Herrgård, L. M. Blank, J. Forster, J. Nielsen and I. Borodina, *Microb. Cell Fact.*, 2016, **15**, 53.
295 Y. Hu, Z. Zhu, J. Nielsen and V. Siewers, *Open Biol.*, 2019, **9**, 190049–190059.
296 S. Li, Q. Zhang, J. Wang, Y. Liu, Y. Zhao and Y. Deng, *J. Biotechnol.*, 2021, **325**, 83–90.
297 D. Yang, W. Kim, S. M. Yoo, J. H. Choi, S. H. Ha, M. H. Lee and S. Y. Lee, *Proc. Natl. Acad. Sci. U. S. A.*, 2018, **115**, 9835–9844.
298 P. Lin, Z. Fu, X. Liu, C. Liu, Z. Bai, Y. Yang and Y. Li, *ACS Synth. Biol.*, 2023, **12**, 1599–1607.
299 S. Li, T. Si, M. Wang and H. Zhao, *ACS Synth. Biol.*, 2015, **4**, 1308–1315.
300 S. He, Z. Zhang, C. Zhang and W. Lu, *Processes*, 2022, **10**, 2660.
301 M.-L. Sun, Y. Xu, L. Lin, J. Gao, R. Ledesma-Amaro, K. Wang and X.-J. Ji, *J. Agric. Food Chem.*, 2025, **73**, 6050–6058.
302 S. Ito, S. Nishikawa, N. Terasaka and K. Fujishima, *ACS Synth. Biol.*, 2025, **14**, 3245–3251.
303 J. Li, X. Mu, W. Dong, Y. Chen, Q. Kang, G. Zhao, J. Hou, R. Gonzalez, L. Bai, Y. Feng, C. Yang, T. Liu and Z. Tan, *Nat. Catal.*, 2024, **7**, 361–374.
304 C. Zhan, G. Lan, Q. Dan, N. Qin, A. Pearson, P. Mellinger, Y. Liu, Z. Wang, S. Cheong, C. Dou, C. Li, R. Haushalter and J. D. Keasling, *Metab. Eng.*, 2025, **90**, 106–116.
305 S. H. Klass, M. Wesselkamper, A. E. Cowan, N. Lee, N. Lanclos, S. Cheong, Z. Wang, Y. Chen, J. W. Gin, C. J. Petzold and J. D. Keasling, *Nat. Chem. Biol.*, 2025, **21**, 1214–1225.
306 J. Wang, Y. Hong, Z. Wu, A. Fishman and P. Xu, *Metab. Eng.*, 2026, **94**, 99–109.
307 C. Zhan, N. Lee, G. Lan, Q. Dan, A. Cowan, Z. Wang, E. E. K. Baidoo, R. Kakumanu, B. Luckie, R. C. Kuo, J. McCauley, Y. Liu, L. Valencia, R. W. Haushalter and J. D. Keasling, *Nat. Metab.*, 2023, **5**, 1127–1140.
308 G. R. Nickles, B. Oestereicher, N. P. Keller and M. T. Drott, *Nucleic Acids Res.*, 2023, **51**, 7220–7235.
309 W. Zhang, L. Du, Z. Qu, X. Zhang, F. Li, Z. Li, F. Qi, X. Wang, Y. Jiang, P. Men, J. Sun, S. Cao, C. Geng, F. Qi, X. Wan,

C. Liu and S. Li, *Proc. Natl. Acad. Sci. U. S. A.*, 2019, **116**, 13305–13310.
310 C. You, F. Li, X. Zhang, L. Ma, Y.-Z. Zhang, W. Zhang and S. Li, *FEBS J.*, 2021, **288**, 5768–5780.
311 B. Fan, Y. Liu, L.-p. Chi, C. Yang, S. Li and W. Zhang, *Adv. Sci.*, 2025, **12**, e08826.
312 J. F. Martín and P. Liras, *Int. J. Mol. Sci.*, 2024, **25**, 1224.
313 S. Wu, Q. Zhang, W. Zhang, W. Huang, Q. Kong, Q. Liu, W. Li, X. Zou, C.-M. Liu and S. Yan, *J. Agric. Food Chem.*, 2022, **70**, 15928–15944.
314 S. Upadhyay, X. Xu, D. Lowry, J. C. Jackson, R. W. Roberson and X. Lin, *Cell Rep.*, 2016, **14**, 2511–2518.
315 Y. Wang, L. Cao, L. Rong, C. Ding, C. Liu, Q. Ye, Q. Huang, C.-y. Zhang, N. Xu, J. Mao, J. L. Foo and A. Yu, *Chem. Eng. J.*, 2025, **524**, 169279.
316 P. S. Grewal, J. A. Samson, J. J. Baker, B. Choi and J. E. Dueber, *Nat. Chem. Biol.*, 2021, **17**, 96–103.
317 M.-Q. Yin, K. Xu, T. Luan, X.-L. Kang, X.-Y. Yang, H.-X. Li, Y.-H. Hou, J.-Z. Zhao and X.-M. Bao, *Microbiol. Res.*, 2024, **286**, 127815.
318 P. Santhiya, M. N. Bharathi, R. R. Menon, K. Rajalakshmi and J. Manikandan, *Silico Res. Biomed.*, 2025, **1**, 100132.
319 B. T. Lee, O. S. Mohite, M. S. Kwon, H.-S. Kang, T. Weber, S. Y. Lee and H. U. Kim, *Metab. Eng.*, 2025, **92**, 241–251.
320 G. B. Kim, H. R. Kim and S. Y. Lee, *Nat. Commun.*, 2025, **16**, 2869.
321 D. Yang, W. D. Jang and S. Y. Lee, *J. Am. Chem. Soc.*, 2021, **143**, 5364–5377.
322 D. Yang, H. Eun, C. P. S. Prabowo, S. Cho and S. Y. Lee, *Curr. Opin. Biotechnol.*, 2022, **77**, 102760.
323 L. Liu, D. Ding, H. Wang, X. Ren, S. Y. Lee and D. Zhang, *Adv. Sci.*, 2025, **12**, e10649.
324 K. Blin, S. Shaw, K. Steinke, R. Villebro, N. Ziemert, S. Y. Lee, M. H. Medema and T. Weber, *Nucleic Acids Res.*, 2019, **47**, W81–W87.

 